

Structure Effect of Alcohols and Polyglycols on Bubble Rise Velocity

Yue Hua (Hope) Tan

Department of Mining and Materials Engineering
McGill University

Montreal, Canada

August 2013

A thesis submitted to McGill University in partial fulfillment of the
requirements for the degree of
Doctor of Philosophy

© Yue Hua (Hope) Tan
2013

ABSTRACT

Frothers are commonly used in mineral flotation processes to reduce bubble size, slow bubble rise, and stabilize froth. Frother chemistry (structure) plays an important role in determining these functions. In this thesis, over 50 surfactants (mainly from two frother families, alcohols and polyglycols) were investigated to determine the structure effect on bubble rise velocity. The structural variables were: alkyl chain length in alcohols and polyglycols, the number of propylene oxide (PO) and ethylene oxide (EO) groups in polyglycols and location of methyl branch and hydroxyl group in alcohols. The bubble rise velocity profile was determined over 350 cm in a water column. The concentration to reach minimum velocity at 300 cm (CMV) was estimated for each structure. A lower CMV means a structure is more effective in slowing bubble rise. The relationship between CMV and the structural variables and between CMV and HLB (hydrophile-lipophile balance) was investigated.

Increasing alkyl chain length and number of PO or EO units decreases CMV. The hydroxyl group(s) at the terminal position is more effective in reducing CMV than the center position. The effect of methyl branch position is related to the position of the hydroxyl group (OH): The farther the methyl branch from the OH, the lower the CMV. The mechanism slowing bubble rise was related to surfactant surface activity and packing density and the consequent effect on surface tension gradient and surface viscosity.

Linear relationships were found between log CMV and the structural variables and between log CMV and HLB that had a common slope for each surfactant family. Modified HLB group numbers to account for methyl branch and OH position in alcohols were derived in order to include the isomers in the relationship. Noting there were common trends between CMV and the critical coalescence concentration (CCC) linear log CCC vs. HLB relationships were shown using literature data. The mechanism apparently linking CMV and CCC is discussed. The CMV/HLB and CCC/HLB relationships are a step towards predicting frother functions from the structure.

RÉSUMÉ

Les mousses sont communément utilisées en flottaison pour réduire la taille et la vitesse de la bulle et stabiliser la buse de flottaison. La chimie structurale de la buse de flottaison joue un rôle majeur dans la détermination de ces fonctions. Dans cette thèse, plus de 50 surfactants (principalement ceux appartenant aux familles d'alcools et de poly glycols ont été étudiés afin d'en déterminer l'effet structural lors de la montée de la bulle. Les variables structurales considérées étaient: la longueur de la chaîne alkylée dans les alcools et poly glycols, le nombre de groupes d'oxyde de propylene (PO) et d'oxyde d'éthylène (EO), l'emplacement de la branche méthylique et celui du groupe hydroxylique dans les alcools. La vitesse de la bulle a été établie sur 350 cm dans la colonne d'eau. La concentration correspondant à la vitesse minimale à 300 cm (CMV) était évaluée pour chaque structure. Une valeur basse du CMV indique que la structure est effective dans le retardement de la bulle. La relation entre le CMV et les variables structurales et celle entre le CMV et HLB (budget hydrophile- lipophile) étaient étudiées.

En augmentant la longueur de la chaîne alkylée et le nombre de PO et EO, le CMV diminue. Les groupes hydroxyl en position terminale sont plus effectifs dans la réduction du CMV qu'en position central. L'effet découlant de la position du groupe methyl est en relation avec la position du groupe hydroxyl (OH): Le CMV est d'autant plus faible que le groupe methyl est éloigné du groupe OH. Le mécanisme traduisant la montée de la bulle était en relation avec l'activité en

surface du surfactant et la densité de l'empaquetage et l'effet résultant du gradient de la tension superficielle et la viscosité de surface.

Des relations linéaires étaient obtenues entre le log CMV et les variables structurales d'une part et d'autre part entre logCMV and HLB. Ces relations ont révélé des pentes similaires pour chaque famille de surfactants. Pour tenir compte des groupes methyl et du groupe OH dans les alcools, les coefficients des HLB modifiés étaient calculés. Il est à noter qu'il y a des tendances similaires entre le CMV et la concentration de coalescence critique (CCC) et (log CCC en fonction de HLB). Les relations de HLB provenaient des données existant dans la littérature. L'on discute du mécanisme connectant MMV et CCC. Les relations entre CMV/HLB et CCC/HLB sont une étape dans la prédiction des fonctions structurales.

ACKNOWLEDGEMENTS

I would like to express my utmost gratitude to my supervisor, Prof. James A. Finch, for his continuous encouragement and guidance and for his valuable academic insights. I benefitted greatly from his positive attitude toward research and life and from the way he patiently mentors and nurtures his students.

My sincere thanks to Dr. Cesar O. Gomez for setting up apparatus and providing critical guidance throughout my research; to Mr. Raymond Langlois and Dr. Mirnezami for assistance in experiments; and to the Late Dr. Rao for helping me when my supervisor was on sabbatical.

I would like to acknowledge all of my other colleagues in the mineral processing group at McGill University for their selfless help, support, encouragement and constructive suggestions and comments especially during the more challenging parts of my project.

I am grateful to have benefitted from the MEDA (McGill Engineering Doctoral Awards) scholarship, and from financial support through the Chair in Mineral Processing sponsored by Vale, Teck, Xstrate Process Support, Barrick Gold, Shell Canada, SGS Lakefield Research, COREM and Flottec under the NSERC (Natural Sciences and Engineering Research Council of Canada) and CRD (Collaborative Research and Development) program.

My special thanks to my Christian friends, Georgia and Brian Ludgate, who have been like family to me for many years. They supported me during the hardest times of my life while I was a newcomer to Canada.

Last but not least, I would like to thank my son, Ying Peng Cheng, for his ongoing support and for his practical help in my experimental work.

I could never express adequately my appreciation to all the people around me. Without their encouragement and continuous support, I would never have accomplished my goals.

TABLE OF CONTENTS

| | |
|---|------|
| ABSTRACT..... | I |
| RÉSUMÉ | III |
| ACKNOWLEDGEMENTS..... | V |
| TABLE OF CONTENTS..... | VII |
| NOMENCLATURE | XI |
| LIST OF FIGURES | XIV |
| LIST OF TABLES..... | XVII |
| Chapter 1 – Introduction | 1 |
| 1.1 Frother classification..... | 2 |
| 1.2 Frother structure and properties | 3 |
| 1.3 Characterization properties | 4 |
| 1.4 Single bubble rise velocity..... | 5 |
| 1.6 Objective of the study | 8 |
| 1.7 Structure of the thesis..... | 8 |
| References..... | 10 |
| Chapter 2 – Literature Review | 15 |
| 2.1 Physicochemical hydrodynamics of surfactant at interface | 15 |
| 2.1.1 Models of adsorption kinetics at the air/water interface | 18 |
| 2.1.2 Surface tension and structure relationship | 23 |
| 2.2 Physico-chemical hydrodynamics of a rising bubble..... | 28 |
| 2.2.1 Distribution of surfactant molecules on bubble surface—Marangoni effect ... | 29 |
| 2.2.2 Physico-chemical hydrodynamics..... | 30 |
| 2.2.3 Mass transfer | 33 |
| 2.3 Bubble rise velocity | 40 |
| 2.3.1 Bubble size and bubble shape | 40 |

| | |
|---|----|
| 2.3.2 Single bubble rise velocity | 41 |
| 2.3.3 Relation of bubble shape and rise velocity | 45 |
| References..... | 48 |
| Chapter 3 – Experimental Part..... | 61 |
| 3.1 Equipment..... | 61 |
| 3.1.1 Single bubble column setup | 61 |
| 3.1.2 Camera moving device | 62 |
| 3.2 Procedure | 63 |
| 3.3 Reagents..... | 63 |
| 3.3.1 Replication: profile in tap water..... | 65 |
| 3.3.2 Replication: frother solutions..... | 66 |
| References..... | 68 |
| Chapter 4 – Effect of alkyl chain length in alcohols and polyglycol alkyl ethers..... | 70 |
| 4.1 Introduction..... | 70 |
| 4.2 Reagents..... | 71 |
| 4.2.1 Alcohols..... | 71 |
| 4.2.2 Polyglycol ethers..... | 71 |
| 4.3 Results..... | 72 |
| 4.3.1 Bubble rise velocity profile..... | 72 |
| 4.3.2 Velocity at 300 cm..... | 75 |
| 4.3.3 Concentration to reach minimum velocity (CMV) | 81 |
| 4.3.4 Effect of alkyl chain length on CMV | 84 |
| 4.4 Discussion..... | 87 |
| 4.5 Summary | 91 |
| References..... | 92 |
| Chapter 5 – Effect of methyl branch and hydroxyl positions in alcohols | 95 |
| 5.1 Introduction..... | 95 |

| | |
|---|-----|
| 5.2 Reagents..... | 97 |
| 5.3 Results..... | 99 |
| 5.3.1 Hydroxyl position | 99 |
| 5.3.2 Methyl branch position | 103 |
| 5.4 Discussion..... | 105 |
| 5.5 Summary..... | 109 |
| References..... | 111 |
| Chapter 6 – Effect of number of PO and EO units in polyglycols..... | 115 |
| 6.1 Introduction..... | 115 |
| 6.2 Reagents..... | 116 |
| 6.3 Results..... | 118 |
| 6.3.1 Velocity at 300 cm and CMV | 118 |
| 6.3.2 Effect of PO (m) number and EO (l) number on CMV | 124 |
| 6.4 Discussion..... | 125 |
| 6.5 Summary..... | 128 |
| References..... | 130 |
| Chapter 7 – Relationship between CMV and HLB..... | 133 |
| 7.1 Introduction..... | 133 |
| 7.1.1 Hydrophilic-Lipophilic Balance (HLB)..... | 133 |
| 7.1.2 Critical Coalescence Concentration (CCC) | 136 |
| 7.2 HLB, CMV and CCC values | 137 |
| 7.3 CCC vs. HLB..... | 139 |
| 7.4 CMV vs. HLB..... | 141 |
| 7.4.1 Effect of alkyl chain length (n) | 141 |
| 7.4.2 Effect of PO/EO group (m/l) number | 143 |
| 7.4 Relationship between CMV and CCC | 145 |
| 7.5 Discussion..... | 148 |

| | |
|--|-----|
| 7.6 Summary | 150 |
| References..... | 151 |
| Chapter 8 – CMV vs. HLB modified to include isomers..... | 157 |
| 8.1 Introduction..... | 157 |
| 8.2 Relationship between CMV and HLB in alcohol isomers | 158 |
| 8.2.1 Effect of hydroxyl group position..... | 158 |
| 8.2.2 Effect of methyl branch position..... | 158 |
| 8.3 HLB modification in isomers..... | 161 |
| 8.3.1 Hydroxyl position | 161 |
| 8.3.2 Methyl branch position | 162 |
| 8.4 Discussion..... | 166 |
| 8.5 Summary | 169 |
| References..... | 170 |
| Chapter 9 – Conclusions, claims to original research and suggestions for future work . | 172 |
| 9.1 Conclusions..... | 172 |
| 9.1.1 Experimental setup..... | 172 |
| 9.1.2 Structural effect..... | 172 |
| 9.2 Claims for original research..... | 174 |
| 9.3 Recommendations for future work | 175 |

NOMENCLATURE

| | | |
|---------------------------------|--------------------------|--|
| A: | [cm ²] | Reference area |
| a ₀ : | | Frumkin isotherm interaction parameter |
| C : | [mol/cm ³] | Bulk concentration |
| C ₀ | [mol/cm ³] | Equilibrium bulk concentration |
| C _d : | | Drag coefficient |
| D: | [m ² /s] | Mass diffusivity coefficient |
| D _{diff} : | [cm ² /s] | Diffusion coefficient |
| D _L : | [m/s] | Mass transfer coefficient |
| d: | [cm] | Bubble diameter |
| d _{sol} : | [cm] | Equivalent spherical diameter of the solute molecule |
| E _a ⁰ | [J] | Adsorption activation energy |
| E _d ⁰ | [J] | Desorption activation energy |
| g: | [cm ² /s] | Gravitational acceleration |
| J _{ad} | [cm/s] | Adsorption flux |
| J _{des} : | [cm/s] | Desorption flux |
| k _B : | [J/k] | Boltzman constant ; k _B = 1.3806488×10 ⁻²³ |
| k _{ad} : | [cm/s] | Adsorption rate constant |
| k _{des} : | [mol/cm ² .s] | Desorption rate constant |
| k _L ^{ad} | [cm/s] | Langmuir adsorption rate constant |
| k _L ^{des} : | [mol/cm ² .s] | Langmuir desorption rate constant |
| K: | [m/s] | Mass transfer coefficient |

| | | |
|------------------------|------------------------|--|
| K_F : | [mol/cm ²] | Frumkin equilibrium adsorption constant |
| k_F^{ad} : | | Frumkin kinetics adsorption rate constant |
| k_F^{des} : | | Frumkin kinetics desorption rate constant |
| K_G : | [m/s] | Gas film mass transfer coefficient |
| K_H : | [cm] | Henry constant; $K_H = k_H^{ad} / k_H^{des}$ |
| K_L | [m/s] | Liquid film mass transfer coefficient |
| K_L | [mol/cm ²] | Langmuir equilibrium adsorption constant $K_L = k_L^{ad} / k_L^{des} \Gamma_\infty$ |
| M_{solvent} : | [g/mol] | Molecular weight of the solvent |
| r : | [μm] | Capillary orifice radius |
| R : | [J/mol.K] | Gas constant |
| Re_c : | | Reynold number |
| Sc_c : | | Schmidt number |
| T : | [K] | Absolute temperature |
| U : | [cm/s] | Bubble rise velocity |
| U_{st} : | [cm/s] | Velocity of bubble calculated by Stokes' Law |
| U_{H-R} : | [cm/s] | Terminal velocity described by Hadamard and Rybczynski |
| U_T : | [cm/s] | Terminal velocity |
| V_b : | [cm ³ /mol] | Molar volume of solute at the boiling point |
| V'_b : | [cm ³ /mol] | LeBas molar volume of solute at the boiling point |
| X : | | Association parameter for solvent polarity |

| | | |
|--------------------------|--|---|
| α : | | Pre-exponential factor |
| α_0 : | [J] ; [J/mol] | Interaction energy parameter |
| β : | | Pre-exponential factor |
| ρ_L : | [kg/m ³] | Density of the surrounding fluid |
| ρ_g : | [kg/m ³] | Density of the air |
| $\Delta\rho$: | [kg/m ³] | Density difference between liquid and gas |
| γ : | [mN/m] | Interfacial tension |
| Γ_0 : | [mol/cm ²] | Equilibrium surface concentration |
| σ : | [mol/cm ²] | Surfactant solution surface tension |
| θ : | | Modification parameter; $\theta = \frac{\Gamma}{\Gamma_\infty}$ |
| Γ : | [mol/cm ²] | Surface adsorption concentration |
| Γ_∞ : | [mol/cm ²] | Maximum surface concentration |
| Γ/Γ_∞ : | | Fraction of the surface coverage |
| μ : | [N·s/m ²] ; [kg/m·s]; [g/cm.s] | Dynamic viscosity of the surrounding fluid |
| μ' : | [Pa·s] | internal viscosity of the bubble |
| μ_g : | [Pa·s] | dynamic viscosity of the gas |
| ν : | [m/s] | kinematic viscosity of the liquid |

LIST OF FIGURES

| | |
|---|-------------------------------------|
| Figure 2.1 – Accumulation of surfactants at the gas/water interface (Dukhin et al. 1995) | 17 |
| Figure 2.2 – Equilibrium surface tension vs. concentration for n-alkanoic acid (n= 5-12) (Danov et al. 2006)..... | 25 |
| Figure 2.3 – Surface tension vs. solute concentration at 25°C for octaethyleneglycol n- alkyl ethers (Ueno et al. 1981) | 25 |
| Figure 2.4 – Dynamic surface tension of some alcohol solutions: A, B and C at 3.44×10^{-3} mole/liter; D: at 2.43×10^{-3} mole/liter (Defay et al. 1966) | 26 |
| Figure 2.5 – Surface tension for 1-alcohol aqueous solutions as a function of temperature (Vochten and Petre 1973)..... | 28 |
| Figure 2.6 – A cross-section meridional-plane view of an air bubble rising through a surfactant solution and the interfacial surfactant transport processes (Nguyen and Schulze 2004) | 30 |
| Figure 2.7 – A water molecule structure (a) and H-bonding between water molecules (b) | Error! Bookmark not defined. |
| Figure 2.8 – Single bubble velocity profile (Sam 1995)..... | 42 |
| Figure 2.9 – Terminal velocity of air bubbles at 20 °C (Clift et al. 1978)..... | 45 |
| Figure 2.10 – Velocity and aspect ratio for maximum concentration test (Kracht and Finch 2010) | 47 |
| Figure 2.11 – Bubble velocity and aspect ratio for water, frothers, polymer and inorganic salts (Maldonado et al. 2013) | 47 |
| Figure 3.1 – The experimental setup for single bubble rise velocity..... | 62 |
| Figure 3.2 – Bubble velocity profiles in tap water at different times showing acceptable cleanliness to commence a test..... | 66 |
| Figure 3.3 – Demonstration or replication: bubble velocity profiles in 0.4 mmol/l 1- pentanol and 1-hexanol | 67 |
| Figure 4.1 – Bubble velocity profile in presence of 1, 2- butanediol at selected concentrations..... | 73 |
| Figure 4.2 – Bubble velocity profile in presence of three dipropylene glycol ethers (0.05 mmol/L)..... | 74 |
| Figure 4.3 – Velocity at 300 cm for alcohols as a function of concentration: (a) 1-alcohols; (b) 1, 2-diols | 76 |

| | |
|--|-----|
| Figure 4.4 – Velocity at 300 cm for PPGAE as a function of concentration and alkyl chain length: (a) $m = 1$; (b) $m = 2$; (c) $m = 3$ | 79 |
| Figure 4.5 – Velocity at 300 cm for PEGAE as a function of concentration and alkyl chain length: (a) $l = 1$; (b) $l = 2$; (c) $l = 3$ | 81 |
| Figure 4.6 – Method to determine concentration to reach minimum velocity (CMV) | 82 |
| Figure 4.7 – Log CMV for diethylene glycol alkyl ethers at 150cm and 300cm as a function of carbon number | 83 |
| Figure 4.8 – Log CMV of 1-alcohols and 1, 2-diols as a function of carbon number n .. | 84 |
| Figure 4.9 – Log CMV as a function of carbon number n for polyglycol alkyl ethers: (a) PPGAE; (b) PEGAE..... | 86 |
| Figure 4.10 – Log CCC95 as a function of number of carbon in alkyl chain (PPGAE) .. | 91 |
| Figure 5.1 – Effect on velocity at 300 cm of hydroxyl position in alcohols: (a) five-carbon; (b) six-carbon | 100 |
| Figure 5.2 – Effect on velocity at 300 cm of hydroxyl position in branched (3-methyl-) alcohols: (a) five-carbon; (b) six-carbon | 101 |
| Figure 5.3 – Effect on velocity at 300 cm of position of the second hydroxyl in diols: (a) five-carbon; (b) six-carbon..... | 103 |
| Figure 5.4 – Effect on velocity at 300 cm of the methyl branch position in alcohols: (a) five-carbon; (b) six-carbon..... | 104 |
| Figure 5.5 – Illustration of effect of hydroxyl position on packing density | 107 |
| Figure 5.6 – Illustration of effect of methyl position on packing density..... | 108 |
| Figure 6.1 – Velocity at 300 cm as a function of concentration for polypropylene glycols and their alkyl ethers: (a) $n = 0$ (i.e., PPG); (b) $n = 1$; (c) $n = 3$; (d) $n = 4$ | 120 |
| Figure 6.2 – Velocity at 300 cm as a function of concentration for polyethylene glycols and their alkyl ethers: (a) $n = 0$ (i.e., PEG); (b) $n = 1$; (c) $n = 2$; (d) $n = 3$; (e) $n = 4$ | 123 |
| Figure 6.3 – Log CMV as a function of: (a) PO (m) number; (b) EO (l) number | 124 |
| Figure 6.4 – Log CCC as a function of (a): PO (m) number; (b) EO (l) number | 128 |
| Figure 7.1 – Log CCC vs. HLB for PPGAE family as a function of: (a) carbon (n); (b) PO (m) number (dashed lines are least squares best fit)..... | 140 |
| Figure 7.2 – Log CCC vs. HLB for PEGAE family as a function of: (a) carbon (n); (b) EO (l) number (dashed lines are least squares best fit) | 141 |

| | |
|--|-----|
| Figure 7.3 – Log CMV versus HLB as a function of n: (a) 1-alcohols and 1, 2 diols; (b) PPGAE; (c) PEGAE (dashed lines are least squares best fit)..... | 143 |
| Figure 7.4 – Log CMV versus HLB value as a function of m or l: (a) PPGAE; (b) PEGAE (dashed lines are least squares best fit)..... | 144 |
| Figure 7.5 – Log CMV versus log CCC95 as a function of n: (a) 1-alcohols; (b) PPGAE; (c) PEGAE (dashed lines are least squares best fit) | 146 |
| Figure 7.6 – Log CMV versus log CCC95 as a function of m or l: (a) PPGAE; (b) PEGAE | 147 |
| Figure 8.1 – Log CMV as a function of hydroxyl position in five/six alcohols (x indicates the position of hydroxyl group)..... | 158 |
| Figure 8.2 – Log CMV as a function of methyl branch position in five-/six- carbon alcohols with hydroxyl group located at: (a) 1C; (b) 2C; (c) 3C position (x indicates the methyl branch position)..... | 160 |
| Figure 8.3 – Log CMV as a function of modified HLB (dashed line is best fit for 1-alcohols) | 163 |
| Figure 8.4 – Log CMV as a function of modified HLB including x-hexanol/x-pentanol as branch chained (x stands for 2 or 3) | 165 |
| Figure 8.5 – Log CCC as a function of modified HLB number (CCC 95 from literature: Zhang 2012) | 169 |

LIST OF TABLES

| | |
|--|-----|
| Table 1.1 - Classification of frothers..... | 2 |
| Table 2.1 - Diffusion coefficient of 1-alcolhols and 1, n-diols in water with increasing chain length* | 36 |
| Table 2.2 - Diffusion coefficient of alcohols in water with changing OH position..... | 37 |
| Table 2.3 - Bubble size and motion in various Reynolds number region (Aybers and Tapucu 1969)..... | 45 |
| Table 3.1 - Alcohols for chain length study..... | 64 |
| Table 3.2 - Polyglycols for chain length of alkyl chain and EO/PO unit study | 64 |
| Table 3.3 - Alcohols tested for methyl branch and hydroxyl position..... | 65 |
| Table 4.1 - Alcohols tested for alkyl chain length | 71 |
| Table 4.2 - Polyglycol ethers for alkyl chain length study | 72 |
| Table 4.3 - CMV for diethylene glycol alkyl ethers at 150 cm and 300 cm | 82 |
| Table 4.4 - CMV: alcohols..... | 84 |
| Table 4.5 - CMV: Polyglycol ethers at a given m/l | 85 |
| Table 5.1 - Five-carbon alcohol isomers tested | 97 |
| Table 5.2 - Six-carbon alcohol isomers tested | 98 |
| Table 5.3 - Diols tested for hydroxyl position study..... | 99 |
| Table 5.4 - CMVs for five- and six-carbon alcohols | 105 |
| Table 5.5 - CMVs for five- and six-carbon diols..... | 105 |
| Table 6.1 - Polypropylene glycol surfactants tested in this study..... | 117 |
| Table 6.2 - Polyethylene glycol surfactants tested in this study | 117 |
| Table 6.3 - CMV for polyglycol ethers as function of PO/EO number | 123 |
| Table 6.4 - Constants in Eq. 6.1 and 6.2 | 126 |
| Table 7.1 - Selected group number HLB value used in Davies method | 134 |
| Table 7.2 - Aliphatic alcohols: HLB, CMV and CCC | 138 |
| Table 7.3 - Polypropylene and polyethylene alkyl glycol ethers: HLB, CMV and CCC..... | 138 |
| Table 8.1 - Hydroxyl group and methyl branch position modification coefficient..... | 164 |
| Table 8.2 - Modified HLB in five-/six-carbon alcohol isomers..... | 165 |

Chapter 1 – Introduction

Froth flotation (or simply ‘flotation’) was first introduced into the mining industry towards the end of the nineteenth century. It is a process widely applied to separate valuable minerals from gangue by taking advantage of differences in particle hydrophobicity, where hydrophobic particles attach to air bubbles and rise to be collected while hydrophilic particles remain in the pulp (or slurry).

Flotation is a relatively low cost and highly versatile separation method used to recover minerals from various sources ranging from coal deposits to ores of copper, lead, molybdenum, nickel, tungsten and zinc. Flotation enables processing of low-grade ores (Hernández et al. 2004; Senior and Thomas 2005) and fine-grained multi-mineral ores (Tong et al. 2008) which require fine grinding for adequate liberation (Beas-Bustos and Crozier 1992).

Various reagents are introduced into flotation systems to effect the separation by modifying the properties of the solid/liquid and liquid/gas interfaces. Two almost universal reagents are collectors and frothers, which are surface-active agents (surfactants). Collectors are used to change the properties of the solid/liquid interface to render valuable minerals hydrophobic; frothers control the air/liquid interfacial properties to help produce fine bubbles (Harris 1976), reduce bubble rise velocity (Klimpel and Isherwood 1991) and stabilize the froth (Rao and Leja 2004). Linking frother functions to frother structure is the theme of my thesis.

There have been three distinct periods of frother development over the 100 years

of flotation. The first period (prior to 1920s) was characterized by using large amounts of frothing agent (up to 10 kg/ton of ore) of a variety of natural products, such as pine-oil and cresylic acid. These natural products were often poorly soluble and contained a range of chemicals, some effective as frothers others not. The second period (1921–1950) saw chemicals developed in several other industries (e.g., rubber, tanning, agriculture) applied to flotation. Short-chain water-soluble organic molecules such as alcohols were introduced and consumption dropped to < 0.5 kg/ton of ore. The third period, 1951 to present, is characterized by development of reagents specifically for flotation, such as polyglycols (Chander and Nagaraj 2007).

1.1 Frother classification

Several classifications of flotation frothers have been proposed, depending on their properties and behavior in solution. Table 1.1 shows the classification of Dudenkov et al. (Bulatovic 2007) based on application at different pH.

Table 1.1 - Classification of frothers

| Frother classification | Example |
|----------------------------------|--|
| Acidic | Phenols; Alkyl sulfates |
| Neutral (nonionic surfactant) | Aliphatic alcohols; Cyclic alcohols (alpha terpeneols); Alkoxy paraffins; Polypropylene glycol ethers; Polyglycol ethers; Polyglycol glycerol ethers |
| Basic | Pyridine base |

The acidic frothers, which are restricted to low pH, were extensively used up to the 1960s but applications have since diminished because of environmental concerns. The basic frothers, represented by pyridine and homologs, are still used in flotation for some base-metal ores. Neutral frothers are the most important and

widely used. They can be sub-divided into four groups. The first group consists of aromatic alcohols such as α -cresol and 2, 3-xyleneol. The second group is the alkoxy types such as triethoxy butane (TEB). The third group consists of aliphatic alcohols such as 2-ethyl hexanol, diacetone and methyl isobutyl carbinol (MIBC). In recent years, a fourth group of synthetic frothers, loosely referred to as 'polyglycols' comprising PEO (polyethylene oxide), PPO (polypropylene oxide) and PBO (polybutylene oxide) types, has been introduced (Gupta et al. 2007).

Today, the two principal frother families are alcohol-based and polyglycol-based. Among the alcohol frothers branched or cyclic hydrocarbon chains (chain length 5 to 8 carbons), such as MIBC (Methyl Isobutyl Carbinol, or 4-methyl-2-pentanol, a branched-chain aliphatic alcohol) are the most common. Frothers in the polyglycol family are derivatives of polyglycol and polyglycol ether. Molecular weights range up to 600 g/mol with the reagents remaining readily soluble in water. Two well-known examples are Dow Froth 250 ($\text{CH}_3\text{-(OC}_3\text{H}_6)_4\text{-OH}$) and Flottec 150 ($\text{H-(OC}_3\text{H}_6)_7\text{-OH}$).

1.2 Frother structure and properties

Frothers are hetero-polar surfactants containing polar and non-polar (hydrocarbon chain) groups. The polar groups include: hydroxyl ($-\text{OH}$), carbonyl ($>\text{C}=\text{O}$) and ether linkages ($-\text{O}-$). Hydrocarbon chains may be straight or branched, saturated or unsaturated. The general understanding is that this hetero-polar structure results in frother molecule adsorption at the water/air interface with the polar group oriented to the water-side and the hydrocarbon chain to the air-side. As a consequence, interface-related properties, e.g. surface tension and surface

viscosity, are modified and lead to the three principal frother functions: to produce small bubbles, reduce bubble rise velocity, and enhance froth stability.

Frother structure and flotation performance are related (Edwards et al. 1991; Harvey et al. 2005). It is reported that effective flotation frothers have a branched hydrocarbon structure and this 'bulkier' structure forms a loosely packed gaseous films at the liquid/gas interface (Laskowski 1993). A bulkier structure can be accomplished by adding a second hydrophilic group into the molecules, some distance from the first one, or by replacing a hydrophobic group with a short, highly branched hydrocarbon chain. In a flotation system, the bulkier structure of branched frothers compared to straight chain frothers may not only provide the appropriate film to give the needed degree of froth stability, but also may foster interaction with collector adsorbed on the mineral particles, the so-called penetration model (Rao and Leja 2004). However, the structure-function link is not well understood: the link is the focus of this research.

1.3 Characterization properties

To attack the problem measurement of a suitable response or property is required. Many characterization techniques have been proposed to evaluate frothers including: surface tension, rate of bubble coalescence, flotation recovery, foam stability, bubble size distribution, bubble motion (e.g., rise velocity), electrostatic properties of bubbles (zeta-potential), interaction of frother with the mineral surface (co-adsorption with collector) (Somasundaran and Wang 2006).

What is required is a property sensitive to the structure that is easy to measure.

Surface tension is not sensitive at the low concentrations of frother employed (Aston et al. 1983; Sweet et al. 1997). Bubble size measurement suffers the dual problem of sampling a bubble population and selecting a mean size to represent the distribution. As for froth stability there is no universally measurement method, some researchers adopting static tests (e.g., froth decay rate when gas is shut off) and others dynamic tests (e.g., water overflow rate as a function of gas rate for a given froth height). Measurement of equilibrium froth height may be simple conceptually, but some researchers have found poor reproducibility (Araya et al. 2011) and others have found that the geometry of the vessel is a factor (Watkins 1973; Ross and Suzin 1985; Cunningham and Finch 2009). Bubble rise velocity appears to offer both the required sensitivity and ease of measurement.

1.4 Single bubble rise velocity

The reduction in bubble rise velocity is given as one function of a frother (Klimpel and Isherwood 1991). The connection to flotation is likely the impact on gas holdup. As bubble rise velocity decreases gas holdup increases, which increases the bubble surface area in a flotation cell for bubble capture. Combined with reducing bubble size which also slows bubble rise frother has a pronounced impact on gas holdup (Finch and Dobby 1991). Rise velocity, therefore, offers a function to link with structure and measurement appears straightforward but must recognize that velocity is time-dependent.

The local rise velocity of a bubble as a function of time (or height), defined as the “bubble velocity profile”, was introduced by Sam et al. (1996) in the study of frothers. They used an adjustable speed stage-mounted mobile camera system to

track a bubble generated at a capillary over a distance up to 400 cm. The bubble velocity profile reflects the process of frother adsorption/desorption at the bubble surface (i.e., the air/water interface). Upon initial injection the bubble surface is essentially free of surfactant and as the bubble rises frother (or any surfactant) accumulates at the bubble surface. Accumulation is not uniform on a rising bubble as fluid flow over the surface transports surfactant to the bubble rear. The bubble thus has lower surfactant concentration (adsorption density) at the front (i.e., upstream side) compared to the rear (i.e., downstream side). This increasing adsorption density towards the rear creates a positive surface tension gradient towards the bubble front which opposes the fluid flow and thus increases drag (Clift et al. 1978; Dukhin et al. 1995). This increase in drag slows the bubble as evident in the velocity profile.

This increase in drag is the commonly accepted mechanism explaining why the bubble slows in the presence of surfactant. Given sufficient surfactant concentration and/or bubble rise time dynamic equilibrium is reached and the bubble reaches minimum or terminal velocity. Another mechanism sometimes entertained is an increase in surface viscosity as surfactants accumulate (Nguyen and Schulze 2004).

The adsorption/desorption process of surfactant at the bubble surface is related to its structure. Sam et al (1996) demonstrated that the bubble velocity profile was sensitive to frother type, i.e., frother structure. Others have shown the sensitivity of the profile for a variety of surfactants (Krzan and Malysa 2002; Tomiyama et al. 2002; Krzan et al. 2004; Krzan et al. 2007). Single bubble velocity profile will

be the basis to relate to frother structure in this project.

1.5 Quantifying frother structure

The thesis will use surfactants from the two main frother families, alcohols and polyglycols. One set of structural variables will be alkyl chain length, quantified by the number of carbons (n), and the number of propylene oxide (PO) groups (m) in polypropylene glycols and the number of ethylene oxide (EO) groups (l) in polyethylene glycols. Another set of structural variables will be the location of methyl branch and hydroxyl head group in alcohols.

Correlations with the structure variables (n , m , l) will be explored. As an alternative measure of structure the hydrophilic-lipophilic balance (HLB) number (Rao and Leja 2004) will be investigated. The HLB number is a measure of the degree to which a surfactant is hydrophilic or lipophilic (hydrophobic). The choice of HLB is based on the argument that since it is the heteropolar (i.e., hydrophilic-hydrophobic) character that induces frother adsorption at the air-water interface leading to the frother functions a measure related to the heteropolar character is required. Others have argued similarly (Fuerstenau et al. 1983; Laskowski and Woodburn 1998; Pugh 2000).

The HLB is calculated for straight chain surfactants by summing values assigned to the different functional groups in the molecule. The calculation does not consider the group location and type of neighboring groups in the molecule. In consequence the HLB is the same for isomers, surfactants with the same chemical formula but different structure. From rise velocity data for three isomers of 6-C

alcohols (Rafiei 2009) there appears to a difference depending on the position of the OH and $-CH_3$ groups. This thesis will provide a comprehensive evaluation of isomers of alcohols and explore ways to modify HLB group numbers to reflect position in the molecule. The approach takes previous work modifying HLB group numbers as the precedent.

1.6 Objective of the study

The study is part of the general objective to determine frother structure-property relationships. In this thesis the property is single bubble rise velocity and structure is varied by selecting surfactants from the two main frother families, alcohols and polyglycols. The specific objectives of the thesis are:

1. Determine the effect on rise velocity of structural variables alkyl chain length and position of OH and CH_3 in alcohols, and alkyl chain length and number of propylene oxide and ethylene oxide groups in polyglycols.
2. Determine the concentration to give minimum rise velocity, CMV, as a single metric to quantify the rise velocity property, and relate to structural variables, and to the hydrophilic-lipophilic-balance, HLB.
3. Develop a model to modify the HLB group number to include isomers.
4. Extend analysis to include literature on critical coalescence concentration, CCC, as another property measure.

1.7 Structure of the thesis

Chapter 2: Background and literature review of dynamic and equilibrium surface tension, mass transfer from bulk solution to bubble surface, the Marangoni effect

and the role of surfactants on bubble rise velocity;

Chapter 3: Experimental procedure used in Chapters 4, 5 and 6 and selection of frother chemistries;

Chapters 4, 5, 6: Effect of structural parameters: alkyl chain length, the position of hydroxyl and methyl branch and number of propylene oxide and ethylene groups in the alcohol and polyglycol frother families, respectively. Concentration to reach minimum velocity (CMV) is determined. Each chapter contains a discussion section;

Chapter 7: Relationship between CMV and HLB and between CMV and CCC based on chain length effect;

Chapter 8: Introduces the methodology to modify the HLB group numbers to account for effect of isomers on CMV;

Chapter 9: Overall conclusions, claims to original research and suggestions for further research.

References

- Aston, J. D., Drummond, C. J., Scales, F. J. and Healy, T. W. (1983). Frother chemistry in fine coal processing, In Proc. 2nd Aust. Coal Prep. Congress R. I. Whitmore. Brisbane, Westminster Press: 148-160.
- Araya, R., Maldonado, M., Gomez, C. O. and Finch, J. A. (2011). Technique to automate measurement of water overflow rate in frother characterization testing. *Minerals Engineering* 24(8): 950-952.
- Beas-Bustos, E. and Crozier, R. D. (1992). Moly/copper separation from concentrate of the combined acid and basic circuits at el teniente. *Minerals Engineering* 5(3-5): 357-379.
- Bulatovic, S. M. (2007). *Handbook of flotation reagents: chemistry, theory and practice* Amsterdam Boston: Elsevier. pp: 43-49.
- Chander, S. and Nagaraj, D. R. (2007). *Flotation: Flotation Reagents*. Encyclopedia of Separation Science. D. W. Editor-in-Chief: Ian. Oxford, Academic Press: 1-14.
- Clift, R., Grace, J. R., and Weber, M. E. (1978). *Bubbles, drops, and particles*. Montreal, Academic Press.
- Cunningham, R. R. and Finch, J. A. (2009). Modifications to foam volume measurements. The 48th conference of metallurgists. Sudbury, Ontario, Canada, The Metallurgical Society of the Canadian Institute of Mining, Metallurgy and Petroleum: 193-202.

- Dukhin, S. S., Kretzschmar G., and Miller, R. (1995). Dynamics of adsorption at liquid interfaces: Theory, Experiment, Application, Elsevier Science.
- Edwards, D. A., Shapiro, M., Brenner, H. and Shapira, M. (1991). Dispersion of inert solutes in spatially periodic, two-dimensional model porous media. *Transport in Porous Media* 6(4): 337-358.
- Finch, J. A. and Dobby, G. S. (1991). Column flotation----A selected review. Part 1. *International Journal of Mineral Processing*.
- Fuerstenau, D. W., Rosenbaum, J. M. and Laskowski, J. (1983). Effect of surface functional groups on the flotation of coal. *Colloids and Surfaces* 8(2): 153-173.
- Gupta, A. K., Banerjee, P. K., Mishra, A., Satish, P. and Pradip (2007). Effect of alcohol and polyglycol ether frothers on foam stability, bubble size and coal flotation. *International Journal of Mineral Processing* 82(3): 126-137.
- Harris, C. C. (1976). Flotation machines in flotation, A. M. Gaudin Memorial Volume, Fuerstenau, M. C., Ed.; AIME; New York, NY, USA. Vol 2: 753-815.
- Harvey, P. A., Nguyen, A. V., Jameson, G. J. and Evans, G. M. (2005). Influence of sodium dodecyl sulphate and Dowfroth frothers on froth stability. *Minerals Engineering* 18(3): 311-315.
- Hernández, F., Calero, M. and Blázquez, G. (2004). Flotation of low-grade phosphate ore. *Advanced Powder Technology* 15(4): 421-433.

- Klimpel, R. R. and Isherwood, S. (1991). Some industrial implications of changing frother chemical structure. *International Journal of Mineral Processing* 33(1-4): 369-381.
- Krzan, M., Lunkenheimer, K. and Malysa, K. (2004). On the influence of the surfactant's polar group on the local and terminal velocities of bubbles. *Colloids and Surfaces a-Physicochemical and Engineering Aspects* 250(1-3): 431-441.
- Krzan, M. and Malysa, K. (2002). Profiles of local velocities of bubbles in n-butanol, n-hexanol and n-nonanol solutions. *Colloids and Surfaces A: Physicochemical and Engineering Aspects* 207(1-3): 279-291.
- Krzan, M., Zawala, J. and Malysa, K. (2007). Development of steady state adsorption distribution over interface of a bubble rising in solutions of n-alkanols (C5, C8) and n-alkyltrimethylammonium bromides (C8, C12, C16). *Colloids and Surfaces A: Physicochemical and Engineering Aspects* 298(1-2): 42-51.
- Laskowski, J. S. (1993). Frothers and flotation froth. *Mineral Processing and Extractive Metallurgy Review: An International Journal* 12(1): 61-89.
- Laskowski, J. S. and Woodburn, E. T., (1998). *Frothing in flotation II* Amsterdam, Netherlands Gordon and Breach Science Publishers.
- Nguyen, A. V. and Schulze, H. J. (2004). *Colloidal Science of flotation*. New York, New York Basel.

- Pugh, R. J. (2000). Non-ionic polyethylene oxide frothers in graphite flotation. *Minerals Engineering* 13(2): 151-162.
- Rafiei, A. A. M. (2009). Effects of frother type on single bubble rise velocity. M. Eng, McGill University.
- Rao, S. R. and Leja, J. (2004). Surface chemistry of froth flotation, New York: Kluwer Academic/Plenum Publishers.
- Ross, S. and Suzin, Y. (1985). Measurement of dynamic foam stability. *Langmuir* 1: 145-149.
- Sam, A., Gomez, C. O. and Finch, J. A. (1996). Axial velocity profiles of single bubbles in water/frother solutions. *International Journal of Mineral Processing* 47(3-4): 177-196.
- Senior, G. D. and Thomas, S. A. (2005). Development and implementation of a new flow sheet for the flotation of a low grade nickel ore. *International Journal of Mineral Processing* 78(1):49-61.
- Somasundaran, P. and Wang, D. (2006). Solution chemistry: minerals and reagents. W. Dianzuo, Elsevier. Volume 17: 143-201.
- Sweet, C., Hoogstraten, J. Van, Harris, M. and Laskowski, J. S. (1997). The effect of frothers on bubble size and frothability of aqueous solutions. *Processing of Complex Ores-Proc. 2nd UBC-McGill Int. Symposium (J .A. Finch, S. R. Rao and I. Holubec, eds.)* Sudbury.
- Tong, X., Song, S., He, J. and Lopez-Valdivieso, A. (2008). Flotation of indium-

beard marmatite from multi-metallic ore. *Rare Metals* 27(2): 107-111.

Tomiyama, A., Celata, G. P., Hosokawa, S. and Yoshida, S (2002). Terminal velocity of single bubbles in surface tension force dominant regime. *International Journal of Multiphase Flow* 28(9): 1497-1519.

Watkins, R. C. (1973). An improved foam test for lubricating oil. *Journal of the institute of Petroleum* 59: 106-113.

Chapter 2 – Literature Review

2.1 Physicochemical hydrodynamics of surfactant at interface

Surface active agents (surfactants) are compounds, which in very small quantities (a few ppm) can significantly alter air-water interfacial properties while not affecting other properties such as solution viscosity and density. Surfactants are added to reduce surface tension in processes where interface formation is required, such as detergency, creation of coatings or sprays, and formation of foams and emulsions. Surfactants play important roles in biological and biochemical systems (Brown et al. 1990; Valentini et al. 1991) such as development of agricultural pesticide sprays (Knoche et al. 1991), enhanced oil recovery (Liu et al. 2007), textile processing (Notter and Morrow 1975; Notter and Finkelstein 1984). They also have key functions in mineral processing.

Amphiphile, which means both hydrophilic (water-loving) and hydrophobic (water-fearing) properties exist in one molecule, is sometimes used as a synonymous term for surfactant. This amphiphilic nature of the structure causes surfactant molecules to adsorb at the air-water interface in a particular orientation, the hydrophilic (polar) part on the water-side of the interface and the hydrophobic (usually a hydrocarbon chain) part on the air-side. Accordingly, both the hydrophilic and hydrophobic properties are satisfied simultaneously.

When an air-water interface (i.e., bubble) is freshly formed in an aqueous surfactant solution, the surface concentration or adsorption density, Γ (units:

mole/m²), is initially close to zero. The adsorption process then commences and with time an equilibrium condition at the interface is established. If the interface is stationary the equilibrium adsorption density is related to the equilibrium surface tension by the Gibbs adsorption isotherm (de Nevers 2012; Rosen and Kunjappu 2012). If the bubble is moving (i.e., is rising through the solution) the fluid motion over the bubble surface transports surfactant to the rear of the bubble (downstream side). This means the adsorption density increases towards the rear and thus creates a gradient in the surface tension. The surface tension gradient has a profound effect on the bubble behavior, causing the bubble to become more spherical and slowing the bubble down. Both of these effects are usually explained by the surface tension gradient producing a force opposing bubble deformation and increasing drag (Dukhin et al. 1995). Equilibrium adsorption on a rising bubble's surface is dynamic between the adsorption process predominantly at the front of the bubble, transport along the surface, and desorption from the bubble rear. The velocity associated with reaching dynamic equilibrium is the terminal velocity.

The thermodynamic driving force for adsorption is the lowering of the free energy of the system. In the presence of surfactant it is the reduced surface tension, or surface energy. The driving force for mass transfer is a concentration gradient. The following argument describes how the concentration gradient arises. When a bubble surface is freshly formed in a solution containing soluble surfactant, those surfactant molecules close to the interface adsorb onto the interface. Thus the concentration in the layer immediate to the bubble surface is depleted, termed the

subsurface. There is now a concentration gradient from the subsurface to the bulk that drives the mass transfer of surfactant to the subsurface. Adsorption of surfactants at the air/water interface is then treated as occurring in two consecutive steps as depicted in Fig. 2.1:

- Surfactants are transported from the bulk to the subsurface
- Surfactants are transferred/adsorbed from the subsurface onto the interface

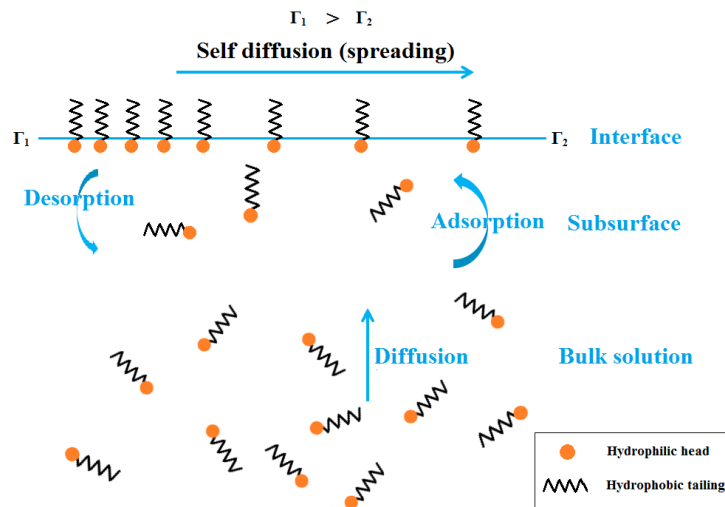


Figure 2.1 – Accumulation of surfactants at the gas/water interface (Dukhin et al. 1995)

Three regions are thus defined: the interface, where the surfactant molecules accumulate; the subsurface, which is adjacent to the interface and assumed to be in equilibrium with the interface at all times; and the bulk solution which has a uniform concentration of surfactant.

The impact of a surfactant on surface tension depends on the (bulk) concentration and surface activity. Surface activity, a synonym of tensioactivity, can be thought of as the extent to which surface tension is reduced per molecule adsorbed.

Surface activity is controlled by the surfactant structure (Holmberg et al. 2003). For example, a structure that allows one surfactant to pack more closely on the surface than another will produce a lower surface tension at equal bulk concentration, i.e., will have a higher surface activity. The rate of surfactant transport to the surface by diffusion, is also controlled by structure. The kinetics of adsorption is described by different models as discussed below.

2.1.1 Models of adsorption kinetics at the air/water interface

Adsorption is a kinetic process resulting from the balance between the adsorptive flux (J_{ad}) to an interface and desorptive flux (J_{des}) from the interface where the rate of change in surface coverage $d\Gamma/dt$ is given by:

$$\frac{d\Gamma}{dt} = J_{ad} - J_{des} \quad 2.1$$

For single component systems with low surface coverage and non-interacting molecules which form a gaseous-type monolayer, a simple linear model is that due to Henry (Erbil 2009):

$$\frac{d\Gamma(t)}{dt} = k_{ad}C(0, t) - k_{des}\Gamma \quad 2.2$$

where the surface concentration is given by Henry's adsorption isotherm:

$$\Gamma = K_H C \quad 2.3$$

A measure of the surface activity is the equilibrium adsorption constant $K_H (= k_{ad}/k_{des})$. It provides an important reference scale for the so-called dynamic subsurface adsorption layer.

Assuming no interaction between solute and solvent molecules, Langmuir derived the following model (Dukhin et al. 1995), the most commonly used to describe surfactant adsorption kinetics:

$$\frac{d\Gamma(t)}{dt} = k_{ad}C(0, t) \left(1 - \frac{\Gamma}{\Gamma_{\infty}}\right) - k_{des} \frac{\Gamma}{\Gamma_{\infty}} \quad 2.4$$

where the surface concentration is given by the Langmuir adsorption isotherm:

$$\Gamma = \Gamma_{\infty} \cdot \frac{K_L C}{1 + K_L C} \quad 2.5$$

In Langmuir's model, the adsorption rate depends on subsurface concentration, and the fraction of uncovered surface $(1 - \Gamma/\Gamma_{\infty})$. There is a theoretical upper limit Γ_{∞} of surface concentration. At low concentration or when $K_L C \ll 1$, the Langmuir model (Eq. 2.3) can be approximated by the Henry model, where $K_H = \Gamma_{\infty} \cdot K_L$.

In practice, it is the surface tension not the adsorption density that is measured experimentally; an equation relating surface tension and adsorption density is required. When equilibrium is reached, the Gibbs adsorption isotherm relates the surfactant surface concentration to the surface tension, which for a non-ionic surfactant is Eq. 2.6:

$$\Gamma = -\frac{1}{RT} \frac{\partial \gamma}{\partial \ln c} \quad 2.6$$

From a plot of surface tension (γ) against natural logarithm of the concentration ($\ln C$) the slope at any point (i.e., the tangent) is proportional to Γ , the equilibrium surface concentration. Substituting the Gibbs adsorption isotherm into the Langmuir kinetic model, the Frumkin kinetic model (Frumkin 1925) is derived:

$$\frac{d\Gamma(t)}{dt} = k_F^{ad} C(0, t) \left(1 - \frac{\Gamma}{\Gamma_\infty}\right) - k_F^{des} \Gamma \exp(\alpha_0 (\Gamma/\Gamma_\infty)) \quad 2.7$$

where the Frumkin adsorption isotherm is:

$$C = \frac{1}{K_F} \frac{\Gamma}{\Gamma_\infty - \Gamma} \exp(-\alpha_0 (\frac{\Gamma}{\Gamma_m})) \quad 2.8$$

where α_0 is a parameter representing the intermolecular force between surfactant molecules in the interface. Frumkin introduced the additional interaction force to account for non-ideal conditions. When α_0 is positive, there is attraction between the molecules; when α_0 is negative, there is repulsion; and when α_0 equals to zero, the surface is ideal, and the Frumkin kinetic model reduces to the Langmuir kinetic model (Gibbs 1906).

Based on Langmuir's kinetic model, Chang and Franses (1992) proposed a modification (Eq. 2.9) by introducing an empirical parameter β , which is compatible with an activation energy barrier. A linear extra term in exponential, $\exp(-\beta\theta)$, form was chosen:

$$\frac{d\Gamma(t)}{dt} = k_L^{ad} C(0, t) \left(1 - \frac{\Gamma}{\Gamma_\infty}\right) \exp(-\beta\theta) - k_L^{des} \exp(-\beta\theta) \quad 2.9$$

In this model the same β parameter is used in both the adsorption and desorption rate terms. Equation 2.9 better describes the efficiency of the interfacial monolayer at capturing additional molecules than the prior models. It can describe either an activation energy barrier for adsorption and desorption, or cooperative adsorption caused by attractive interaction between the monolayer and the molecules in the bulk. In this equation, k_L^{ad} and β are empirical and depend on the bulk concentration.

Intermolecular force in the interface has been considered by many researchers trying to explain variance between theory and experiment. Miller and Lunkenheimer (1986) tried to explain the adsorption of n-alkanols and n-alkanoic acids by considering surface concentration dependent activation energy for adsorption in the Frumkin model. The continued disagreement between theory and experiment was assumed to be due to neglecting cohesive forces.

In order to account for intermolecular cohesive forces among the adsorbed surfactant molecules, Lin et al. (1991) considered cooperative adsorption due to enhanced intermolecular attractions and derived:

$$\frac{\Gamma}{\Gamma_{\infty}} = x = \frac{c}{a \exp(kx^n) + c} \quad 2.10$$

where $k = (v_a - v_d) \Gamma_{\infty}^n / RT$ and $a = (\alpha/\beta) \exp [(E_a^0 - E_d^0)/RT]$. This model well described adsorption for surfactant molecule structures with long, slender hydrocarbon chains and small polar groups. This success was ascribed to strong, attractive van der Waals forces when surface crowding causes inter-chain contact. The presence of a cohesive intermolecular force which increases with surface

coverage and decreases the desorption rate (relative to that of adsorption) corresponds to $k < 0$ (Lin et al. 1991).

Different chemical structures give different surface activities. The adsorption kinetics of highly surface-active compounds (usually at low concentration) is rate limiting (e.g. diffusion controlled in non-turbulent systems), the transfer from the subsurface to the interface being much faster than from the bulk to the subsurface and can be considered 'instantaneous'. Under this circumstance, local equilibrium between the subsurface and the interface is established in the time range of the diffusion process. However, for less tensioactive molecule structures, the bulk concentration has to be high to achieve an appreciable surface tension reduction. In this case, due to the high concentration gradient, the diffusion process is fast, and the transfer from the subsurface to the interface becomes the rate controlling step. For surfactant molecules with intermediate tensioactivity both diffusion and subsurface-interface mass transfer have to be included in a mixed model (Bleys and Joos 1985). For many surfactants similar to commercial frothers, the mixed model applies (Chang and Franses 1995).

The adsorption rate constant depends on chain length. Among alcohols, 1-propanol, 1-butanol, and 1-pentanol show transfer-controlled kinetics, while 1-hexanol and 1-heptanol show mixed kinetics, i.e., both diffusion-controlled and transfer-controlled kinetics, and 1-octanol shows diffusion controlled kinetics (Joos and Serrien 1989).

2.1.2 Surface tension and structure relationship

2.1.2.1 Equilibrium surface tension

Surfactant adsorption to a fresh interface is a time-dependent process. As there is no easy direct way of measuring air/water interface surface concentration, surface tension data are used in studying the effect of surfactant adsorption. Many methods for measuring surface tension are available. They mainly fall into the following four categories:

1. Force methods: e.g. Du Noüy ring (Boucher et al. 1967; Mankowich 1967; Löfgren et al. 1984) and Wilhelmy plate (Padday and Russell 1960; Pike and Bonnet 1970; Furlong and Hartland 1979)
2. Shape methods: pendant and sessile drops or bubbles (Girault et al. 1984) and spinning drop or bubble (Coltharp and Franses 1996; Viades-Trejo and Gracia-Fadrique 2007; Martin and Velankar 2008)
3. Pressure methods - small bubble surfactometer (Horozov et al. 1996; Lenghor et al. 2005); oscillating jet method (Defay and Hommelen 1958; Hansen et al. 1958; Hansen and Wallace 1959)
4. Other methods: capillary rise (Lane 1973), inclined plate (Van Den Bogaert and Joos 1979), drop volume (Harkins and Brown 1919; Tornberg 1978), and growing bubble method (MacLeod and Radke 1993)

Usually, for single-component surfactants, the equilibrium tension decreases monotonically with the increase of surfactant concentration, and stays approximately constant above the critical micelle concentration (CMC). Figs. 2.2

and 2.3 show the surface tension (mN/m) vs. concentration for n-alkanoic acids ($n = 5 - 12$) (Danov et al. 2006) and octaethylene glycol n-alkyl ethers $[C_nH_{2n+1}(EO)_8OH]$ with alkyl (hydrocarbon) chain length $n = 9 - 15$ (Ueno et al. 1981), respectively. It can be seen the rate of decrease in surface tension with concentration increases with increasing hydrocarbon chain length. That is, surface activity increases with the number of carbons in the molecule structure. In a homologous series of surfactants, the bulk concentration to achieve a given surface coverage decreases by about three times for every additional $-CH_2-$ group in the hydrocarbon chain (Traube rule) (Traube 1891). Alcohols with branched radicals are less surface-active than the corresponding straight chain alcohols (Addison 1945). For surfactant concentrations below the CMC, the surface concentration Γ may be estimated from the slope of a γ -ln c plot at constant temperature, based on the Gibbs adsorption equation with the ideal dilute solution assumption.

In conclusion, surface activity is a function of surfactant chemical structure, especially the hydrocarbon chain length.

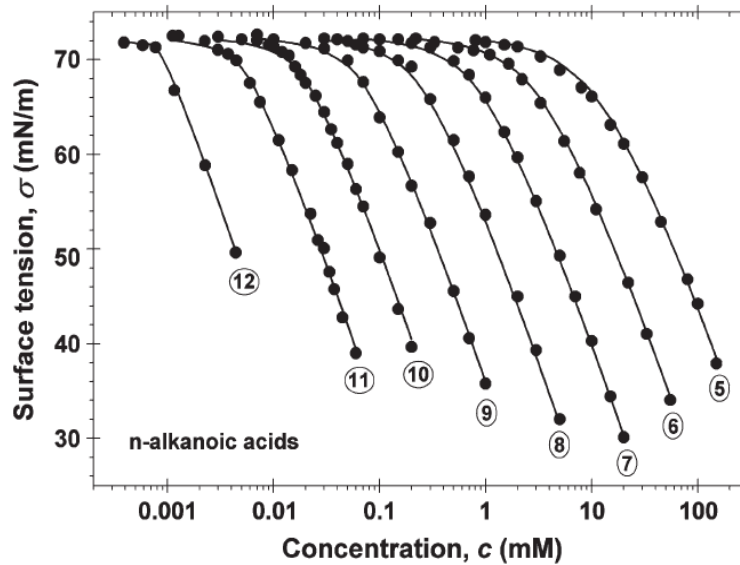


Figure 2.2 – Equilibrium surface tension vs. concentration for n-alkanoic acid ($n=5-12$) (Danov et al. 2006)

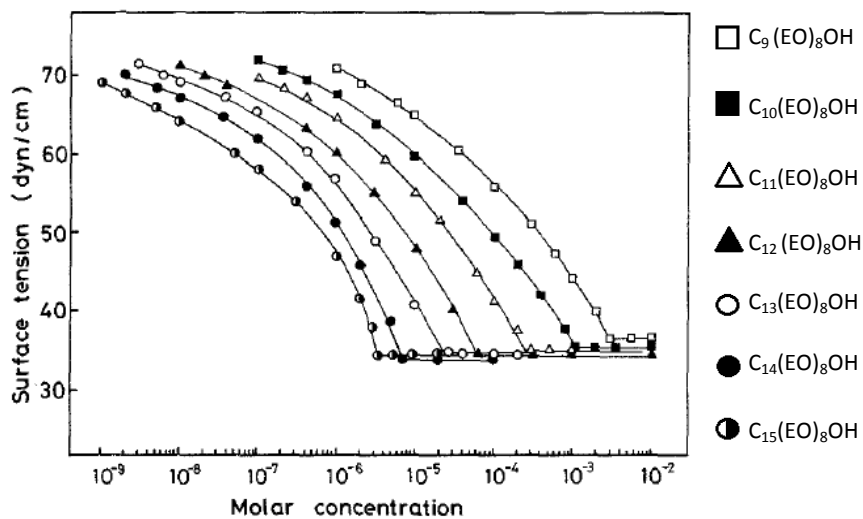


Figure 2.3 – Surface tension vs. solute concentration at 25°C for octaethyleneglycol n-alkyl ethers (Ueno et al. 1981)

2.1.2.2 Dynamic surface tension (DST)

The time-dependent interfacial surfactant accumulation (adsorption) results in a time-dependent or dynamic surface tension (DST). A typical surface tension-time curve (Rosen and Hua 1990) can be divided into four stages: induction, fast decrease, meso-equilibrium, and equilibrium. In general, the time to reach equilibrium is dependent on the surfactant type (surfactant structure) and concentration. Fig 2.4 shows DST for straight chain alcohols with $n = 6$ to 8 ; the equilibrium adsorption time of shorter chain alcohols would be less (Leja 1982).

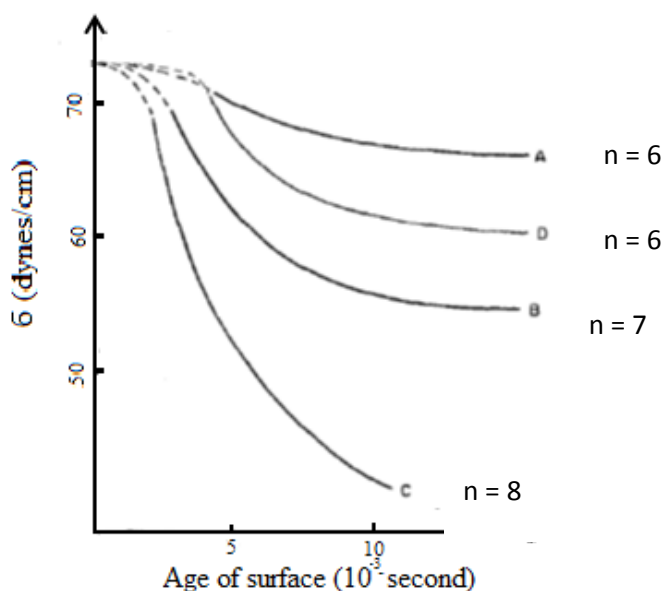


Figure 2.4 – Dynamic surface tension of some alcohol solutions: A, B and C at 3.44×10^{-3} mole/liter; D: at 2.43×10^{-3} mole/liter (Defay et al. 1966)

2.1.2.3 Temperature effect on adsorption:

The surface tension of liquids generally decreases with increasing temperature (Legros 1986). The surface tension of aqueous alcohol solutions with chain lengths longer than 4 carbons presents a minimum value with temperature. For a particular alcohol, the value of the surface tension minimum at the temperature is a monotonic decreasing function of the concentration. This phenomenon was observed with both normal and branched alcohols (Vochten and Petre 1973). Vochten and Petre (1973) used a series of 1-alcohols ($n = 4 - 10$) to study the effect of chain length, the effect of position of the hydroxyl group in a nine carbon straight chain alcohol and the effect of branch (CH_3) position. The temperature corresponding to the minimum surface tension decreases with the increasing length of the hydrocarbon chain (Fig. 2.5). In the 9-carbon alcohol, the temperature at which the minimum surface tension was achieved increased with shift of the OH-group from the C-1 to C-5 position. The effect of temperature, therefore, depends on surfactant structure.

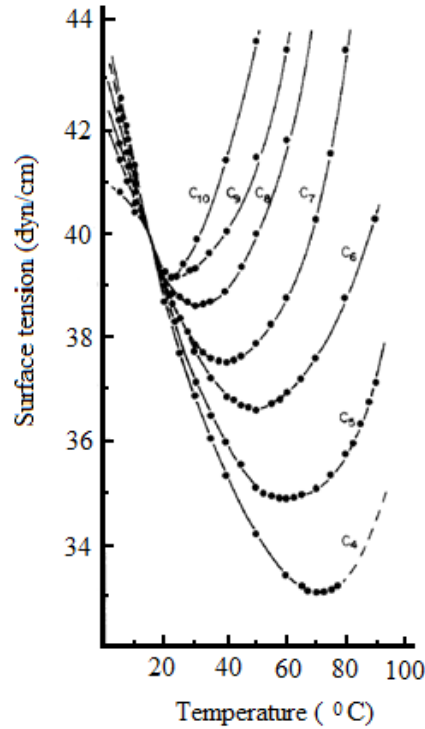


Figure 2.5 – Surface tension for 1-alcohol aqueous solutions as a function of temperature (Vochten and Petre 1973)

2.2 Physico-chemical hydrodynamics of a rising bubble

In the absence of extensive agitation, once a bubble forms it will move under the prevailing buoyancy and drag forces. In clean water (more specifically for this discussion water without surfactant), the bubble surface (air-water interface) is freely mobile. However, the presence of even small quantities of surfactant (frother) will lead to the adsorption and accumulation of surfactant on the rising bubble which hinders its surface mobility (Clift et al. 1978).

2.2.1 Distribution of surfactant molecules on bubble surface—Marangoni effect

The flow of liquid over the surface of a moving bubble results in an uneven distribution of the adsorbed surfactant molecules, as illustrated in Fig. 2.6. As a consequence the adsorbed surfactants on a rising bubble are ‘pushed’ to the rear of the bubble. As shown in the figure, the leading part of the bubble surface is considered to remain mobile, is stretched and the adsorption coverage is lower than the equilibrium, while the lower part of the bubble is compressed, immobile and the adsorption coverage is higher than the equilibrium. The non-uniformity of surfactant distribution on the surface induces a tangential gradient of surface tension, which in turn causes a tangential stress opposing the flow shear stress (Scriven 1960). The surface tension gradient leads to the associated phenomena of Gibbs elasticity and the Marangoni effect (Frumkin and Levich 1947).

The constantly created fresh sections of the leading surface receive adsorbing surfactant, while from the compressed part of the bubble surface surfactant is desorbing. These desorption/adsorption processes occur everywhere on the bubble surface but adsorption is focused on the leading side and desorption at the rear. A stagnant cap is formed if the interfacial convection is faster than the interfacial and bulk diffusion. This induced surface tension gradient generates a tangential shear stress which retards the surface velocity and increases the drag coefficient. Experimentally, Warszynski et al. (1996) demonstrated a non-uniform surfactant distribution over the surface changes with the life of the bubble, i.e. after rising different distances.

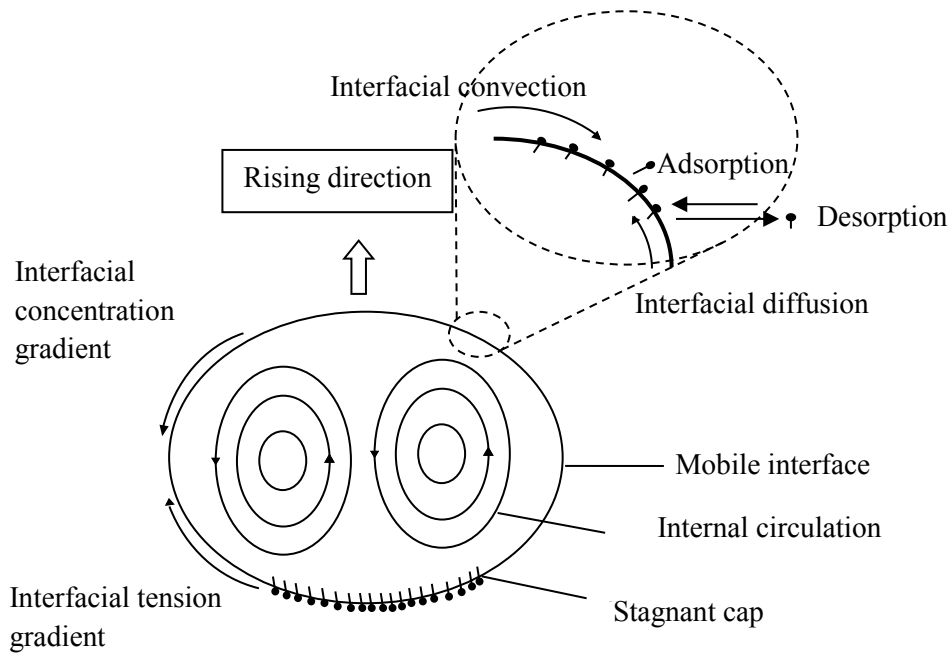


Figure 2.6 – A cross-section meridional-plane view of an air bubble rising through a surfactant solution and the interfacial surfactant transport processes (Nguyen and Schulze 2004)

2.2.2 Physico-chemical hydrodynamics

2.2.2.1 Hydrogen bonding

In an aqueous solution of surfactant, the extent of interaction between surfactant molecules at interface depends on the nature and relative strength of the solute-solute, solute-solvent and solvent-solvent molecular interactions (Israelachvili 2010). One interaction is hydrogen bonding.

Water molecules interact with neighboring water molecules through hydrogen bonding. A popular depiction of the water structure is shown in Fig. 2.7a. The intra-molecular O-H is a covalent bond with a distance of 0.1 nm. The inter-

molecular O···H bond has a distance of 0.176 nm, i.e., longer than the 0.1 nm intra-molecular bond but less than 0.26 nm which is sum of the van der Waals radii of oxygen and hydrogen (Israelachvili 2010). This indicates that the inter-molecular O···H bond possesses some weak covalent or quasi-covalent character. Hydrogen bonds play a prominent role in defining water properties since each oxygen atom with its two hydrogen atoms can participate in four such linkages with other water molecules (Fig 2.7 b).

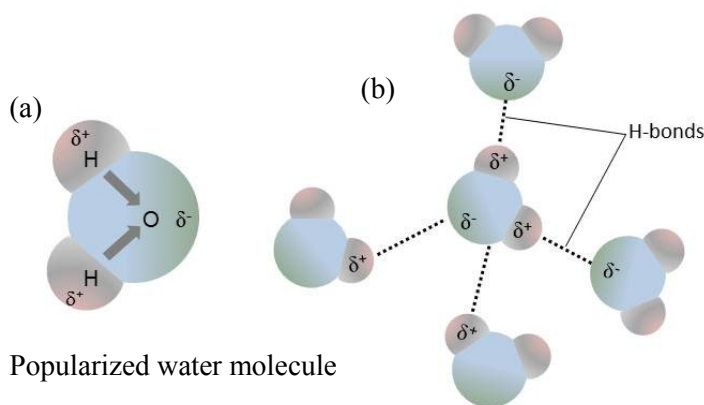


Figure 2.7– A water molecule structure (a) and H-bonding between water molecules (b)

Hydrogen bonds are special in that they only involve hydrogen atoms, which have a tendency to become positively polarized and coupled with their small size can interact strongly with nearby electronegative atoms (e.g., O, N, F, Cl). A hydrogen bond is formed with three atoms: one hydrogen atom and two other electronegative atoms. The hydrogen atom is covalently bonded to one of the electronegative atoms, called the hydrogen bond donor. The other electronegative atom is named the hydrogen bond acceptor. The two electronegative atoms may take up some electron density from the hydrogen atom. As a result, each

electronegative atom carries partial negative charge and the hydrogen atom carries partial positive charge to form predominantly an electrostatic attraction.

Hydrogen bonds are not strong but are somewhat directional which can result in weak three-dimensional short range “structure” (Fig. 2.7b). The strength of the hydrogen bond depends on the donor and acceptor as well as their environment. The strength of most hydrogen bonds lies between 10 to 40 kJ/mole, which makes them stronger than a typical van der Waals ‘bond’ (~ 1kJ/mole) but still much weaker than covalent or ionic bonds (~500 kJ/mole) (Maréchal 2007). Hydrogen bonding also occurs between surfactant molecules and water molecules. The amphiphilic nature of the surfactant structure causes surfactant molecules to orient with the polar part on water side and the hydrocarbon chain in air side of the air-water interface. The oxygen atom(s) in the polar part(s) of the surfactant molecule interacts with neighboring water molecules through hydrogen bonding. The specific inter-molecular interactions between the hydrophilic surfactant head and the closest surrounding water molecules may be the critical factor determining the overall behavior of the adsorption layer at the air/water interface (Ivanova et al. 2005) and is likely to play a decisive role in determining the physical behavior of the system (Chanda and Bandyopadhyay 2006). The formation and breaking of hydrogen bonds in liquid water is responsible for many of its exotic structural and dynamical properties (Chanda and Bandyopadhyay 2006). The dynamics of breaking and forming hydrogen bonds in the air/water interface is faster than in the bulk water (Liu et al. 2005). The surface viscosity reflects this phenomenon. Studies showed that the surface viscosity of long chain

polyethylene glycol alkyl ethers ($\text{CH}_3(\text{CH}_2)_n\text{-OCH}_2\text{CH}_2\text{OH}$, $n = 16, 18, 20, 22$) increased with the increasing n (Katti et al. 1966; Katti and Patil 1968). The increase of surface viscosity increases drag (Nguyen and Schukze 2004).

The regular hydrogen bond network in water alone becomes disrupted in aqueous solutions containing hydrogen bonding solutes. From a thermodynamic point of view the surfactant molecules cause an increase in entropy and enthalpy, which is balanced by the decrease in entropy and enthalpy created by the more oriented structure at the interface than in the solution.

2.2.3 Mass transfer

Mass transfer is the movement of any identifiable species from one spatial location to another. Mass transfer occurs when a concentration gradient/difference exists within a phase. Velocities of single rise bubble are affected by mass transfer to the bubble surface (Leonard and Houghton 1963).

In a surfactant solution when a bubble is formed and released from an orifice, the fresh surface of bubble is essentially free of surfactant. As the bubble rises, surfactant molecules transport to, adsorb and accumulate on the bubble surface, the surface becomes less mobile and the drag force increases. Apart from adsorption/desorption two other rate processes control the surfactant distribution on a rising bubble:

- Diffusion in the continuous phase induced by bulk motion of fluid with different concentrations

- Surface diffusion induced by concentration differences on the bubble interface

(1) Diffusion in the continuous phase induced by bulk motion of fluid

As a bubble rises, surfactant molecules transfer from bulk solution to the bubble surface and gradually accumulate and redistribute on the surface. Molecular diffusion can be described by Fick's First Law:

$$J = -D_{diff} \frac{\partial c}{\partial x} \quad 2.11$$

where D_{diff} is the diffusion coefficient of the solute in the solvent (water in the current case). It is defined as the proportionality constant of the diffusive flux and the negative of the composition gradient ($\partial C/\partial x$). Therefore, the diffusive flux depends on the diffusion coefficient (D_{diff}) and the gradient of concentration with distance.

Since diffusion in liquids involves one molecule in close contact with other molecules, Einstein developed a relationship based on Stokes' law of frictional drag known as the Einstein-Stokes relationship, expressed as (Frenkel 1955):

$$D_{diff} = \frac{k_B T}{3\pi\mu d_{sol}} \quad 2.12$$

Highly viscous solvents (like molasses or glycerin) will have a lower diffusivity than low viscosity solvents (like water) all other factors being equal. In general, large molecules (with large equivalent diameter) will have lower diffusion coefficient than small molecules (Gulliver 2007).

Othmer and Thakar (1953) determined diffusivities of dissolved substances in water and found the following correlation:

$$D_{diff} = \frac{1.4 \times 10^{-4}}{\mu^{1.1} V_b^{0.6}} \quad 2.13$$

Wilke and Chang (1955) developed an empirical relationship based on the temperature and viscosity parameters of the Einstein-Stokes relationship. It incorporates the size of solvent molecules and a parameter for polarized solvents. The relationship is as follows:

$$D_{diff} = 7.4 \times 10^{-8} \frac{T (X M_{solvent})^{1/2}}{\mu V_b^{0.6}} \quad 2.14$$

where V_b is the molar volume of the solute at the boiling point. If the molar volume is unknown, one of two relationships can be used, $V_b = 0.285 V_c^{1.048}$ or $V_b = 0.9 V'_b$ where V_c is the critical volume, i.e., V_b at critical temperature and pressure. The critical volume is given for a number of compounds by Reid et al. (1977). The V'_b is the “LeBas volume” and can be computed using the additive volume increments from the chemical structure (Le Bas 1915).

Hayduk and Laudie (1974) developed a relationship specifically for water as solvent. Based on diffusivities of some 87 different substances in dilute aqueous solutions, they revised the Wilkie-Chang equation and eliminated some of the solvent-specific parameters:

$$D_{diff} = \frac{1.326 \times 10^{-4}}{\mu^{1.14} V_b'^{0.589}} \quad 2.15$$

Taylor dispersion is a commonly used method to measure mutual diffusion coefficients in binary liquid systems (Van de Ven-Lucassen et al. 1995). Diffusion coefficients at infinite dilution in water as a function of temperature are listed in Table 2.1 and Table 2.2 (Yaws 1995). The correlation for diffusion coefficient at infinite dilution in water as a function of temperature is given by the equation:

$$\log_{10} D_A^0 = A + B/T \quad 2.16$$

where A and B are regression coefficients specific to a chemical compound.

Table 2.1 - Diffusion coefficient of 1-alcolhols and 1, n-diols in water with increasing chain length*

| Name | Formula | $\text{Log}_{10} D_A^0 = A+B/T$ (D_A^0 : cm ² /s; T: K) | | | |
|-----------------|---|---|----------|----------|----------|
| | | -A | -B | D_A^0 | |
| | | | | 25 | 100 |
| 1-propanol | C ₃ H ₈ O | 1.7742 | 959.211 | 1.02E-05 | 4.52E-05 |
| 1-butanol | C ₄ H ₁₀ O | 1.6250 | 1006.263 | 1.00E-05 | 4.77E-05 |
| 1-pentanol | C ₅ H ₁₂ O | 1.5090 | 1060.968 | 8.56E-06 | 4.44E-05 |
| 1-hexanol | C ₆ H ₁₄ O | 1.5385 | 1064.866 | 7.76E-06 | 4.05E-05 |
| 1-heptanol | C ₇ H ₁₆ O | 1.5665 | 1068.571 | 7.07E-06 | 3.71E-05 |
| 1-octanol | C ₈ H ₁₈ O | 1.5906 | 1071.754 | 6.53E-06 | 3.45E-05 |
| 1-nonanol | C ₉ H ₂₀ O | 1.6095 | 1074.256 | 6.13E-06 | 3.25E-05 |
| 1,4-butanediol | C ₄ H ₁₀ O ₂ | 1.4922 | 1058.754 | 9.05E-06 | 4.68E-05 |
| 1,5-pentanediol | C ₅ H ₁₂ O ₂ | 1.5252 | 1063.116 | 8.11E-06 | 4.22E-05 |
| 1,6-hexanediol | C ₆ H ₁₄ O ₂ | 1.5531 | 1066.792 | 7.39E-06 | 3.87E-05 |

* All the data adopted from literature: (Yaws 1995)

Table 2.2 - Diffusion coefficient of alcohols in water with changing OH position

| Name | Formula | $\text{Log}_{10} D_A^0 = A+B/T$ (D_A^0 : cm ² /s; T: K) | | | |
|------------|----------------------------------|---|----------|----------|----------|
| | | -A | -B | D_A^0 | |
| | | | | 25°C | 100°C |
| 1-butanol | C ₄ H ₁₀ O | 1.6250 | 1006.263 | 1.00E-05 | 4.77E-05 |
| 2-butanol | | 1.473 | 1056.220 | 9.65E-06 | 4.97E-05 |
| 1-pentanol | C ₅ H ₁₂ O | 1.5090 | 1060.968 | 8.56E-06 | 4.44E-05 |
| 2-pentanol | | 1.5109 | 1061.218 | 8.51E-06 | 4.42E-05 |
| 1-hexanol | C ₆ H ₁₄ O | 1.5385 | 1064.866 | 7.76E-06 | 4.05E-05 |
| 2-hexanol | | 1.5392 | 1064.959 | 7.74E-06 | 4.04E-05 |
| 1-heptanol | C ₇ H ₁₆ O | 1.5665 | 1068.571 | 7.07E-06 | 3.71E-05 |
| 2-heptanol | | 1.5661 | 1068.514 | 7.08E-06 | 3.72E-05 |
| 1-octanol | C ₈ H ₁₈ O | 1.5906 | 1071.754 | 6.53E-06 | 3.45E-05 |
| 2-octanol | | 1.5896 | 1071.625 | 6.55E-06 | 3.46E-05 |
| 1-nonanol | C ₉ H ₂₀ O | 1.6095 | 1074.256 | 6.13E-06 | 3.25E-05 |
| 2-nonanol | | 1.6142 | 1074.868 | 6.04E-06 | 3.20E-05 |

* All the data from literature (Yaws 1995)

Table 2.1 and Table 2.2 show diffusion coefficients for alcohols and 1, n-diols as a function of chain length and position of the hydroxyl group. The trend is that as hydrocarbon chain length increases the diffusion coefficient decreases whether at 25 °C or 100 °C (Table 2.1). The effect of hydroxyl position on the diffusion coefficient is minor (Table 2.2). Funazukuri and Nishio (1999) studied binary diffusion coefficients of five-carbon isomers in dilute water solution and found that diffusion coefficient of isomers increase with the boiling point.

(2) Diffusion at the interface

The rate of adsorption is controlled by the rates of diffusion of solute through the surface films of gas and liquid at the gas-liquid boundary. The volumetric mass transfer coefficient ($K_{L\alpha}$) is a parameter to describe the film on the gas side of an air-water interface. At ambient temperature and pressure, gas-phase diffusion coefficients are of the order of $10^{-5} \sim 10^{-6}$ m²/s (Rousseau 1987).

The non-uniform surfactant distribution on the surface resulting from the motion of liquid over the surface means mass transfer is maximal at the front of a moving bubble and decreases along the bubble surface toward the rear.

An important factor determining surface mobility is bubble size. Gas bubbles of diameter smaller than 0.3 mm in water behave as rigid spheres regardless of presence of surfactant and above this diameter a toroidal circulation sets in, which persists throughout the rise (Garner and Hammerton 1954). For the liquid-side mass transfer coefficient for a rigid bubble surface (bubble diameter < 0.3 mm), two correlations are considered, one proposed by Frössling (Frössling 1938) and the other by Calderbank and Moo-Young (1961).

$$\text{Frössling equation: } K_L^{rigid} = \frac{D}{d_B} (2 + 0.6R_e^{1/2} S_c^{1/3}) \quad 2.17$$

$$\text{Calderbank Moo-Young equation: } K_L^{rigid} = 0.31(g\mu_L/\rho_L)^{1/3} S_c^{-2/3} \quad 2.18$$

There are empirical and theoretical correlations for determining K_L for bubble diameters greater than 3.5 mm with mobile bubble surface. The correlations of Higbie (1935) and Calderbank and Moo-Young (1961) are probably the most often employed.

$$\text{Higbie equation: } k_L = 2 \sqrt{\frac{D}{\pi t_e}} \quad 2.19$$

$$\text{Calderbank and Moo-Young: } k_L = 0.42 \left(\frac{\rho_L - \rho_G}{\rho^2} \mu_L g \right)^{1/3} S_c^{-1/2} \quad 2.20$$

Gas-liquid mass transfer between a bubble and surrounding liquid depends upon overall surface mobility, which is affected by surfactants. For the stagnant cap model, it is assumed that a moving bubble surface consists of two parts: a totally mobile upper part and a rigid lower part. The upper value of mass transfer coefficient of an air bubble with a totally mobile surface is expressed as:

$$K_L^{mobile} = 2\sqrt{\frac{D}{\pi t_e}} = 1.13\sqrt{\frac{u}{d}}D^{1/2} \quad 2.21$$

The value of mass transfer coefficient for a totally rigid bubble surface may be predicted using an equation proposed by Frössling using laminar boundary layer theory with $C = 0.6$:

$$K_L^{rigid} = C\sqrt{\frac{u}{d}}D^{2/3}\nu^{-1/6} \quad 2.22$$

If a bubble of relatively constant diameter is introduced in a liquid medium with a finite surface-active contamination concentration, the mass transfer coefficient should decrease with time as surfactant is adsorbed from the liquid bulk.

Based on aliphatic alcohols, Raymond and Zieminski (1971) have shown that the concentration, molecule size and structure have a pronounced effect on mass transfer as well as the drag coefficient of the rising bubble. The overall mass transfer coefficients are defined as follows for both straight chain alcohols and their isomers:

$$k_L = -0.126C_d + 0.1120 \text{ (straight chain length alcohols)} \quad 2.23$$

$$k_L = -0.089C_d + 0.0903 \quad (\text{alcohol isomers}) \quad 2.24$$

There is a small but significant difference between these relationships that suggests the relationship is not independent of molecule structure. As noted by Laskowski (1993), frother mass transfer rates are related to structure. Factors such as the length of the hydrophobic chain or introducing a branch changes the mass transfer rate and alters packing of the surfactant molecules at the interface. As a note, bubble size needs to be accounted for when measuring mass transfer as small bubbles spend a longer time in the experimental apparatus than large bubbles due to lower rise velocity, and thus are subject to larger contamination periods.

2.3 Bubble rise velocity

2.3.1 Bubble size and bubble shape

For a single bubble generated at a submerged capillary at sufficiently low gas rate, the size of the released bubble can be estimated by the force balance between upward buoyancy and surface tension, known as Tate's law, which is applied for spherical bubbles:

$$d = 2\left(\frac{3r\sigma\cos\theta}{2\Delta\rho g}\right)^{1/3} \quad 2.25$$

It is usually assumed that the capillary material is well wetted and θ is zero (i.e. $\cos\theta = 1$).

In reality, bubbles have variable shapes (e.g., from spherical to ellipsoidal),

depending on the size of the orifice, conditions of generation and the presence of surfactant (or other solutes such as high concentrations of inorganic salts). Small bubbles (diameter < 1.5 mm) tend to be spherical. In the case of non-spherical bubbles, a bubble volume equivalent spherical diameter (d_{eq}) is usually calculated, assuming axial symmetry over the direction of movement (Raymond and Zieminski 1971; Sam et al. 1996; Hernandez-Aguilar et al. 2004; Alves et al. 2005; Kracht and Finch 2010):

$$d_{eq} = [2a \times (2b)^2]^{1/3} \quad 2.26$$

where a and b are minor and major radii of the ellipsoidal bubble, respectively.

The shape of ellipsoidal bubbles can be characterized by the aspect ratio (AR), the ratio of major to minor axis (or the ratio of minor to major axis) obtained from an image. The closer the AR to 1, the more spherical is the bubble.

2.3.2 Single bubble rise velocity

Two velocities are needed to describe the rising bubble: local velocity and terminal velocity.

2.3.2.1 Local velocity

Local velocity is determined as a function of distance/time from the point of bubble formation. The plot of local velocity vs. distance (or time) is the velocity profile or ‘time-history’. Sam (1995), using a video camera mounted on an adjustable speed platform, was the first to study single bubble velocity profile in frother solutions. The general pattern of the velocity profile was found to display three regions (Fig. 2.8) (Sam 1995): an initial rapid increase in velocity (acceleration) to reach a maximum followed by the rise velocity slowing (deceleration) as

surfactant accumulates and increases drag, and, given sufficient distance (time), the third region is reached where velocity becomes constant, i.e., terminal velocity is reached. The velocity profile reflects the surfactant adsorption density distribution on the rising bubble surface and how it changes with time.

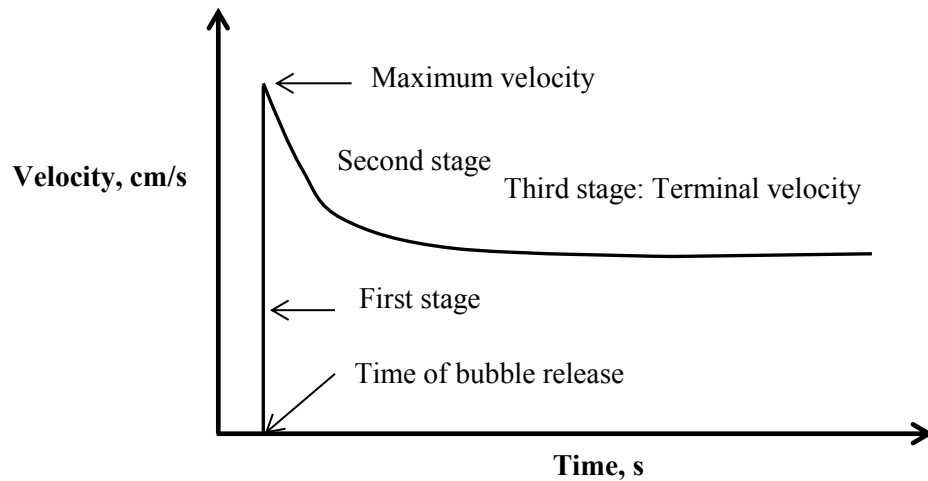


Figure 2.8 – Single bubble velocity profile (Sam 1995)

Sam et al. (1996) noted that there was a strong dependence of the profile on surfactant type and concentration but found that terminal velocity (provide it was reached) was independent of concentration and only weakly dependent on frother type. Rafiei et al. (2009) confirmed these observations.

2.3.2.2 Terminal velocity

Single bubble terminal velocity is of fundamental importance in gas/liquid phase flow theory. It is associated with the constant velocity region in the velocity profile. Many equations to predict bubble terminal velocity have been proposed.

For a small bubble ($<1\text{mm}$, $\text{Re} \ll 1$) with immobile surface rising in a viscous liquid, Stokes' law applies:

$$U_{st} = \frac{2R_b^2 \Delta \rho g}{9\mu} \quad 2.27$$

The velocity of a rising bubble with a mobile surface was investigated by Hadamard and Rybczynski (as discussed by Aybers and Tapucu, 1969). They considered that the tangential stress induces vorticity within the sphere, resulting in the dissipation of energy in the dispersed medium as well as in the continuous phase. Under these conditions the terminal velocity is expressed as:

$$U_{H-R} = \frac{2R_b^2 \Delta \rho g}{3\mu} \frac{\mu + \mu'}{2\mu + 3\mu'} \quad 2.28$$

where μ' is the internal viscosity of the bubble and μ the viscosity of the liquid medium. When the internal viscosity is insignificant (i.e., $\mu' \ll \mu$) the mobile surface should be incapable of supporting any tangential stress, in which case Eq 2.28 becomes:

$$U_{H-R} = \frac{R_b^2 \Delta \rho g}{3\mu} = \frac{3}{2} U_{st} \quad 2.29$$

It can be seen in the Hadamard–Rybczynski theory, due to the fluidity of the bubble interface and internal circulation within the bubble, that the velocity is 50% higher than predicted by Stokes' law for a rigid sphere of the same dimensions and fluid properties.

If a high viscosity thin liquid layer is considered to exist near the fluid-liquid interface, the terminal velocity is predicted by Boussinesq's equation where the Boussinesq number (Bou) is a dimensionless group that represents the ratio of interfacial to bulk viscous forces:

$$U = \frac{2R_b^2 \Delta \rho g}{9\mu} \frac{3+2B_{ou}}{2+2B_{ou}} \quad 2.30$$

There are also many semi-empirical and empirical equations proposed to predict bubble rise velocity. In general, there is no single equation that can describe the bubble rise velocity for the entire range of Reynolds number. It is common for $Re < 130$ to take C_d corresponding to that given by the “standard drag curve” (Clift et al., 1978). For $Re > 130$ the $C_d = 0.95$ approximation can be used (Karamanev, 1996). A general model, modified by Sawi for surfactant-contaminated solutions, is used by Karamanev (1996):

$$U_T = \sqrt{\frac{4g\Delta\rho d_{eq}}{3\rho C_d}} \quad 2.31$$

By substituting $C_d = 0.95$ one of the simplest models is achieved:

$$U_T = 37.1\sqrt{d_{eq}} \quad 2.32$$

From this equation it can be seen that in the $Re > 130$ region, terminal velocity is dependent only on bubble size. A good fit between the predicted terminal velocity using Eq. 2.32 and experiment was observed by Zhang et al (2003).

The mass transfer from bulk solution to the bubble surface depends on bubble Reynolds number (Re) and the state of the bubble surface. Clift et al. (1978) reviewed work on mass transfer for mobile bubbles and rigid spheres. At high Re , the thin concentration boundary layer approximation is valid and the mass transfer from bulk solution to a spherical surface has been solved numerically from boundary layer theory.

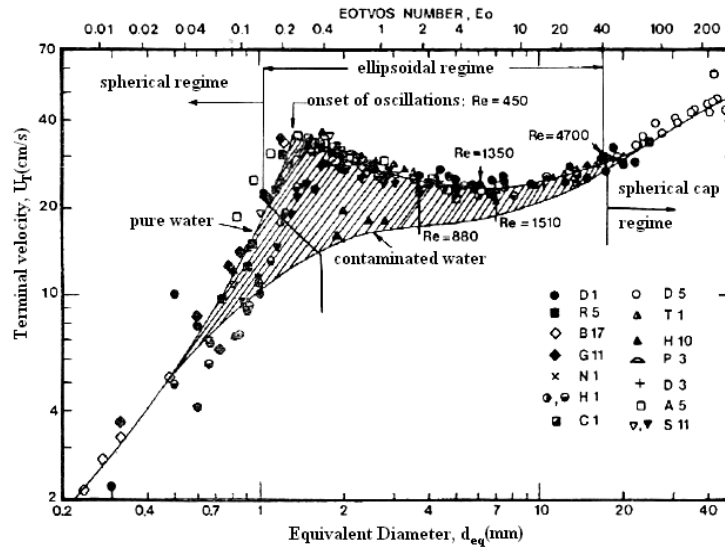


Figure 2.9 – Terminal velocity of air bubbles at 20 °C (Clift et al. 1978)

2.3.3 Relation of bubble shape and rise velocity

A qualitative correlation of bubble shape and motion as a function of bubble size or Reynolds number was put forward by Ayber and Tapucu (1969), as shown in Table 2.3.

Table 2.3 - Bubble size and motion in various Reynolds number region (Aybers and Tapucu 1969)

| d_{eq} (cm) | Re | Bubble shape and motion |
|--------------------------|--------------------|---|
| <0.04 | $Re < 70$ | spherical bubbles, rectilinear |
| $0.04 < d_{eq} < 0.062$ | $70 < Re < 400$ | spherical bubbles, rectilinear |
| $0.062 < d_{eq} < 0.077$ | $400 < Re < 500$ | oblate spheroid, rectilinear |
| $0.077 < d_{eq} < 0.24$ | $500 < Re < 1100$ | oblate spheroid, helical |
| $0.24 < d_{eq} < 0.35$ | $1100 < Re < 1600$ | Irregular oblate spheroid; almost rectilinear |
| $0.35 < d_{eq} < 0.88$ | $1600 < Re < 5000$ | transition from oblate spheroid to spherical caps; almost rectilinear |
| $0.88 < d_{eq}$ | $Re > 5000$ | spherical caps, rectilinear |

Sam et al. (1996) noted that bubble shape changed in the presence of frother as the bubble rose and slowed down. Tomiyama et al. (2002) concluded that bubble shape and velocity are related based on experiments in clean (distilled) water and

water with surfactants. A corollary is that velocity is sensitive to the initial shape generated. Wu and Gharib (2002) noted this shape-velocity dependence, finding that spherical bubbles move significantly slower than ellipsoidal ones of equivalent volume with or without surfactants. Krzan et al. (2004) noted the presence of surfactant made the bubble more spherical and decreased the rise velocity compared to clean water. Kracht and Finch (2010) reported a relationship between single bubble velocity and bubble shape (AR, ratio of major and minor diameters) for a variety of frothers (and salt, NaCl). The relationship for two alcohols and two commercial polyglycols is shown in Fig. 2.10. The figure confirms a strong relationship between shape and bubble rise velocity. the more spherical the bubble, the slower it rises in agreement with the work of Wu and Gharib (2002). Maldonado et al. (2013) showed a unique relationship between bubble shape (in this case ratio of minor to major diameters) and rise velocity, which is independent of solute type or concentration (Fig. 2.11). The shape-velocity relationship represents a possible property for the study of the frother structure-property link.

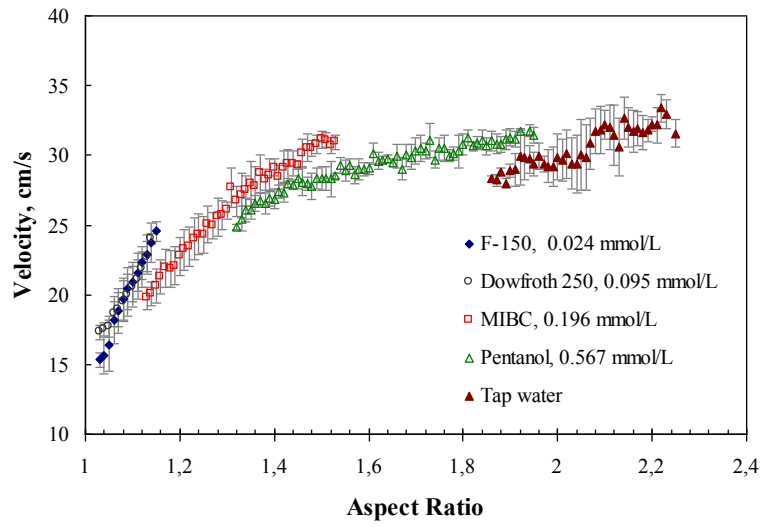


Figure 2.10 – Velocity and aspect ratio for maximum concentration test (Kracht and Finch 2010)

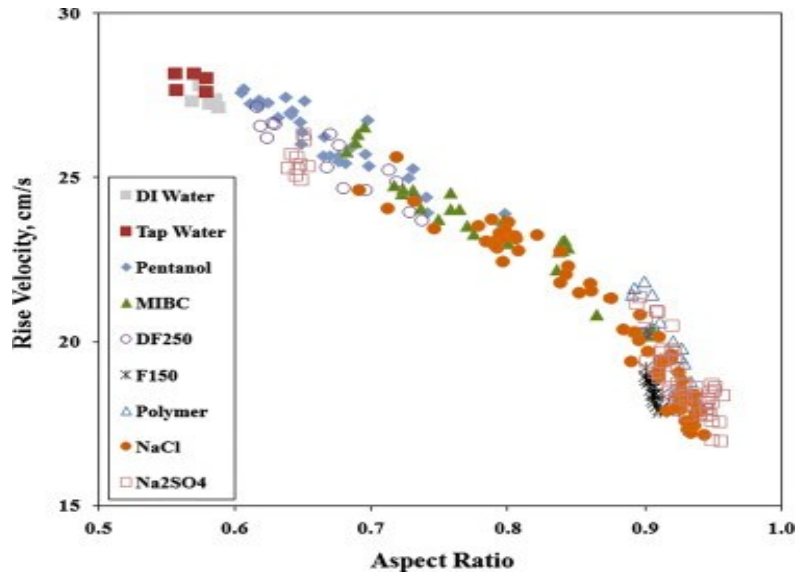


Figure 2.11 – Bubble velocity and aspect ratio for water, frothers, polymer and inorganic salts (Maldonado et al. 2013)

References

- Addison, C. C. (1945). The properties of freshly formed surfaces. Part IV. The influence of chain length and structure on the static and the dynamic surface tensions of aqueousalcoholic solutions. *Journal of the Chemical Society (Resumed)*: 26: 98-106.
- Alves, S. S., Orvalho, S. P. and Vasconcelos, J. M. T. (2005). Effect of bubble contamination on rise velocity and mass transfer. *Chemical Engineering Science* 60(1): 1-9.
- Aybers, N. M. and Tapucu, A. (1969). The motion of gas bubbles rising through stagnant liquid. *Heat and Mass Transfer* 2(2): 118-128.
- Bleys, G. and Joos, P. (1985). Adsorption kinetics of bolaform surfactants at the air/water interface. *The Journal of Physical Chemistry* 89(6): 1027-1032.
- Boucher, E. A., Grinchuk, T. M. and Zettlemyer, A. C. (1967). Measurement of surface tensions of surfactant solutions. *Journal of Colloid and Interface Science* 23(4): 600-603.
- Brown, L., Narsimhan, G. and Wankat, P. C. (1990). Foam fractionation of globular proteins. *Biotechnology and Bioengineering* 36(9): 947-959.
- Calderbank, P. H. and Moo-Young, M. B. (1961). The continuous phase heat and mass-transfer properties of dispersions. *Chemical Engineering Science* 16(1-2): 39-54.
- Chanda, J. and Bandyopadhyay, S. (2006). Hydrogen Bond Lifetime Dynamics at

the Interface of a Surfactant Monolayer. *The Journal of Physical Chemistry B* 110(46): 23443-23449.

Chang, C. H. and Franses, E. I. (1995). Adsorption dynamics of surfactants at the air/water interface: a critical review of mathematical models, data, and mechanisms. *Colloids and Surfaces A: Physicochemical and Engineering Aspects* 100(0): 1-45.

Chang, C. H. and Franses, E. I. (1992). Modified Langmuir—Hinselwood kinetics for dynamic adsorption of surfactants at the air/water interface. *Colloids and Surfaces* 69(2–3): 189-201.

Clift, R., Grace, J. R. and Weber, M. E. (1978). *Bubbles, drops, and particles*. Montreal, Academic Press.

Coltharp, K. A. and Franses, E. I. (1996). Equilibrium and dynamic surface tension behavior of aqueous soaps: sodium octanoate and sodium dodecanoate (sodium laurate). *Colloids and Surfaces A: Physicochemical and Engineering Aspects* 108(2–3): 225-242.

Danov, K. D., Kralchevsky, P. A., Ananthapadmanabhan, K. P. and Lips, A. (2006). Interpretation of surface-tension isotherms of n-alkanoic (fatty) acids by means of the van der Waals model. *Journal of Colloid and Interface Science* 300(2): 809-813.

Defay, R. and Hommelen, J. R. (1958). I. Measurement of dynamic surface tensions of aqueous solutions by the oscillating jet method. *Journal of*

Colloid Science 13(6): 553-564.

de Nevers, N. (2012). Minimization of Gibbs Energy. Physical and Chemical Equilibrium for Chemical Engineers, John Wiley & Sons, Inc.: 49-60.

Defay, R. I., Prigogine, A. B. and Everett, D. H. (1966). Surface tension and adsorption. London, Longmans.

Dukhin, S. S., Kretzschmar, G. and Miller, R. (1995). Dynamics of Adsorption at Liquid Interfaces: Theory, Experiment, Application, Elsevier Science.

Erbil, H. Y. (2009). Liquid Solution Surfaces. Surface Chemistry, Blackwell Publishing Ltd.: 156-222.

Frenkel, J. A. (1955). Kinetic theory of liquids. New York, Dover Publications.

Frössling, N. (1938). Über die verdunstung fallenden tropfen, (Evaporation of falling drops). Gerlands Beitäge zur Geophysik 52: 170-216 (cited in Griffith, 1962).

Frumkin, A. (1925). Zeitschrift für Physikalische Chemie. 116: 466.

Frumkin, A and Levich V.G (1947). On surfactants and interfacial motion. Zh. Fiz. Khim. 21, 1183–1204.

Funazukuri, T. and Nishio, M. (1999). Infinite Dilution Binary Diffusion Coefficients of C5-Monoalcohols in Water in the Temperature Range from 273.2 K to 353.2 K at 0.1 MPa. Journal of Chemical & Engineering Data 44(1): 73-76.

- Furlong, D. N. and Hartland, S. (1979). Wall effect in the determination of surface tension using a wilhelmy plate. *Journal of Colloid and Interface Science* 71(2): 301-315.
- Garner, F. H. and Hammerton, D. (1954). Circulation inside gas bubbles. *Chemical Engineering Science* 3(1): 1-11.
- Gibbs, J. W. (1906). *The Scientific Papers of J. Williard Gibbs*. London, Longmans Green.
- Girault, H. H. J., Schiffrin, D. J. and Smith, B. D. V. (1984). The measurement of interfacial tension of pendant drops using a video image profile digitizer. *Journal of Colloid and Interface Science* 101(1): 257-266.
- Gulliver, J. S. (2007). *Introduction to Chemical Transport in the Environment*. Cambridge, Cambridge University.
- Hansen, R. S., Purchase, M. E. Wallace, T. C. and Woody, R. W. (1958). Extension of the vibrating jet method for surface tension measurement to jets of non-uniform velocity profiles. *Journal of Physical Chemistry* 62(2): 210-214.
- Hansen, R. S. and Wallace, T. C. (1959). The kinetics of adsorption of organic acids at the water-air interface. *Journal of Physical Chemistry* 63(7): 1085-1091.
- Harkins, W. D. and Brown, F. E. (1919). The determination of surface tension (free surface energy), and the weight of falling drops: The surface tension

of water and benzene by the capillary height method. *The Journal of the American Chemical Society* 41(4): 499-524.

Hayduk, W. and Laudie, H. (1974). Prediction of diffusion coefficients for nonelectrolytes in dilute aqueous solutions. *AIChE Journal* 20(3): 611-615.

Hernandez-Aguilar, J. R., Coleman, R. G., Gomez, C. O. and Finch, J. A. (2004). A comparison between capillary and imaging techniques for sizing bubbles in flotation systems. *Minerals Engineering* 17(1): 53-61.

Higbie, R. (1935). The rate of absorption of a pure gas into a still liquid during short periods of exposure. *Transactions of the American Institution of Chemical Engineers* 31: 365-389.

Holmberg, K., Jönsson, B., Kronberg, B. and Lindman, B. (2003). Introduction to Surfactants. *Surfactants and Polymers in Aqueous Solution*, John Wiley & Sons, Ltd: 1-37.

Horozov, T. S., Dushkin, C. D., Danov, K. D., Arnaudov, L. N., Velev, O. D., Mehreteab, A. and Broze, G. (1996). Effect of the surface expansion and wettability of the capillary on the dynamic surface tension measured by the maximum bubble pressure method. *Colloids and Surfaces A: Physicochemical and Engineering Aspects* 113(1-2): 117-126.

Israelachvili, J. N. (1991). *Intermolecular and surface forces*. London, Academic Press.

Israelachvili, J. N. (2010). *Intermolecular and Surface Forces (3rd Edition)*. Saint

Louis, MO, USA, Elsevier Science & Technology.

Ivanova, A., Tadjer, A. Tyutyulkov, N. and Radoev, B. (2005). Hydrophilic Interactions between Organic and Water Molecules as Models for Monolayers at the Gas/Water Interface. *The Journal of Physical Chemistry A* 109(8): 1692-1702.

Joos, P. and Serrien, G. (1989). Adsorption kinetics of lower alkanols at the air/water interface: Effect of structure makers and structure breakers. *Journal of Colloid and Interface Science* 127(1): 97-103.

Karamanev, D. G. (1996). Equations for calculation of the terminal velocity and drag coefficient of solid spheres and gas bubble. *Chemical Engineering Communications* 147(1): 75-84.

Katti, S. S., Kulkarni, S. B., Gharpurey, M. K. and Biswas, A. B. (1966). Surface viscosity of monomolecular films of n-long chain alcohols and n-alkoxy ethanols. *Journal of Colloid and Interface Science* 22(3): 207-213.

Katti, S. S. and Patil, G. S. (1968). Surface viscosity of monomolecular films of n-alkoxy ethanols at various temperatures and pressures. *Journal of Colloid and Interface Science* 28(2): 227-239.

Knoche, M., Tamura, H. and Bukovac, M. J. (1991). Performance and stability of the organosilicone surfactant L-77: Effect of pH, concentration, and temperature. *Journal of Agricultural and Food Chemistry* 39(1): 202-206.

Kracht, W. and Finch, J. A. (2010). Effect of frother on initial bubble shape and

- velocity. *International Journal of Mineral Processing* 94(3-4): 115-120.
- Krzan, M., Lunkenheimer, K. and Malysa, K. (2004). On the influence of the surfactant's polar group on the local and terminal velocities of bubbles. *Colloids and Surfaces A: Physicochemical and Engineering Aspects* 250(1-3): 431-441.
- Lane, J. E. (1973). Correction terms for calculating surface tension from capillary rise. *Journal of Colloid and Interface Science* 42(1): 145-149.
- Laskowski, J. S. (1993). Frothers and Flotation Froth. *Mineral Processing and Extractive Metallurgy Review: An International Journal* 12(1): 61-89.
- Le Bas, G. (1915). *The molecular volumes of liquid chemical compounds*. New York, Longmans Green.
- Legros, J. C. (1986). Problems related to non-linear variations of surface tension. *Acta Astronautica* 13(11-12): 697-703.
- Leja, J. (1982). *Surface chemistry of froth flotation*, Plenum Press.
- Lenghor, N., Staggemeier, B. A., Hamad, M. L., Udnan, Y., Tanikkul, S., Jakmune, J., Grudpan, K., Prazen, B. J. and Synovec, R. E. (2005). A dynamic liquid-liquid interfacial pressure detector for the rapid analysis of surfactants in a flowing organic liquid. *Talanta* 65(3): 722-729.
- Leonard, J. H. and Houghton, G. (1963). Mass transfer and velocity of rise phenomena for single bubbles. *Chemical Engineering Science* 18(2): 133-142.

- Lin, S. Y., McKeigue, K. and Maldarelli, C. (1991). Diffusion-limited interpretation of the induction period in the relaxation in surface tension due to the adsorption of straight chain, small polar group surfactants: theory and experiment. *Langmuir* 7(6): 1055-1066.
- Liu, Q., Dong, M., Ma, S. and Tu, Y. (2007). Surfactant enhanced alkaline flooding for Western Canadian heavy oil recovery. *Colloids and Surfaces A: Physicochemical and Engineering Aspects* 293(1–3): 63-71.
- Liu, P., Harder, E. and Berne, B. J. (2005). Hydrogen-Bond Dynamics in the Air–Water Interface. *The Journal of Physical Chemistry B* 109(7): 2949-2955.
- Löfgren, H., Neuman, R. D., Scriven, L. E. and Davis, H. T. (1984). Laser light-scattering measurements of interfacial tension using optical heterodyne mixing spectroscopy. *Journal of Colloid and Interface Science* 98(1): 175-183.
- MacLeod, C. A. and Radke, C. J. (1993). A Growing Drop Technique for Measuring Dynamic Interfacial Tension. *Journal of Colloid and Interface Science* 160(2): 435-448.
- Maldonado, M., Quinn, J. J., Gomez, C. O. and Finch, J. A. (2013). An experimental study examining the relationship between bubble shape and rise velocity. *Chemical Engineering Science* 98(0): 7-11.
- Mankowich, A. M. (1967). Capabilities of the du noüy tensiometer. *Journal of*

Colloid and Interface Science 25(4): 590.

Maréchal, Y. (2007). 1 - The Hydrogen Bond: Formation, Thermodynamic Properties, Classification. *The Hydrogen Bond and the Water Molecule*. Amsterdam, Elsevier: 3-24.

Martin, J. D. and Velankar, S. S. (2008). Unusual behavior of PEG/PPG/Pluronic interfaces studied by a spinning drop tensiometer. *Journal of Colloid and Interface Science* 322(2): 669-674.

Miller, R. and Lunkenheimer, K. (1986). Adsorption kinetics measurements of some nonionic surfactants. *Colloid & Polymer Science* 264(4): 357-361.

Notter, R. H. and Finkelstein, J. N. (1984). Pulmonary surfactant: An interdisciplinary approach. *Journal of Applied Physiology Respiratory Environmental and Exercise Physiology* 57(6): 1613-1624.

Notter, R. H. and Morrow, P. E. (1975). Pulmonary surfactant: A surface chemistry viewpoint. *Annals of Biomedical Engineering* 3(2): 119-159.

Nguyen, A. V. and Schulze H. J. (2004), *Colloidal Science of Flotation*. Surfactant Science Series, vol. 118 Marcel Dekker, New York.

Othmer, D. F. and Thakar, M. S. (1953). Correlating Diffusion Coefficient in Liquids. *Industrial & Engineering Chemistry* 45(3): 589-593.

Padday, J. F. and Russell, D. R. (1960). The measurement of the surface tension of pure liquids and solutions. *Journal of Colloid Science* 15(6): 503-511.

- Patil, G. S., Katti, S. S. and Biswas, A. B. (1967). Surface viscosity of monomolecular films of n-long chain alcohols at various temperatures and pressures. *Journal of Colloid and Interface Science* 25(4): 462-481.
- Pike, F. P. and Bonnet, J. C. (1970). The end-correction in the Wilhelmy technique for surface tension measurements. *Journal of Colloid and Interface Science* 34(4): 597-605.
- Rafiei, A. A. M. (2009). Effects of frother type on single bubble rise velocity. M. Eng, Thesis, McGill University.
- Raymond, D. R. and Zieminski, S. A. (1971). Mass transfer and drag coefficients of bubbles rising in dilute aqueous solutions. *AIChE Journal* 17(1): 57-65.
- Reid, R., Poling, B. E. and Prausnitz, J. M. (1977). *The Properties of Gases and Liquids*. New York, McGraw-Hill.
- Rosen, M. J. and Hua, X. Y. (1990). Dynamic surface tension of aqueous surfactant solutions: 2. Parameters at 1s and at mesoequilibrium. *Journal of Colloid and Interface Science* 139(2): 397-407.
- Rosen, M. J. and Kunjappu, J. T. (2012). *Micelle Formation by Surfactants. Surfactants and Interfacial Phenomena*, John Wiley & Sons, Inc.: 123-201.
- Rousseau, R. W. (1987). *Handbook of Separation Process Technology*, John Wiley & Sons: 75-76.
- Sam, A. (1995). Single bubble behaviour study in a flotation column. Ph. D dissertation, McGill University.

- Sam, A., Gomez, C. O. and Finch, J. A. (1996). Axial velocity profiles of single bubbles in water/frother solutions. *International Journal of Mineral Processing* 47(3-4): 177-196.
- Scriven, L. E. (1960). Dynamics of a fluid interface Equation of motion for Newtonian surface fluids. *Chemical Engineering Science* 12(2): 98-108.
- Tomiyama, A., Celata, G. P., Hosokawa, S., and Yoshida, S. (2002). Terminal velocity of single bubbles in surface tension force dominant regime. *International Journal of Multiphase Flow* 28(9): 1497-1519.
- Tornberg, E. (1978). The application of the drop volume technique to measurements of the adsorption of proteins at interfaces. *Journal of Colloid and Interface Science* 64(3): 391-402.
- Traube, J. (1891). Ueber die Capillaritätsconstanten organischer Stoffe in wässrigen Lösungen. *Justus Liebigs Annalen der Chemie* 265(1): 27-55.
- Ueno, M., Takasawa, Y., Miyashige, H., Tabata, Y. and Meguro, K. (1981). Effects of alkyl chain length on surface and micellar properties of octaethyleneglycol-n alkyl ethers. *Colloid & Polymer Science* 259(7): 761-766.
- Valentini, J. E., Thomas, W. R., Sevenhuysen, P., Jiang, T. S., Lee, H. O., Liu, Y., and Yen, S. C. (1991). Role of dynamic surface tension in slide coating. *Industrial & Engineering Chemistry Research* 30(3): 453-461.
- Van de Ven-Lucassen, I. M. J. J., Kieviet F. G. and Kerkhof, P. J. A. M. (1995).

- Fast and Convenient Implementation of the Taylor Dispersion Method. *Journal of Chemical & Engineering Data* 40(2): 407-411.
- Van Den Bogaert, R. and Joos, P. (1979). Dynamic surface tensions of sodium myristate solutions. *Journal of Physical Chemistry* 83(17): 2244-2248.
- Vasconcelos, J. M. T., Orvalho, S. P. and Alves, S. S. (2002). Gas-liquid mass transfer to single bubbles: Effect of surface contamination. *AIChE Journal* 48(6): 1145-1154.
- Viades-Trejo, J. and Gracia-Fadrique, J. (2007). Spinning drop method: From Young-Laplace to Vonnegut. *Colloids and Surfaces A: Physicochemical and Engineering Aspects* 302(1-3): 549-552.
- Vochten, R. and Petre, G. (1973). Study of the heat of reversible adsorption at the air-solution interface. II. Experimental determination of the heat of reversible adsorption of some alcohols. *Journal of Colloid and Interface Science* 42(2): 320-327.
- Warszyński, P., Jachimska, B. and Małyśa, K. (1996). Experimental evidence of the existence of non-equilibrium coverages over the surface of the floating bubble. *Colloids and Surfaces A: Physicochemical and Engineering Aspects* 108(2-3): 321-325.
- Wilke, C. R. and Chang, P. (1955). Correlation of diffusion coefficients in dilute solutions. *AIChE Journal* 1(2): 264-270.
- Wu, M. and Gharib, M. (2002). Experimental studies on the shape and path of

small air bubbles rising in clean water. *Physics of Fluids* 14(7): L49-L52.

Yaws, C. L. (1995). *Handbook of Transport Property Data*. Houston, London, Paris, Zurich, Tokyo, Gulf Publishing Company.

Yoon, R.-H. and Ravishankar, S. A. (1996). Long-Range Hydrophobic Forces between Mica Surfaces in Dodecylammonium Chloride Solutions in the Presence of Dodecanol. *Journal of Colloid and Interface Science* 179(2): 391-402.

Zhang, J., Yoon, R.-H. and Eriksson, J. C. (2007). AFM surface force measurements conducted with silica in CnTACl solutions: Effect of chain length on hydrophobic force. *Colloids and Surfaces A: Physicochemical and Engineering Aspects* 300(3): 335-345.

Zhang, Y., Sam, A. and Finch, J. A. (2003). Temperature effect on single bubble velocity profile in water and surfactant solution. *Colloids and Surfaces A: Physicochemical and Engineering Aspects* 223(1-3): 45-54.

Chapter 3 – Experimental Part

3.1 Equipment

3.1.1 Single bubble column setup

The setup used to determine the velocity as a function of distance, i.e., velocity profile, is shown in Fig. 3.1. It comprises a circular Plexiglas column 6.35 cm diameter by 350 cm high (20 liter capacity) surrounded by a square Plexiglas water jacket (8×8×350 cm). The water jacket maintains a uniform temperature (at $23\pm 1^\circ\text{C}$) and, being square, eliminates the optical distortion associated with curved surfaces. An overflow outlet was positioned at the 350 cm level to give reproducible water height (i.e., hydrostatic pressure) above the bubble generating capillary. A measuring tape was placed along the central axis of the column to locate the position of the bubble. A glass capillary with nominal internal diameter 51 μm was used to generate bubbles using dry air delivered from a compressor. Two measurements of bubble size made at right angles near the capillary were corrected to conditions at the 350 cm level (top of water column) giving a mean value 1.45 ± 0.061 mm diameter (standard deviation based on 30 measurements). A 1.45 mm size bubble is in a range sensitive to surfactant addition (Clift et al. 1978) and is relevant to the size of bubbles in flotation systems (0.5~2.5 mm) (Finch and Dobby 1990). The 20-liter test solution was prepared with Montréal tap water (Remillard et al. 2009).

Air was provided from the McGill compressed air system with flow rate adjusted by an online monitoring system. A minimum input gas rate to just generate a bubble was applied, which respected the bubble frequency of < 80 bubbles per minute recommended by Sam et al. (1996).

3.1.2 Camera moving device

A digital video camera (CCD Canon GL2, 30 frames/s) mounted on a stage on a chain controlled by a variable speed motor was driven manually to track a single bubble during its rise. Limit speed sensors were placed at the bottom and the top track to arrest the movement.

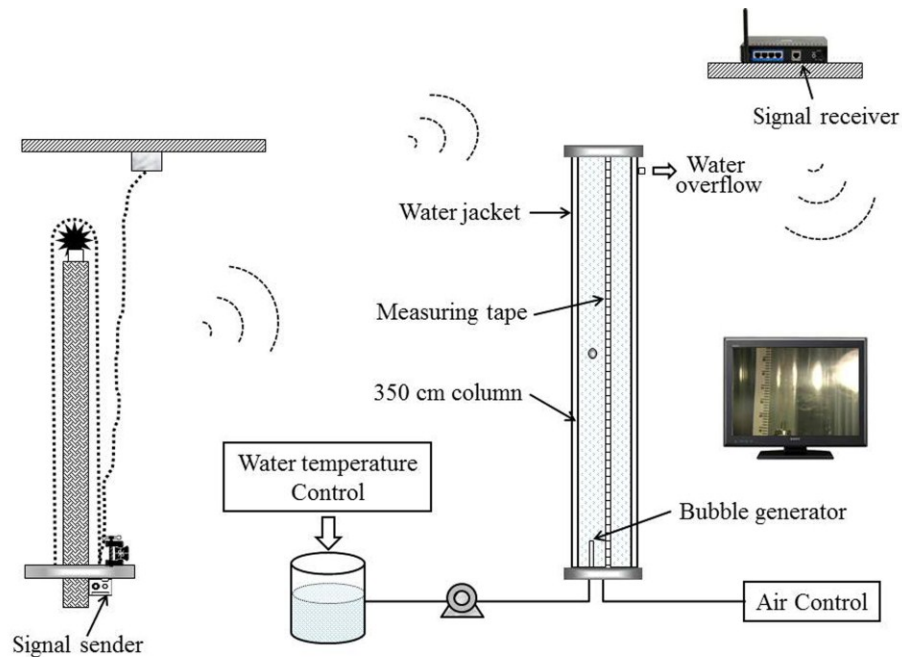


Figure 3.1 – The experimental setup for single bubble rise velocity

3.2 Procedure

The experiment was initiated by activating the camera at the moment a bubble released from the capillary and the experimenter adjusted speed to maintain the bubble in the field of view. The images were continuously displayed on the monitor (Sony PVM-1340) through a signal sender and receiver set (Radio Shack 15-2572). After recording, the images were processed offline to give position and from sequential images, the local velocity. All results were entered into a database developed using Microsoft Excel to calculate the local rise velocity profile.

3.3 Reagents

Reagents from two prime families, alcohols (Table 3.1) and polyglycols (Table 3.2) were used. Table 3.1 lists the 1-alcohols and 1, 2-diols (two hydroxyl groups at one end, i.e., the 1, 2 positions) in the effect of alkyl chain length study. Table 3.2 lists the polyglycols used for both the alkyl chain and PO/EO unit chain length studies. Table 3.3 gives the five-carbon and six-carbon alcohols and diols isomers used for the methyl branch and hydroxyl position studies. The surfactants represent those that are readily available ($n = 2$ PPGAE is not, for example), and can be safely disposed.

Table 3.1 - Alcohols for chain length study

| Frother family | Chemical structure | n |
|----------------|---|-----|
| Alcohols | $\begin{array}{c} \text{Alkyl group} \\ \underbrace{\hspace{2cm}} \\ \text{C}_n\text{H}_{2n+1}\text{OH} \\ \underbrace{\hspace{1.5cm}} \\ \text{Hydroxyl group} \end{array}$ | 4~7 |
| 1,2- diols | $\begin{array}{c} \text{Alkyl group} \\ \underbrace{\hspace{2cm}} \\ \text{C}_{n-2}\text{H}_{2n-3}\text{CHOHCH}_2\text{OH} \\ \underbrace{\hspace{1.5cm}} \quad \underbrace{\hspace{1.5cm}} \\ \text{Hydroxyl group} \end{array}$ | 3~6 |

Table 3.2 - Polyglycols for chain length of alkyl chain and EO/PO unit study

| Frother family | Chemical structure | n | m | l |
|---|---|---------|-----|-----|
| Polypropylene Glycols (PPG) | $\begin{array}{c} \text{Propylene Oxide group} \\ \underbrace{\hspace{2cm}} \\ \text{H} [\text{OC}_2\text{H}_3(\text{CH}_3)]_m \text{OH} \\ \underbrace{\hspace{1.5cm}} \\ \text{Hydroxyl group} \end{array}$ | -- | 1~3 | -- |
| Polypropylene Glycol Alkyl Ethers (PPGAE) | $\begin{array}{c} \text{Propylene Oxide group} \\ \underbrace{\hspace{2cm}} \\ \text{C}_n\text{H}_{2n+1} [\text{OC}_2\text{H}_3(\text{CH}_3)]_m \text{OH} \\ \underbrace{\hspace{1.5cm}} \quad \underbrace{\hspace{1.5cm}} \\ \text{Alkyl group} \quad \text{Hydroxyl group} \end{array}$ | 1, 3, 4 | 1~3 | -- |
| Polyethylene Glycols (PEG) | $\begin{array}{c} \text{Ethylene Oxide group} \\ \underbrace{\hspace{2cm}} \\ \text{H} [\text{OC}_2\text{H}_4]_l \text{OH} \\ \underbrace{\hspace{1.5cm}} \\ \text{Hydroxyl group} \end{array}$ | -- | -- | 1~3 |
| Polyethylene Glycol Alkyl Ethers (PEGAE) | $\begin{array}{c} \text{Ethylene Oxide group} \\ \underbrace{\hspace{2cm}} \\ \text{C}_n\text{H}_{2n+1} [\text{OC}_2\text{H}_4]_l \text{OH} \\ \underbrace{\hspace{1.5cm}} \quad \underbrace{\hspace{1.5cm}} \\ \text{Alkyl group} \quad \text{Hydroxyl group} \end{array}$ | 2, 3, 4 | -- | 1 |
| | | 1~4, 6 | -- | 2 |
| | | 1, 2, 4 | -- | 3 |

Table 3.3 - Alcohols tested for methyl branch and hydroxyl position

| Frother family | n | Name | Position | | |
|-----------------|----------------|---------------------|------------------|-----------------|----|
| | | | -CH ₃ | OH | |
| Alcohols | 5 | 1-pentanol | -- | 1 | |
| | | 2-pentanol | | 2 | |
| | | 3-pentanol | | 3 | |
| | | 2-methyl-1-butanol | 2 | 1 | |
| | | 2-methyl-2-butanol | | 2 | |
| | | 3-methyl-1-butanol | 3 | 1 | |
| | | 3-methyl-2-butanol | | 2 | |
| | 6 | 1-hexanol | -- | 1 | |
| | | 2-hexanol | | 2 | |
| | | 3-hexanol | | 3 | |
| | | 2-methyl-1-pentanol | 2 | 1 | |
| | | 2-methyl-2-pentanol | | 2 | |
| | | 2-methyl-3-pentanol | | 3 | |
| | | 3-methyl-1-pentanol | 3 | 1 | |
| | | 3-methyl-2-pentanol | | 2 | |
| | | 3-methyl-3-pentanol | | 3 | |
| | | 4-methyl-1-pentanol | 4 | 1 | |
| | | 4-methyl-2-pentanol | | 2 | |
| | | Diols | 5 | 1,2-pentanediol | -- |
| 1,4-pentanediol | 4 | | | 1 | |
| 1,5-pentanediol | 5 | | | 1 | |
| 6 | 1,2-hexanediol | | -- | 2 | 1 |
| | 1,5-hexanediol | | | 5 | 1 |
| | 1,6-hexanediol | | | 6 | 1 |

3.3 Validation:

As bubble rise velocity is sensitive to the presence of contaminants (Sam et al. 1996; Krzan and Malysa 2002; Krzan et al. 2004; Parkinson et al. 2008), system cleanliness had to be verified prior to each test.

3.3.1 Replication: profile in tap water

To achieve acceptable replication the system required extensive washing. Before a test the system was flushed repeatedly with tap water till the known velocity profile in tap water was obtained (Fig. 3.2). This could sometimes take 25 times the volume of the column. Reagent testing only commenced once the standard velocity profile in water alone was achieved. This precaution plus the use of

minimum gas rate to just release a bubble gave the replication needed for the study (Tan et al. 2013).

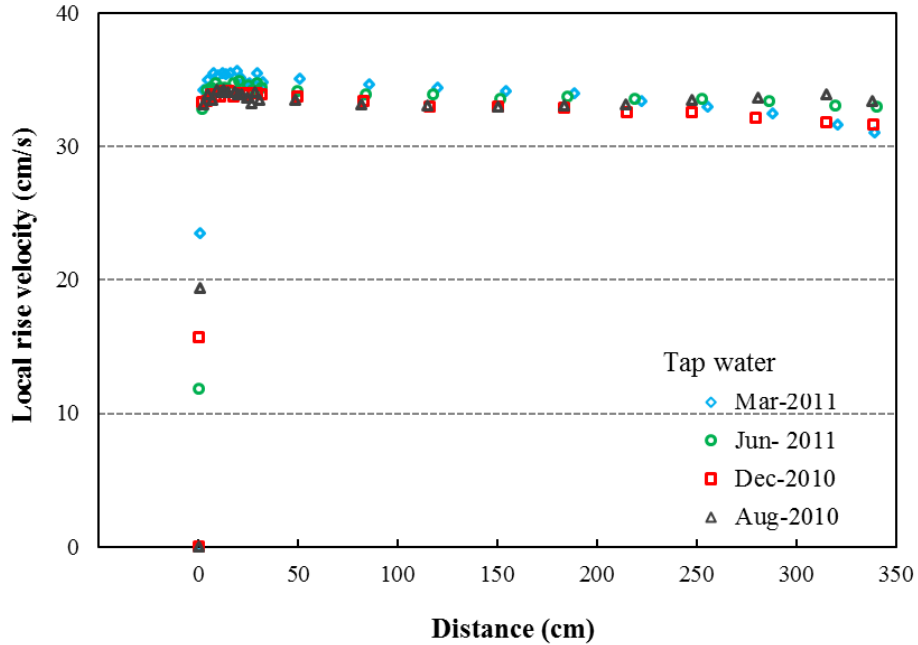


Figure 3.2 – Bubble velocity profiles in tap water at different times showing acceptable cleanliness to commence a test

3.3.2 Replication: frother solutions

Two full repeats tests (i.e., including solution preparation) were conducted with 1-pentanol and 1-hexanol at different times of the year. With the precautions described in 3.3.1 good repeatability was achieved (Fig. 3.3).

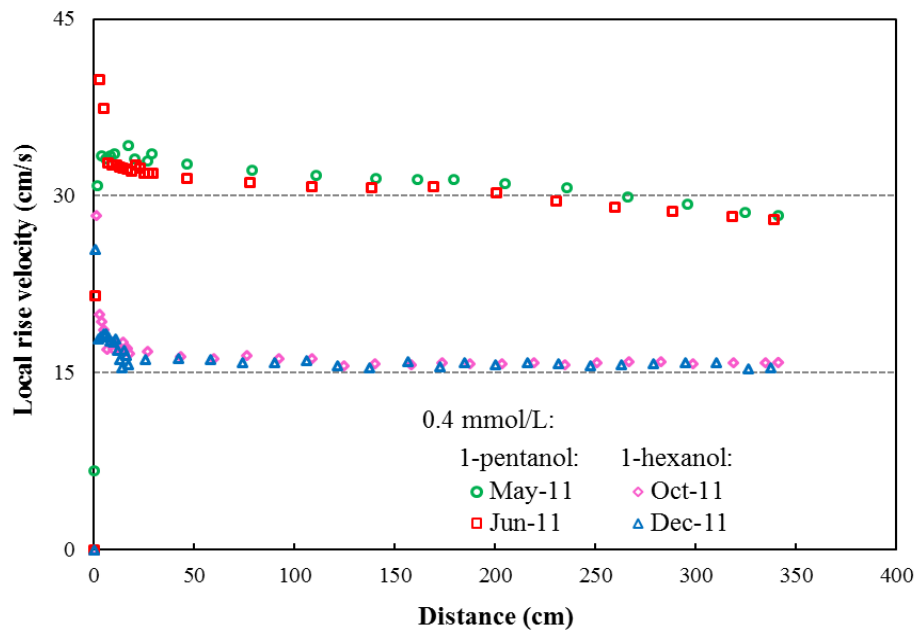


Figure 3.3 – Demonstration or replication: bubble velocity profiles in 0.4 mmol/l 1-pentanol and 1-hexanol

References

- Clift, R., Grace, J. R. and Weber, M. E. (1978). Bubbles, drops, and particles, New York : Academic Press.
- Finch, J. A. and Dobby, G. S. (1990). Column flotation. Oxford, England; New York, Pergamon.
- Krzan, M., Lunkenheimer, K. and Malysa, K. (2004). On the influence of the surfactant's polar group on the local and terminal velocities of bubbles. Colloids and Surfaces a-Physicochemical and Engineering Aspects 250(1-3): 431-441.
- Krzan, M. and Malysa, K. (2002). Profiles of local velocities of bubbles in n-butanol, n-hexanol and n-nonanol solutions. Colloids and Surfaces A: Physicochemical and Engineering Aspects 207(1-3): 279-291.
- Parkinson, L., Sedev, R., Fornasiero, D. and Ralston, J. (2008). The terminal rise velocity of 10-100 μm diameter bubbles in water. Journal of Colloid and Interface Science 322(1): 168-172.
- Remillard, M., Joseph, M. and Laroche, L. (2009). Municipal drinking water produced by Atwater and Charles-J Des Bailleurs drinking water treatment plants: Annual Summary. Montreal: Division de l' expertise technique.

Sam, A., Gomez, C. O. and Finch, J. A. (1996). Axial velocity profiles of single bubbles in water/frother solutions. *International Journal of Mineral Processing* 47(3-4): 177-196.

Tan, Y. H., Rafiei, A. A., Elmahdy, A. and Finch, J. A. (2013). Bubble size, gas holdup and bubble velocity profile of some alcohols and commercial frothers. *International Journal of Mineral Processing* 119: 1-5.

Chapter 4 – Effect of alkyl chain length in alcohols and polyglycol alkyl ethers

4.1 Introduction

Surface-active agents known as frothers play a critical role in many mineral flotation systems helping to control bubble size, reduce bubble rise velocity, and stabilize froth. The frother molecule has two parts: a hydrophobic (nonpolar) hydrocarbon (alkyl) chain and a hydrophilic (polar) part. The general understanding is that the frother molecule adsorbs at the water/air interface with the polar group oriented to the water-side and the hydrocarbon chain to the air-side. As a consequence, interface-related properties are modified that result in the frother functions. The ability of surfactants to change the properties of interfaces is known to be dependent on their chemical structure (Rosen and Dahanayake 2000).

Water/air interfacial properties are related to the hydrocarbon chain length of the surfactant, which is recognized in processes such as flotation, flocculation, foam separation and phenomena such as surface tension, adsorption and micelle formation (Lin et al. 1974; Briggs et al. 1995). Fuerstenau (1976), testing a homologous series of alkyl amine surfactants, showed that the concentration at equal flotation recovery of quartz decreased as hydrocarbon chain length increased. For a homologous series of linear single-chain surfactants the critical micelle concentration (CMC) decreases logarithmically with increasing carbon number (Klevens 1953). Keitel and Onken (1982) studied aqueous solutions of n-

alcohols (C₁-C₈) and diols (C₂-C₅) and showed that with increasing alkyl chain length bubble size reduced and gas holdup increased.

Understanding the relationship between frother structure and properties can help to characterize frothers, explain their action and aid selection for a given duty. The objective of this chapter is to determine the impact on single bubble velocity of hydrocarbon chain length for the two main frother families, alcohols and polyglycols.

4.2 Reagents

4.2.1 Alcohols

Table 4.1 lists the 1-alcohols and 1, 2- diols used to study the effect of alkyl chain length. The 1-alcohols were from Fisher Scientific Company (Canada Ltd) and 1,2-diols were from Sigma-Aldrich Corporation (Canada). All reagents were purchased with the highest purity available from 98% to 99.8%.

Table 4.1 - Alcohols tested for alkyl chain length

| Family | Name | Chemical formula | n | Molecule weight (g/mol) |
|------------|-----------------|--|---|-------------------------|
| 1-alcohols | 1-butanol | C ₄ H ₉ OH | 4 | 74.12 |
| | 1-pentanol | C ₅ H ₁₁ OH | 5 | 88.15 |
| | 1-hexanol | C ₆ H ₁₃ OH | 6 | 102.17 |
| | 1-heptanol | C ₇ H ₁₅ OH | 7 | 116.2 |
| 1,2-diols | 1,2-propanediol | CH ₃ CHOHCH ₂ OH | 3 | 76.09 |
| | 1,2-butanediol | C ₂ H ₅ CHOHCH ₂ OH | 4 | 90.12 |
| | 1,2-pentanediol | C ₃ H ₇ CHOHCH ₂ OH | 5 | 104.15 |
| | 1,2-hexanediol | C ₄ H ₉ CHOHCH ₂ OH | 6 | 118.17 |

4.2.2 Polyglycol ethers

Table 4.2 lists the 20 polyglycol ethers studied, which fall into two sub-families, polypropylene glycol alkyl ether (PPGAE: C_nH_{2n+1}(OC₃H₆)_mOH) and polyethylene glycol alkyl ether (PEGAE: C_nH_{2n+1}(OC₂H₄)_lOH). The polyglycol

ethers are further divided based on the number of propylene oxide (PO) groups ($m = 1, 2, 3$) or ethylene oxide (EO) groups ($l = 1, 2, 3$). All were from Sigma-Aldrich Corporation (Canada) with a purity of 98.5% to 99.5%. All the reagents were used as received.

Table 4.2 - Polyglycol ethers for alkyl chain length study

| Family | Name | n | l/m | Molecule weight (g/mol) | | |
|--------|--------------------------------|---------------------------------|----------------------------------|-------------------------|--------|--------|
| PPGAE | Propylene glycol methyl ether | 1 | 1 | 90.12 | | |
| | Propylene glycol propyl ether | 3 | | 118.17 | | |
| | Propylene glycol butyl ether | 4 | | 132.20 | | |
| | PPGAE | Dipropylene glycol methyl ether | 1 | 2 | 148.2 | |
| | | Dipropylene glycol propyl ether | 3 | | 176.25 | |
| | | Dipropylene glycol butyl ether | 4 | | 190.28 | |
| | | PPGAE | Tripropylene glycol methyl ether | 1 | 3 | 206.28 |
| | | | Tripropylene glycol propyl ether | 3 | | 234.33 |
| | | | Tripropylene glycol butyl ether | 4 | | 248.36 |
| PEGAE | Ethylene glycol ethyl ether | 2 | 1 | 90.12 | | |
| | Ethylene glycol propyl ether | 3 | | 104.15 | | |
| | Ethylene glycol butyl ether | 4 | | 118.17 | | |
| | PEGAE | Diethylene glycol methyl ether | 1 | 2 | 120.15 | |
| | | Diethylene glycol ethyl ether | 2 | | 134.17 | |
| | | Diethylene glycol propyl ether | 3 | | 148.20 | |
| | | Diethylene glycol butyl ether | 4 | | 162.23 | |
| | | Diethylene glycol hexyl ether | 6 | | 190.28 | |
| | | Triethylene glycol methyl ether | 1 | | 3 | 164.20 |
| | Triethylene glycol ethyl ether | 2 | 178.23 | | | |
| | Triethylene glycol butyl ether | 4 | 206.28 | | | |

4.3 Results

4.3.1 Bubble rise velocity profile

Examples of bubble local velocity profiles in surfactants from the alcohol and polyglycol families are shown in Figs 4.1 and 4.2, respectively.

4.3.1.1 Alcohols

Fig. 4.1 gives velocity profiles of 1, 2- butanediol at selected concentrations. At 1 mmol/L, the bubble rise velocity is close to that in water only. At 8 mmol/L, the profile shows a continuous decrease from ca. 34 cm/s to 19 cm/s at 350 cm, which indicates progressive adsorption of the surfactant onto the bubble surface. At 30 mmol/L and 60 mmol/L the profile reaches the minimum velocity of ca. 15-16 cm/s within about 150 and 50 cm from the launch position, respectively. This indicates that these concentrations are sufficient for adsorption to slow the bubble to its minimum velocity within the distance available (350 cm). The minimum velocity is equated with terminal velocity.

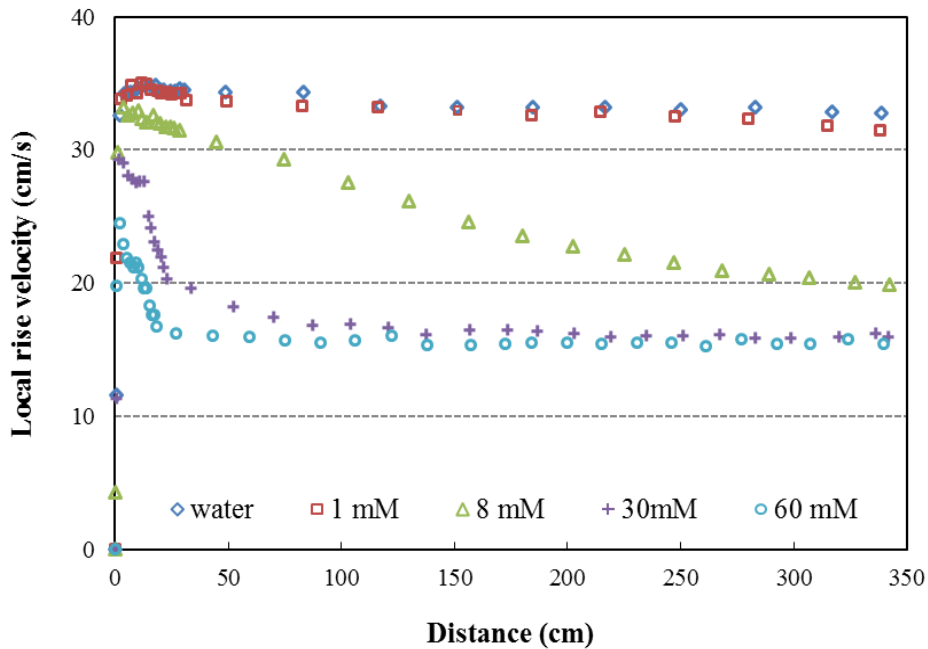


Figure 4.1 – Bubble velocity profile in presence of 1, 2- butanediol at selected concentrations

4.3.1.2 Polyglycol ethers

Fig. 4.2 shows examples of bubble velocity profiles at 0.05 mmol/L for three dipropylene glycol ethers with alkyl chain length $n = 1, 3$ and 4. For the shortest alkyl chain length ($n = 1$, methyl) the profile gradually decreases from ca. 34 cm/s to 25 cm/s at 350 cm while for the longest chain length ($n = 4$, butyl) the minimum velocity, ca. 15 cm/s, is reached within about 25 cm of the launch point. The continuous decrease (deceleration) for the methyl and propyl cases again indicates progressive surfactant adsorption onto the moving bubble.

From the profiles in both alcohols and polyglycols, the bubble rise velocity is evidentially a function of alkyl chain length (i.e., structure), surfactant concentration and the distance travelled.

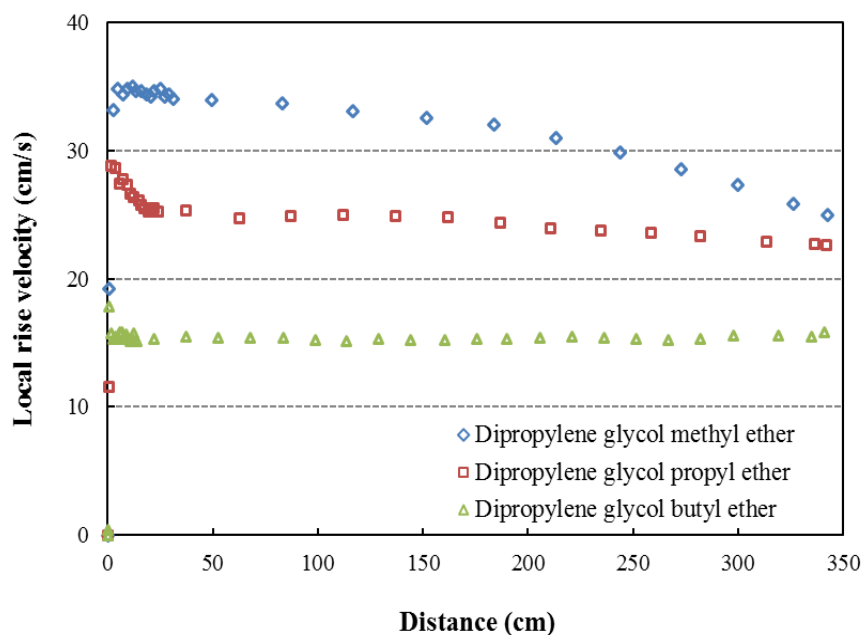


Figure 4.2 – Bubble velocity profile in presence of three dipropylene glycol ethers (0.05 mmol/L)

4.3.2 Velocity at 300 cm

Rather than using the full profile to compare structure, a single metric was selected, namely the velocity at 300 cm. The choice of 300 cm is arbitrary but is partly based on the assumption that any variations in bubble motion, for example due to launch conditions, would be ‘damped’ at this distance. The use of velocity at 300 cm was introduced by Tan et al. (2013).

4.3.2.1 Alcohols

Fig. 4.3 shows the velocity at 300 cm as a function of concentration for 1-alcohols ($n = 4 - 7$) and 1, 2-diols ($n = 3 - 6$). A similar trend is seen in both cases: with increase in concentration the velocity decreased until the minimum velocity, ca. 15 cm/s, is reached. The experimental plan called to increase concentration till the minimum velocity was reached; however, in one case, 1, 2-propanediol, the velocity at 300 cm only reached 24 cm/s with concentration as high as 1.4 mol/L; i.e., the minimum velocity was not achieved.

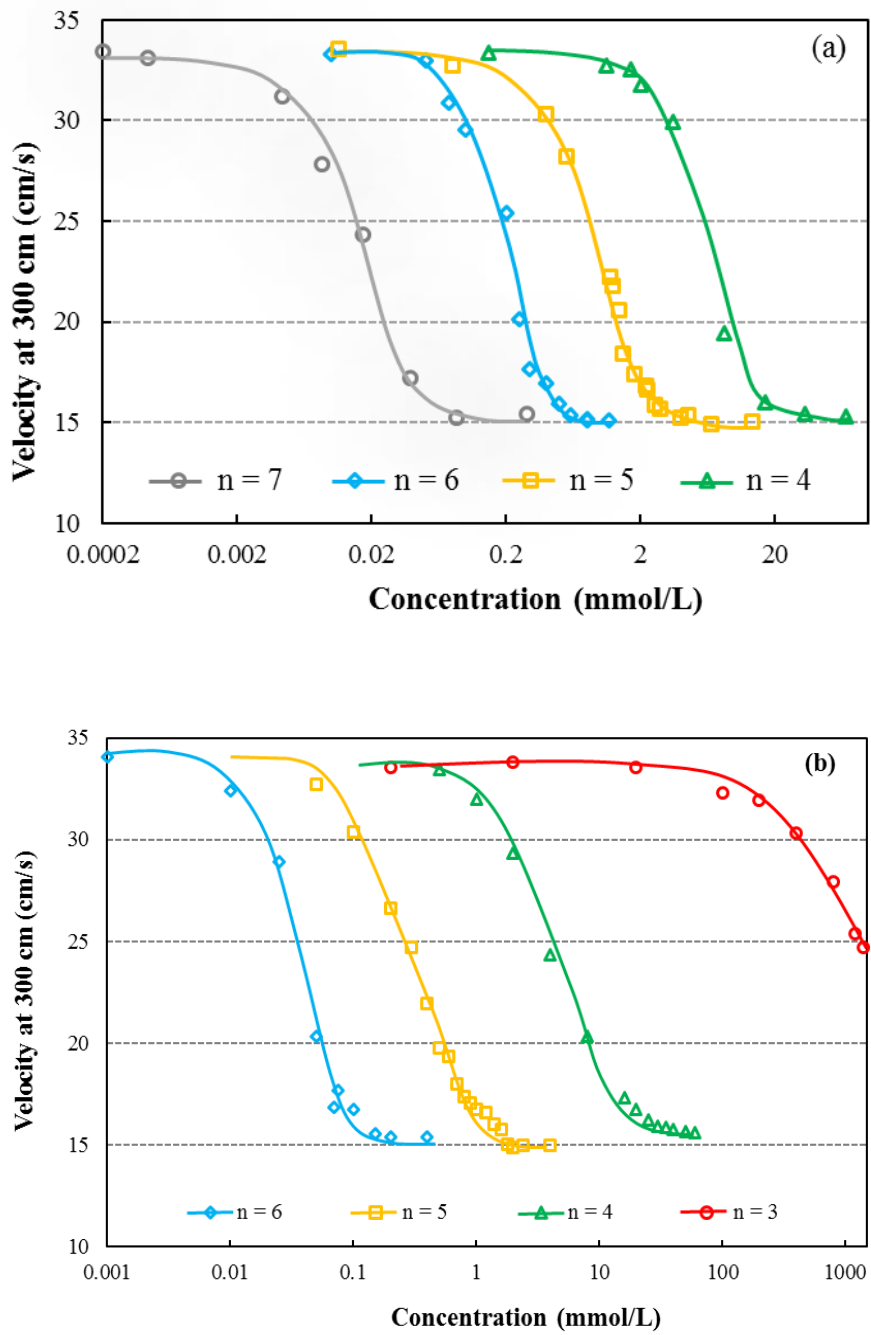


Figure 4.3 – Velocity at 300 cm for alcohols as a function of concentration: (a) 1-alcohols; (b) 1, 2-diols

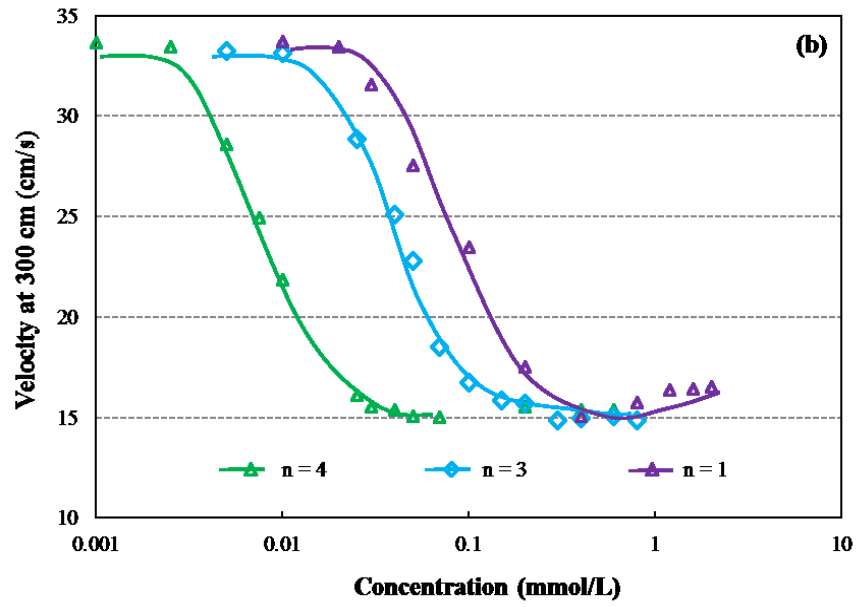
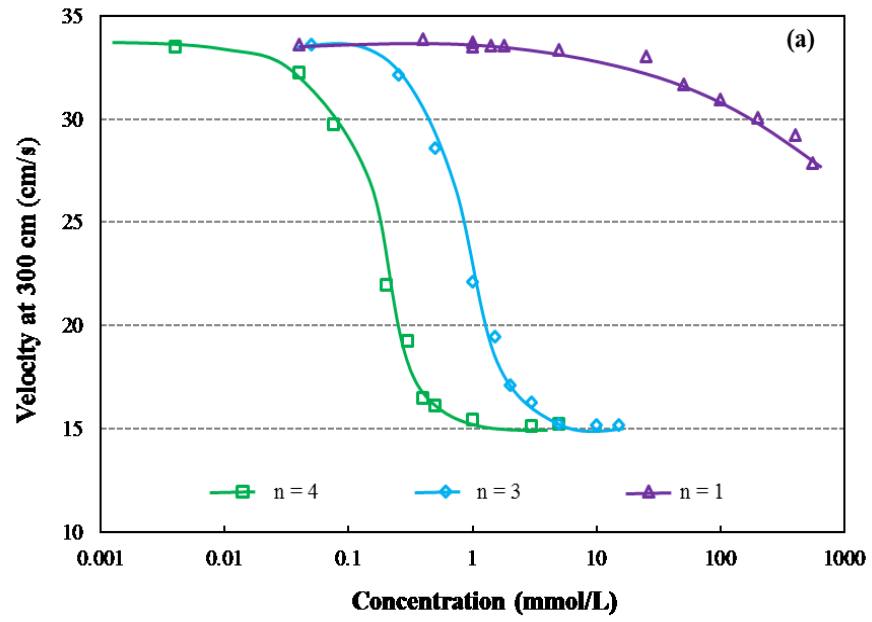
4.3.2.2 Polyglycol ethers

The results for the two polyglycol sub-families, polypropylene glycol alkyl ethers and polyethylene glycol alkyl ethers, are shown in Figs. 4.4 and 4.5, respectively.

4.3.2.2.1 Polypropylene glycol alkyl ethers (PPGAE)

Fig. 4.4 shows the nine polypropylene glycol alkyl ethers of the three subgroups, $m = 1, 2, 3$ with increasing hydrocarbon chain length, $n = 1, 3, 4$. The trends are similar to those seen for alcohols. For each m subgroup, with increase in n the concentration required to reach the minimum velocity decreased. Comparing subgroups, the concentration range decreases by about one order of magnitude for each additional m (note the concentration scales on the figures). This PO number (effectively the PO chain length) effect will be discussed further in Chapter 6.

The minimum concentration was reached with one exception: for propylene glycol methyl ether ($m = 1; n = 1$) the velocity at 300 cm reached only ca. 27 cm/s at a concentration up to 0.55 mol/L. As with 1, 2-propanediol, it was deemed too expensive to go to higher concentrations.



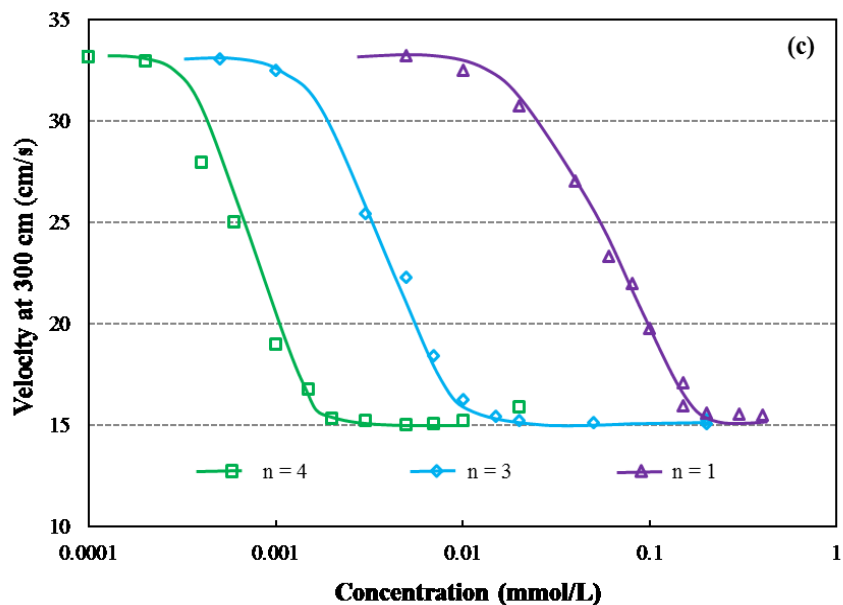
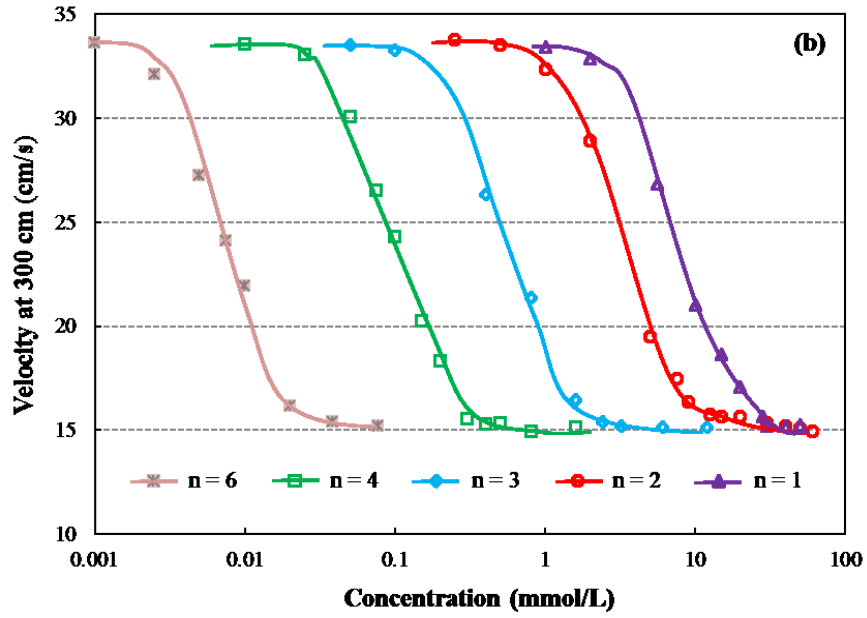
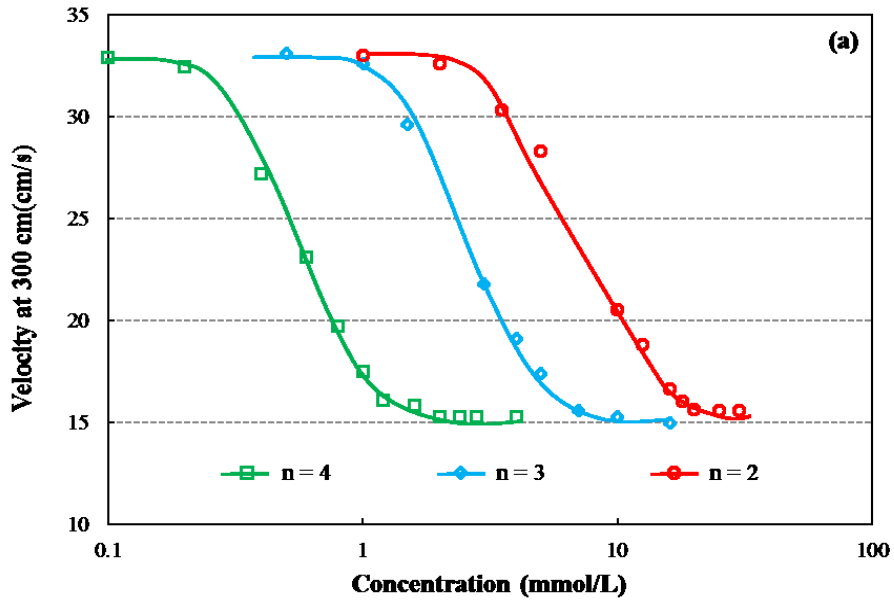


Figure 4.4 – Velocity at 300 cm for PPGAE as a function of concentration and alkyl chain length: (a) $m = 1$; (b) $m = 2$; (c) $m = 3$

4.3.2.2.2 Polyethylene glycol alkyl ethers (PEGAE)

Fig. 4.5 shows the three subgroups of the eleven polyethylene glycol alkyl ethers ($l = 1, 2, 3$) as a function of concentration for different n values. The trend is similar to that for PPGAE but the effect of increasing the EO number (i.e., increasing l) is less significant in reducing the concentration to reach minimum velocity compared to m in the PPGAE structure.



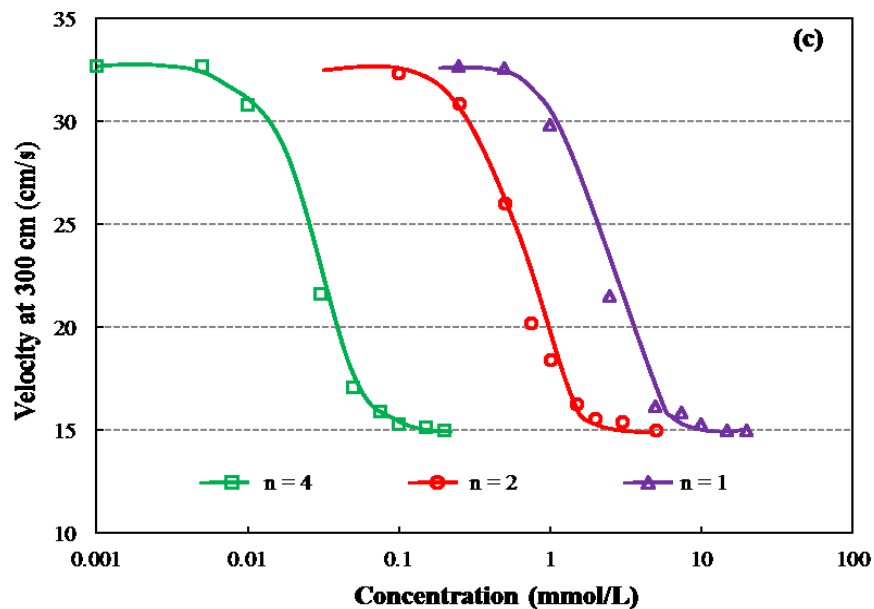


Figure 4.5 – Velocity at 300 cm for PEGAE as a function of concentration and alkyl chain length: (a) $l = 1$; (b) $l = 2$; (c) $l = 3$

4.3.3 Concentration to reach minimum velocity (CMV)

The concentration to reach minimum velocity is a further way to reduce the data to correlate against structure.

4.3.3.1 Determination of CMV

The trend in velocity at 300 cm vs. concentration was similar in all cases: with increase in concentration, the velocity at 300 cm decreased to a minimum (and constant) ca. 15 cm/s at a given concentration referred to as ‘concentration to reach minimum velocity’, CMV. The CMV is estimated graphically from the plot of velocity at 300 cm vs. concentration taking the intersection of the two linear trends imposed on the data as illustrated in Fig. 4.6. Regression analysis was used to estimate the intersection (CMV) and the 95% confidence interval on CMV.

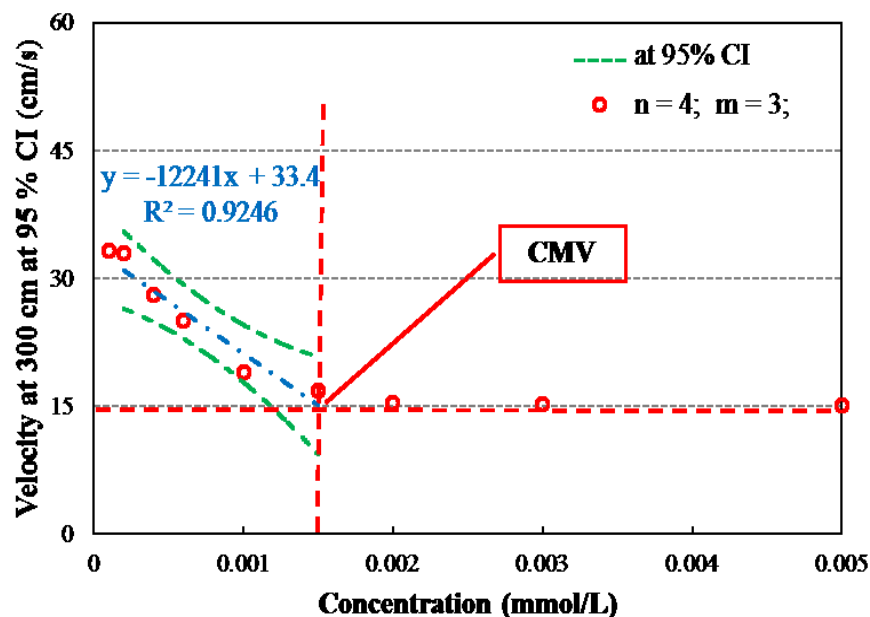


Figure 4.6 – Method to determine concentration to reach minimum velocity (CMV)

The CMV will be used to correlate against structural properties. An example is Fig. 4.7 where log CMV vs. n shows a linear trend. The Figure also includes results when selecting 150 cm as the distance rather than 300 cm.

4.3.3.2 Effect of distance chosen: 150 cm and 300 cm

It is necessary to establish that correlations using CMV defined on 300 cm were independent of the distance chosen. To investigate, for five diethylene glycol alkyl ethers velocity at 150 cm was estimated using the same graphical method as in Fig. 4.6. The results (Fig. 4.7) show the same trend against number of carbons with a slightly higher CMV at 150 cm compared to 300 cm (Table 4.3). For the remainder of the thesis the CMV will refer to the distance of 300 cm.

Table 4.3 - CMV for diethylene glycol alkyl ethers at 150 cm and 300 cm

| Carbon number | 1 | 2 | 3 | 4 | 6 |
|---------------|----|----|-----|-----|-------|
| CMV(mmol/L) | | | | | |
| 300 cm | 25 | 10 | 1.8 | 0.4 | 0.025 |
| 150 cm | 30 | 20 | 4 | 0.5 | 0.04 |

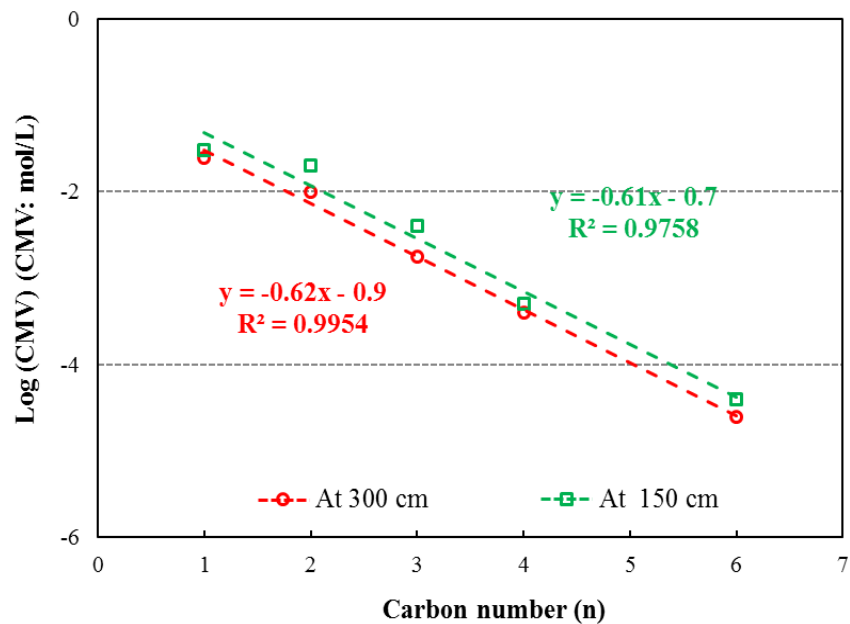


Figure 4.7 – Log CMV for diethylene glycol alkyl ethers at 150cm and 300cm as a function of carbon number

4.3.3.3 Reliability of estimation of CMV value

A confidence interval (CI) is usually used to indicate the reliability of estimation of a population parameter. Probably the most common is the the 95% confidence interval (Zar 1999). The reliability of CMV estimation was investigated on nine surfactants selected from both alcohol and polyglycol families with a range in structure. Regression models were established using simple regression analysis and the 95% CI interval calculated to give the 95% CI on CMV (as in Fig 4.6). The relative 95% CI was calculated (95% CI on CMV/CMV) and the average taken over the nine examples to represent the relative 95% CI for all cases which is the ‘error’ bar on subsequent figures.

4.3.4 Effect of alkyl chain length on CMV

4.3.4.1 Alcohols

Table 4.4 summarizes the CMV values for the alcohol family (recalling no CMV was achieved with 1, 2-propanediol) along with a rough estimate of the percent decrease in CMV for every additional carbon (or $-\text{CH}_2-$). Fig. 4.8 shows log CMV for the two sub-groups of alcohols appears to be a linear function of alkyl chain length (n).

Table 4.4 - CMV: alcohols

| Alcohol sub-group | Name | n | CMV (mmol/L) | % Δ CMV per CH_2 | |
|-------------------|-----------------|---|--------------|----------------------------------|----|
| 1-alcohol | 1-butanol | 4 | 20 | 89 | 78 |
| | 1-pentanol | 5 | 2.3 | | |
| | 1-hexanol | 6 | 0.27 | | |
| | 1-heptanol | 7 | 0.06 | | |
| 1,2-diol | 1,2-ropenediol | 3 | --- | 91 | 90 |
| | 1,2-butanediol | 4 | 20 | | |
| | 1,2-pentanediol | 5 | 1.8 | | |
| | 1,2-hexanediol | 6 | 0.18 | | |

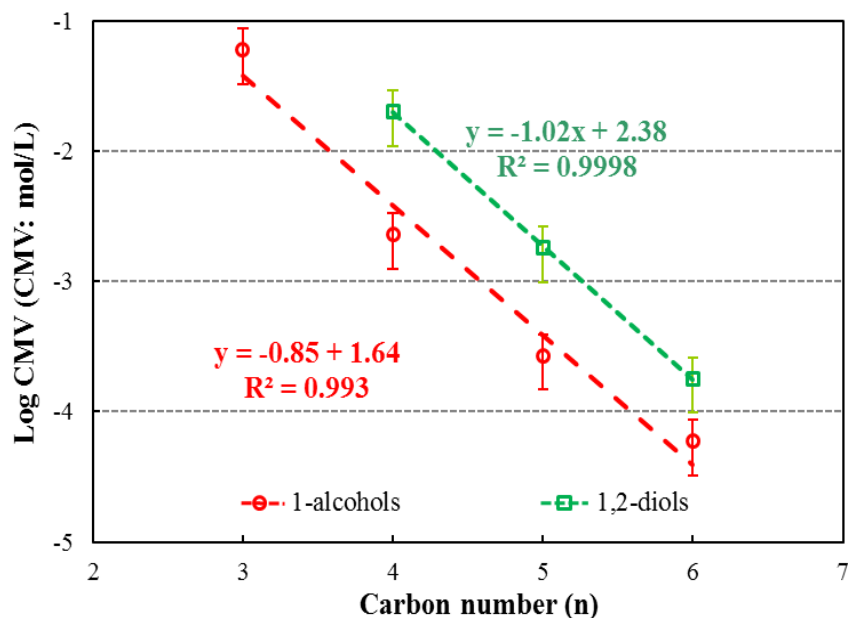


Figure 4.8 – Log CMV of 1-alcohols and 1, 2-diols as a function of carbon number n

4.3.4.2 Polyglycol ethers

Table 4.5 lists the CMV for the 20 polyglycol ethers in the two sub-families (again recalling no CMV was achieved for propylene glycol methyl ether) along with an estimate of the percent decrease in CMV for every additional $-\text{CH}_2-$. The log CMV as a function of number of carbons in the alkyl chain (n) for polyglycol alkyl ethers is shown in Fig. 4.9. Similar to the alcohols, log CMV decreases linearly with increasing n in a series of parallel lines dependent on the m or l number.

Table 4.5 - CMV: Polyglycol ethers at a given m/l

| Frother family | | n | m or l | CMV (mmol/L) | % Δ CMV per CH_2 | | |
|----------------|---------------------------|---|-----------|-----------------|-------------------------------------|----|----|
| PPGAE | Propylene glycol ether | 1 | 1 | --- | 83 | | |
| | | 3 | | 3 | | | |
| | | 4 | | 0.5 | | | |
| | Dipropylene glycol ether | 1 | 2 | 3.5 | 83 | | |
| | | 3 | | 0.14 | | | |
| | | 4 | | 0.024 | | | |
| | Tripropylene glycol ether | 1 | 3 | 0.2 | 86 | | |
| | | 3 | | 0.01 | | | |
| | | 4 | | 0.0014 | | | |
| PEGAE | Ethylene glycol ether | 2 | 1 | 20 | 68 | 83 | |
| | | 3 | | 6.5 | | | |
| | | 4 | | 1.1 | | | |
| | Diethylene glycol ether | 1 | 2 | 25 | 60 | 82 | 78 |
| | | 2 | | 10 | | | |
| | | 3 | | 1.8 | | | |
| | | 4 | | 0.4 | | | |
| | | 6 | | 0.025 | | | |
| | Triethylene glycol ether | 1 | 3 | 7 | 80 | | |
| | | 2 | | 1.4 | | | |
| | | 4 | | 0.08 | | | |

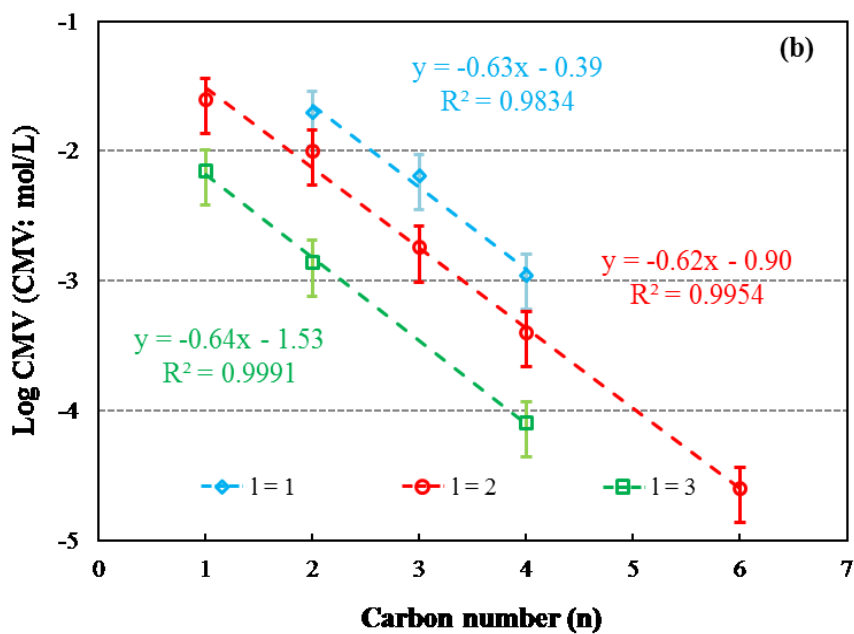
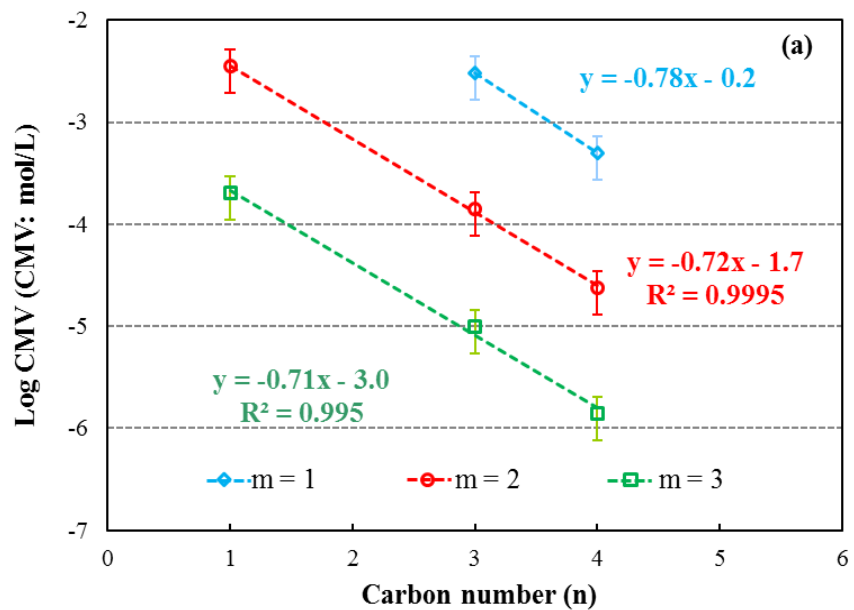


Figure 4.9 – Log CMV as a function of carbon number n for polyglycol alkyl ethers: (a) PPGAE; (b) PEGAE

4.4 Discussion

Predicting a frother's functions according to its structure is of interest to flotation chemical suppliers, modelers and plant operators. The approach here was to determine the effect of hydrocarbon (alkyl) chain length on the bubble rise velocity profile for a series of surfactants from two frother families, alcohols and polyglycols. Previous work had established that the bubble velocity profile was a reliable measure sensitive to surfactant type (Sam et al. 1996).

As the bubble velocity profile is a function of surfactant concentration and distance travelled as well as surfactant structure reducing the profile to single metric greatly aided the analysis. The choice was the concentration to reach minimum velocity at 300 cm, CMV. The choice of 300 cm was based partly on the expectation that factors contributing to bubble velocity had been 'damped' over the distance. It was ascertained that substituting 150 cm as the distance choice would alter the absolute values but not the trends with structural features which is the ambition here.

The graphical method used to estimate CMV is similar to that in determining other physiochemical characteristics of a surfactant, e.g., critical micelle concentration (CMC) from surface tension vs. concentration (Varadaraj et al. 1991; Castro et al. 2001; Holmberg et al. 2003; Adkins et al. 2010), and critical coalescence concentration (CCC) from bubble size vs. frother concentration (Cho and Laskowski 2002; Laskowski 2004; Melo and Laskowski 2006). The

difference here is that reliability of the CMV estimation was quantified by the 95% confidence interval.

The effect of alkyl chain length on CMV was significant: for every additional n (i.e., $-\text{CH}_2-$ group) CMV decreases by ca. 90% for alcohols (Table 4.4) and ca. 70% for polyglycols (Table 4.5). The trend was that \log CMV decreased linearly with increase in n for both the alcohols and polyglycols. Leaving the form of the relationship aside for now let's consider why the increase in n causes CMV to decrease. To do this we must return to the effect of surfactant on bubble rise velocity.

The packing of surfactant molecules at the interface plays a pronounced role in surface properties (Cosgrove 2005), including the tendency to slow bubble rise. At the moment a bubble is released, the initially clean surface is progressively 'contaminated' with surfactant as the bubble rises. Fluid shear over the bubble surface transports surfactant to the rear of the bubble. This increase in packing towards the bubble rear gives a gradient in surface tension which increases in the opposite direction (i.e., towards the front of the bubble) and is credited with increasing drag and thus slowing bubble rise (Dukhin et al. 1995). At dynamic equilibrium the adsorption rate of surfactant (primarily at the bubble front) equals the desorption rate (primarily from the rear) and the bubble attains minimum (equilibrium or terminal) velocity, which in the case of the 1.45 mm here is ca. 15 cm/s.

Armed with this understanding that the slowing of bubble rise is related to surface tension gradients controlled by the distribution of the adsorbed surfactant molecules, an interpretation of the observed effect of alkyl chain length on CMV can be offered.

It is known that increasing alkyl chain length increases surface activity (e.g., the surface tension decreases more per mole as n increases) (Narayanan 2008) which means larger surface tension gradients are generated on the bubble surface as n increases. This is one factor that would slow the bubble more as n increases. In addition, the longer chains can interact (Narayanan 2008), creating a geometry for strong van der Waals intermolecular attraction between the hydrocarbon chains which may increase the packing density. Since there are more molecules towards the bubble rear this interaction mechanism will further increase the packing at the rear adding to the surface tension gradients slowing the bubble rise. The more the bubble is slowed by these phenomena associated with increasing alkyl chain length the lower the concentration of surfactant required to slow the bubble to the minimum velocity, i.e., the lower the CMV.

This argument based on increased surface activity and packing as n increases qualitatively expresses the observation the CMV decreases as n increases. It does not a priori suggest the linear relationship between \log CMV and n . This relationship is represented by the following equation:

$$\log [\text{CMV}] = - a \times n + \text{constant} \quad 4.1$$

where a is constant related to the frother family (ca.0.9 in 1-alcohol; ca.0.74 in PPGAE and ca. 0.63 in PEGAE).

This form of correlation is shown for another surfactant property, the critical micelle concentration (CMC), namely that \log CMC trends linearly with increasing n (Klevens 1953; Lin et al 1974). Zhang et al. (2012) recently determined the critical coalescence concentration (CCC¹) for some of the same surfactants used in the present study. They showed an exponential trend between CCC and n which can be re-arranged as in Fig. 4.10 to show the same \log CCC vs. n trend as observed here for CMV.

This similarity between the relationship with n of CMV and CCC suggests some mechanistic connection between the two. In the case of the CMC trend with n the mechanism is related to a decrease in energy to transfer the surfactant molecule from the bulk solution to the micelle (essentially transfer from aqueous to organic phase) per unit increase in n (i.e., per additional $-\text{CH}_2-$) representing an increase in hydrophobicity. In the case of CMV and CCC surfactant transfer is from bulk to the air-water interface but the dependence on n might again reflect a decrease in energy to transfer as n increases and the molecule becomes more hydrophobic.

Zhang et al. (2012) went on to assess the CCC¹ data against the hydrophilic-lipophilic balance (HLB) (Davis 1957). Following that lead, in Chapter 7 a similar analysis connecting CMV and HLB is attempted.

¹ Note: The CCC and CCC95 data were shown to be similar. The term CCC will be substituted for CCC95 for discussion purposes (see Zhang et al. 2012).

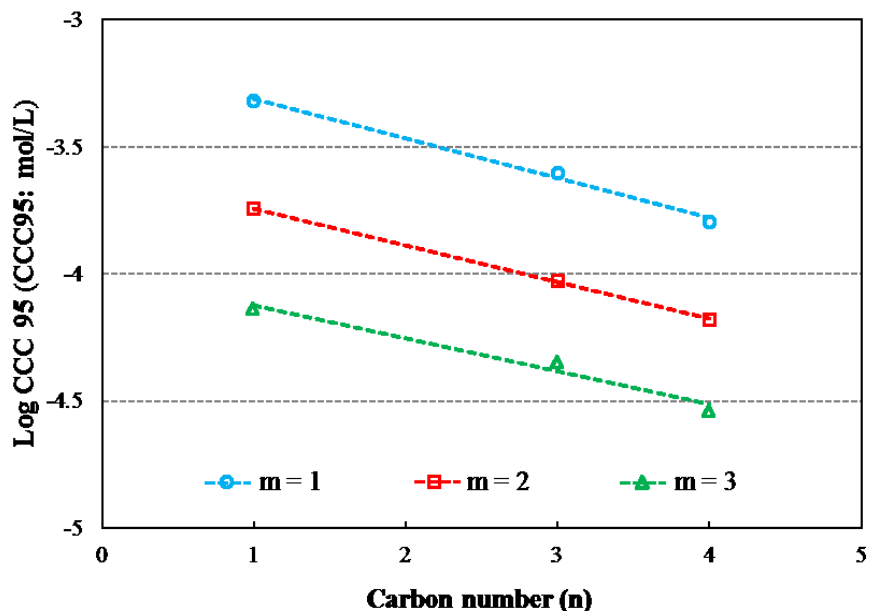


Figure 4.10 – Log CCC95 as a function of number of carbon in alkyl chain (PPGAE)

4.5 Summary

The effect of the number of carbons in the hydrocarbon chain (n) in alcohols and polyglycol alkyl ethers on the single bubble rise velocity profile was determined. The concentration to reach minimum velocity at 300 cm (CMV) was used to correlate against n . The increase in n significantly decreased the CMV: For every additional $-\text{CH}_2-$ group CMV decreases by ca. 90% for alcohols and ca. 70% for polyglycols. The results are interpreted based on the concept of surfactant packing and the resulting surface tension gradient produced. Plotting log CMV vs. n gave a series of linear trends, similar to that reported for other surfactant properties. The findings are a step towards modeling the frother structure-property relationship of potential use in frother selection in flotation systems.

References

- Adkins, S. S., Chen, X., Nguyen, Q. P., Sanders, A. W. and Johnston, K. P. (2010). Effect of branching on the interfacial properties of nonionic hydrocarbon surfactants at the air–water and carbon dioxide–water interfaces. *Journal of Colloid and Interface Science* 346(2): 455-463.
- Briggs, Catherine, B. A., Newington, I. M. and Pitt, A. R. (1995). Synthesis and properties of some novel nonionic polyol surfactants. *Journal of the Chemical Society, Chemical Communications* (3): 379-380.
- Castro, M. J. L., Ritacco, H., Kovensky, J. and Fernández-Cirelli, A. (2001). A simplified method for the determination of critical micelle concentration. *Journal of Chemical Education* 78(3): 347.
- Cho, Y. S. and Laskowski, J. S. (2002). Effect of flotation frothers on bubble size and foam stability. *International Journal of Mineral Processing* 64(2-3): 69-80.
- Cosgrove, T. (2005). Chapter 4 Surfactant Aggregation and Adsorption at Interfaces; *Colloid Science-Principles, Methods and Applications*, Blackwell Publishing., pp : 50-74
- Davies, J. T. (1957). A quantitative kinetic theory of emulsion type: I. Physical chemistry of the emulsifying agent. *Gas/Liquid and Liquid/Liquid Interface Proceedings of the International Congress of Surface Activity*: 426-438

- Dukhin, S. S., Kretzschmar G. and Miller, R. (1995). Dynamics of adsorption at liquid Interfaces: Theory, Experiment, Application, Elsevier Science.
- Fuerstenau, M. C. (1976). Flotation. A. M. Gaudin Memorial Volume, New York, American Institute of Mining, Metallurgical and Petroleum Engineers, Inc.
- Holmberg, K., Jönsson, B., Kronberg, B. and Lindman, B. (2003). Chapter 16: Surface tension and adsorption at the air–water interface. Surfactants and Polymers in Aqueous Solution, John Wiley & Sons, Ltd: 342-345.
- Keitel, G. and Onken, U. (1982). Inhibition of bubble coalescence by solutes in air/water dispersions. Chemical Engineering Science 37(11): 1635-1638.
- Klevens, H. (1953). Structure and aggregation in dilute solution of surface active agents. Journal of the American Oil Chemists' Society 30(2): 74-80.
- Laskowski, J. S. (2004). Testing flotation frothers. Physicochemical Problems of Mineral Processing (38): 13-22.
- Lin, I. J., Moudgil, B. M. and Somasundaran, P. (1974). Estimation of the effective number of -CH₂- groups in long-chain surface active agents. Colloid & Polymer Science 252(5): 407-414.
- Melo, F. and Laskowski, J. S. (2006). Fundamental properties of flotation frothers and their effect on flotation. Minerals Engineering 19(6–8): 766-773.
- Narayanan, R. (2008). Interfacial processes and molecular aggregation of surfactants. Equilibrium adsorption of surfactants at the Gas-liquid

- interface; S. I. Karakashev, A. V. Nguyen and J. D. Miller. Berlin, Springer. (218): pp : 278-281.
- Rosen, M. J. and Dahanayake, M. (2000). *Industrial Utilization of Surfactants - Principles and Practice*, AOCS Press: 169; pp : 171-172.
- Sam, A., Gomez, C. O. and Finch, J. A. (1996). Axial velocity profiles of single bubbles in water/frother solutions. *International Journal of Mineral Processing* 47(3-4): 177-196.
- Tan, Y. H., Rafiei, A. A., Elmahdy, A. and Finch, J. A. (2013). Bubble size, gas holdup and bubble velocity profile of some alcohols and commercial frothers. *International Journal of Mineral Processing* 119(0): 1-5.
- Varadaraj, R., Bock, J., Valint, P., Zushma, S. and Thomas, R. (1991). Fundamental interfacial properties of alkyl-branched sulfate and ethoxy sulfate surfactants derived from Guerbet alcohols. 1. Surface and instantaneous interfacial tensions. *The Journal of Physical Chemistry* 95(4): 1671-1676.
- Zar, J. H. (1999). *Biostatistical analysis*. Upper Saddle River, N.J., Prentice Hall.
- Zhang, W. (2012). *Frothers and frother blends: A Structure – Function Study* (Ph. D dissertation), McGill University.

Chapter 5 – Effect of methyl branch and hydroxyl positions in alcohols

5.1 Introduction

Many surface related properties find their basis in the structural characteristics of a surfactant, such as hydrocarbon chain length, position and type of alkyl chain branch and location of hydroxyl group. In flotation systems, frothers with branched chains (side chains), e.g., MIBC (methyl isobutyl carbinol) and TEB (triethoxybutane), are sometimes considered to possess desirable frothing properties (Somasundaran and Wang 2006). In the previous chapter, the effect of hydrocarbon alkyl chain length (straight-chain) was investigated. In this chapter, the influence of the position of the methyl branch (i.e., branched-chain) and the hydroxyl group is determined.

As a structural parameter, a branched hydrocarbon chain has significant influence on many surfactant interfacial properties (Lin et al. 1974; Varadaraj et al. 1992; Gibbs and Pomonis 1995; Frank et al. 2007; Adkins et al. 2010). Varadaraj et al. (1992) showed that surfactants with branched chain exhibited higher CMC than their straight chain counterparts due to steric effects. The effect of methyl branch on melting temperature depended upon the location of the methyl branch along the molecule (Gibbs and Pomonis 1995). By adding an alkyl branch, the hydrophobic character, e.g., the solubility of the surfactant is modified (Rosen 2004). Replacement of a single straight hydrocarbon chain by a branched chain containing the same number of carbons decreased the extent of surface tension

reduction (Rosen 2004). Not only chain branching but also branch position affects surface properties. Surfactants with two methyl groups on different carbon atoms are more effective in lowering surface tension than two methyl groups on the same carbon atom (Ezrahi et al. 2005). Positioning a methyl group further away from the hydroxyl group enhanced oil recovery at lower alcohol levels (Backlund et al. 1995). Determining the effect of position of the methyl branch in alcohols is a focus of this chapter.

In addition to methyl branch position, the location of the OH also affects surfactant properties. Studies showed that the chemical reactivity of primary alcohols (i.e., hydroxyl group at 1C position) is greater than the reactivity of secondary alcohols (hydroxyl group at 2C position) (Clayden 2001). Along the same line, surfactants with a hydroxyl group at 1C position are more surface active than surfactants with the OH at a central position (Frank et al. 2007; Cosgrove 2005). The closer the OH is to the center of the chain, the higher the critical micelle concentration (CMC) (Lin et al. 1973). As the hydroxyl position plays an important role in surfactant properties, the hydroxyl position is another focus in this chapter.

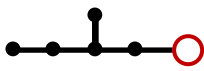

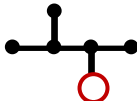
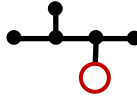
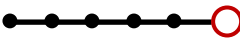
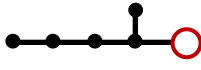
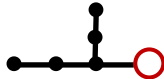
To understand the structure-property relation in alcohols, knowledge of the effect of the position of the methyl branch and hydroxyl group is essential. The objective of this chapter is to determine the impact of OH and $-\text{CH}_3$ position in alcohols using single bubble rise velocity and the concentration to reach minimum velocity (CMV). Diols, which resemble alcohols but with two OH groups, were also tested. One reason to include is that diols with the two OH at terminal

positions are structurally similar to polyglycols, the other major frother family being investigated. This study of diols, therefore, might give some insight into the polyglycol case.

5.2 Reagents

The alcohols comprise seven five-carbon ($C_5H_{12}O$; molecule weight: 88.15 g/mol) and eleven six-carbon ($C_6H_{14}O$, 102.17g/mol) alcohols, listed in Table 5.1 and Table 5.2, respectively. The structural isomers were used to isolate the effect of methyl branch and hydroxyl position from alkyl chain length.

Table 5.1 - Five-carbon alcohol isomers tested

| Name | Structural formula | Structural diagram | Branch position | |
|--------------------|--|--|------------------|----|
| | | | -CH ₃ | OH |
| 2-methyl-1-butanol | CH ₃ CH ₂ CHCH ₃ CH ₂ OH |  | 2 | 1 |
| 3-methyl-1-butanol | CH ₃ CHCH ₃ CH ₂ CH ₂ OH |  | 3 | 1 |
| 2-methyl-2-butanol | CH ₃ CH ₂ CH ₃ COHCH ₃ |  | 2 | 2 |
| 3-methyl-2-butanol | CH ₃ CHCH ₃ CHOHCH ₃ |  | 3 | 2 |
| 1-pentanol | CH ₃ CH ₂ CH ₂ CH ₂ CH ₂ OH |  | - | 1 |
| 2-pentanol | CH ₃ CH ₂ CH ₂ CHOHCH ₃ |  | - | 2 |
| 3-pentanol | CH ₃ CH ₂ CHOHCH ₂ CH ₃ |  | - | 3 |

- Red circle represents hydroxyl group and each black sphere represents a carbon atom


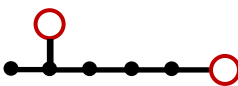


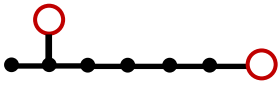

Table 5.2 - Six-carbon alcohol isomers tested

| Name | Structural formula | Structural diagram | Position | |
|---------------------|--|--------------------|------------------|----|
| | | | -CH ₃ | OH |
| 2-methyl-1-pentanol | CH ₃ (CH ₂) ₂ CHCH ₃ CH ₂ OH | | 2 | 1 |
| 3-methyl-1-pentanol | CH ₃ CH ₂ CHCH ₃ (CH ₂) ₂ OH | | 3 | 1 |
| 4-methyl-1-pentanol | CH ₃ CHCH ₃ (CH ₂) ₃ OH | | 4 | 1 |
| 2-methyl-2-pentanol | CH ₃ CH ₂ CHCH ₃ COHCH ₃ | | 2 | 2 |
| 3-methyl-2-pentanol | CH ₃ CH ₂ CHCH ₃ CHOHCH ₃ | | 3 | 2 |
| 4-methyl-2-pentanol | CH ₃ CHCH ₃ CH ₂ CHOHCH ₃ | | 4 | 2 |
| 2-methyl-3-pentanol | CH ₃ CH ₂ CHOHCH ₃ CHCH ₃ | | 2 | 3 |
| 3-methyl-3-pentanol | CH ₃ CH ₂ COHCH ₃ CH ₂ CH ₃ | | 3 | 3 |
| 1-hexanol | CH ₃ (CH ₂) ₅ OH | | - | 1 |
| 2-hexanol | CH ₃ (CH ₂) ₄ OHCH ₃ | | - | 2 |
| 3-hexanol | CH ₃ (CH ₂) ₅ CHOHCH ₂ CH ₃ | | - | 3 |

The diols are listed in Table 5.3 and include five-carbon and six-carbon members selected with one OH at the terminal position and the second OH position changing from 2C to the other terminal position. All reagents were from Sigma-

Aldrich Corporation (Canada) with the highest purity available (> 98%) and were tested as-received.

Table 5.3 - Diols tested for hydroxyl position study

| Name | Structural formula | Structural diagram | Second OH position |
|-----------------|--|--|--------------------|
| 1,2-pentanediol | $\text{CH}_3\text{CH}_2\text{CH}_2\text{CH}(\text{OH})\text{CH}_2\text{OH}$ |  | 1 |
| 1,4-pentanediol | $\text{CH}_3\text{CH}(\text{OH})\text{CH}_2\text{CH}_2\text{CH}_2\text{OH}$ |  | 4 |
| 1,5-pentanediol | $\text{HOCH}_2\text{CH}_2\text{CH}_2\text{CH}_2\text{CH}_2\text{OH}$ |  | 5 |
| 1,2-hexanediol | $\text{CH}_3\text{CH}_2\text{CH}_2\text{CH}_2\text{CH}(\text{OH})\text{CH}_2\text{OH}$ |  | 1 |
| 1,5-hexanediol | $\text{CH}_3\text{CH}(\text{OH})\text{CH}_2\text{CH}_2\text{CH}_2\text{CH}_2\text{OH}$ |  | 5 |
| 1,6-hexanediol | $\text{HOCH}_2\text{CH}_2\text{CH}_2\text{CH}_2\text{CH}_2\text{CH}_2\text{OH}$ |  | 6 |

5.3 Results

5.3.1 Hydroxyl position

Fig 5.1 shows velocity at 300 cm as a function of concentration for three five-carbon (a) and three six-carbon (b) alcohols with OH situated at 1C, 2C, and 3C positions. Noting that the concentration range is about 1 order of magnitude higher for the five-carbon alcohols compared to the six-carbon alcohols otherwise both alcohols show the same trend: the further the OH from the terminal position the less effective the slowing down of the bubble (i.e., the concentration required to reach the same velocity increases).

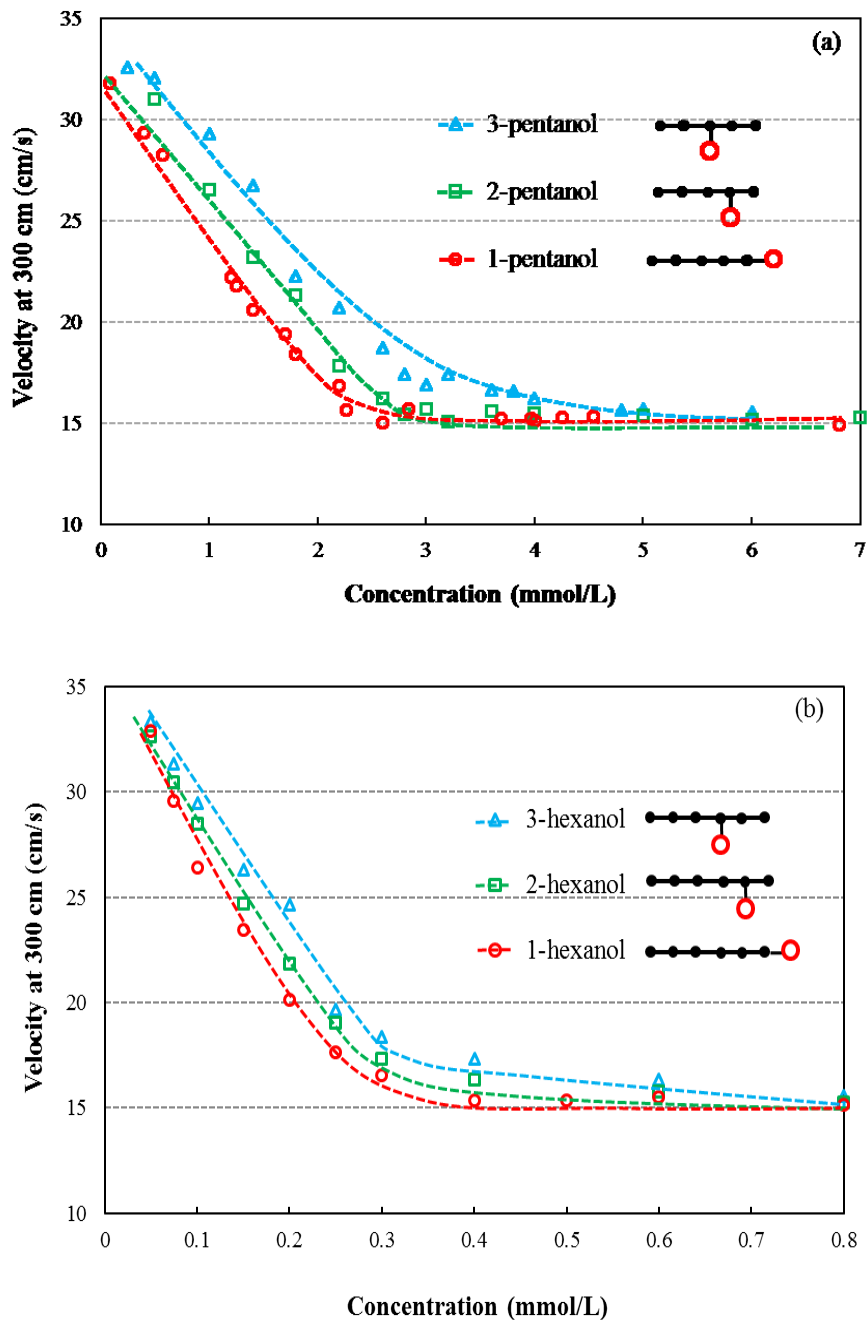


Figure 5.1 – Effect on velocity at 300 cm of hydroxyl position in alcohols: (a) five-carbon; (b) six-carbon

The alcohols with a methyl branch (Fig. 5.2) also showed that moving the OH from the terminal position to 2C, 3C reduced the effectiveness to slow bubble rise

but the impact of OH position was more pronounced than for the straight chain case.

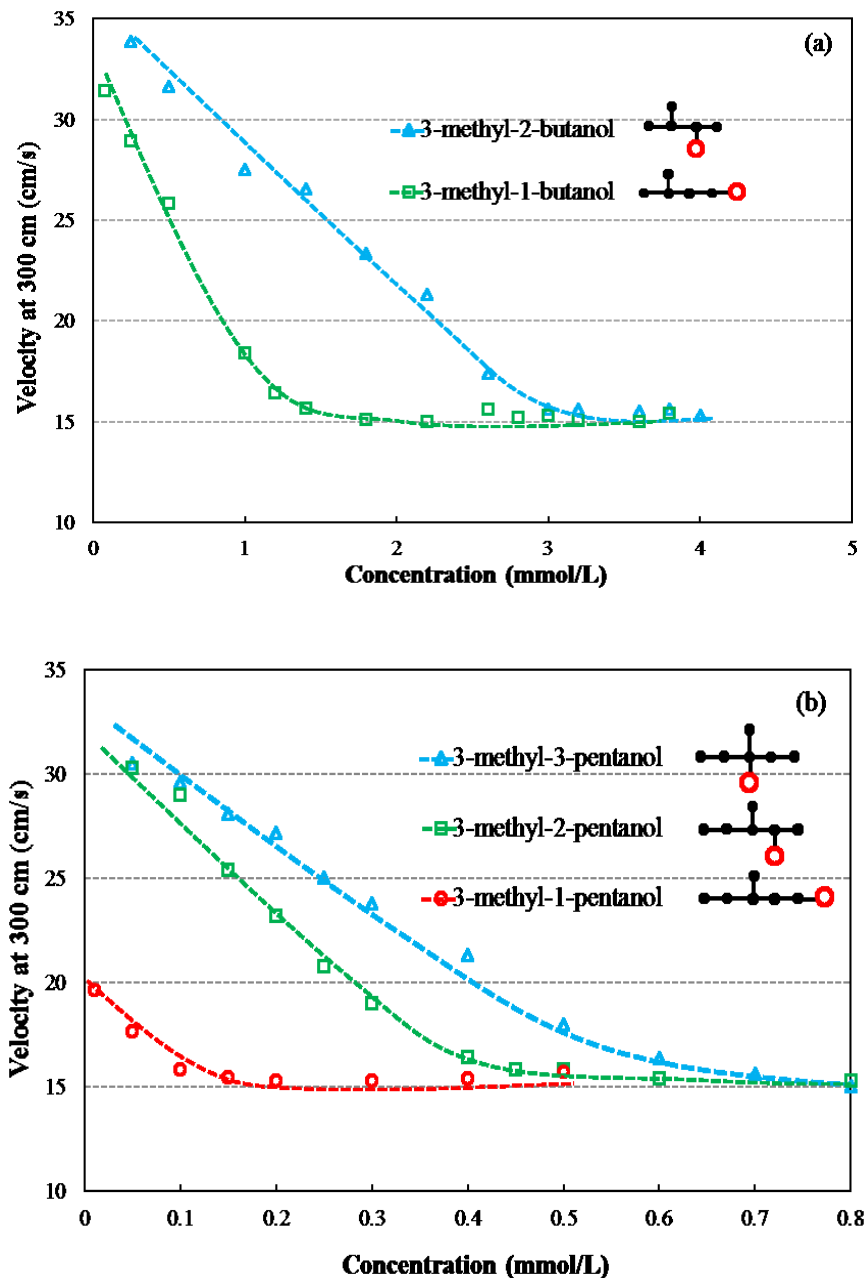
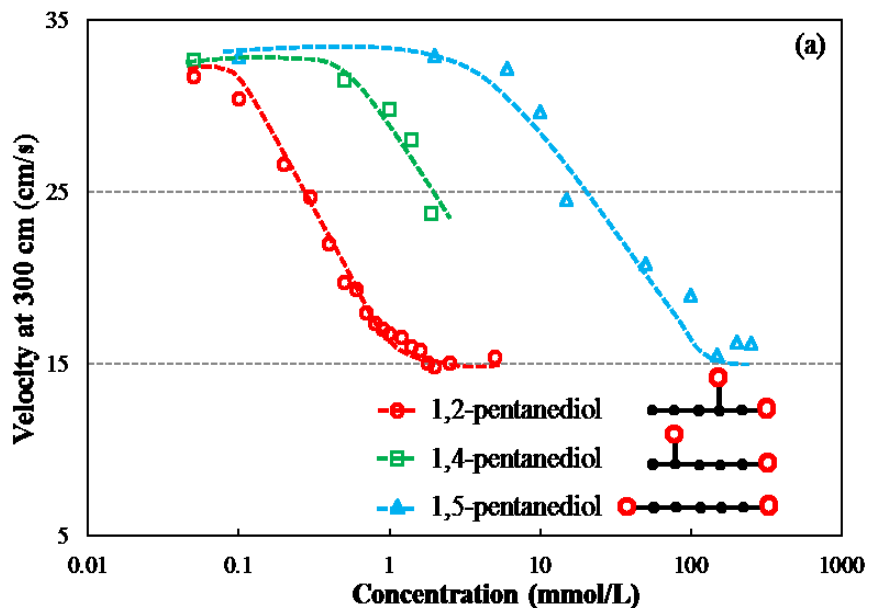


Figure 5.2 – Effect on velocity at 300 cm of hydroxyl position in branched (3-methyl-) alcohols: (a) five-carbon; (b) six-carbon

Fig. 5.3 shows velocity at 300 cm as a function of concentration for three five-carbon diols (Fig. 5.3a) and three six-carbon diols (Fig. 5.3b) with the second OH moving from the 2C position to the far terminal position. Both sets of results show the same significant effect of OH position: that the ability to slow down the bubble rise decreases markedly as the second OH position moves from the 2C position to the other terminus.

The general finding is that there is an impact of the OH position on bubble rise velocity which is more pronounced in the branched alcohols and diols than in the straight chain counterparts.



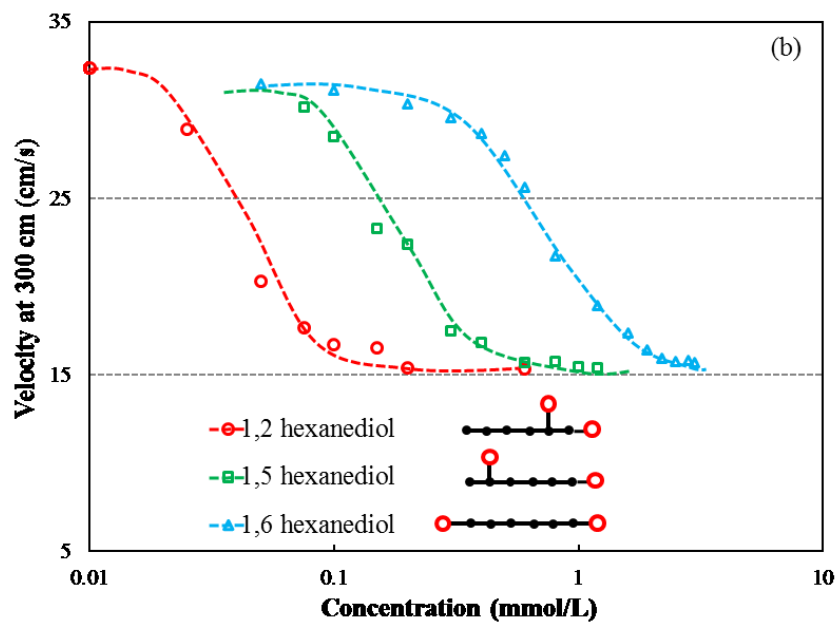


Figure 5.3 – Effect on velocity at 300 cm of position of the second hydroxyl in diols: (a) five-carbon; (b) six-carbon

5.3.2 Methyl branch position

Fig. 5.4a and Fig. 5.4b show the results for the effect of methyl branch position in selected five-carbon and six-carbon alcohols, respectively. They show that the position of methyl branch has a pronounced impact: the further the methyl branch moves away from hydroxyl head group, the more effective the surfactant in slowing down the bubble.

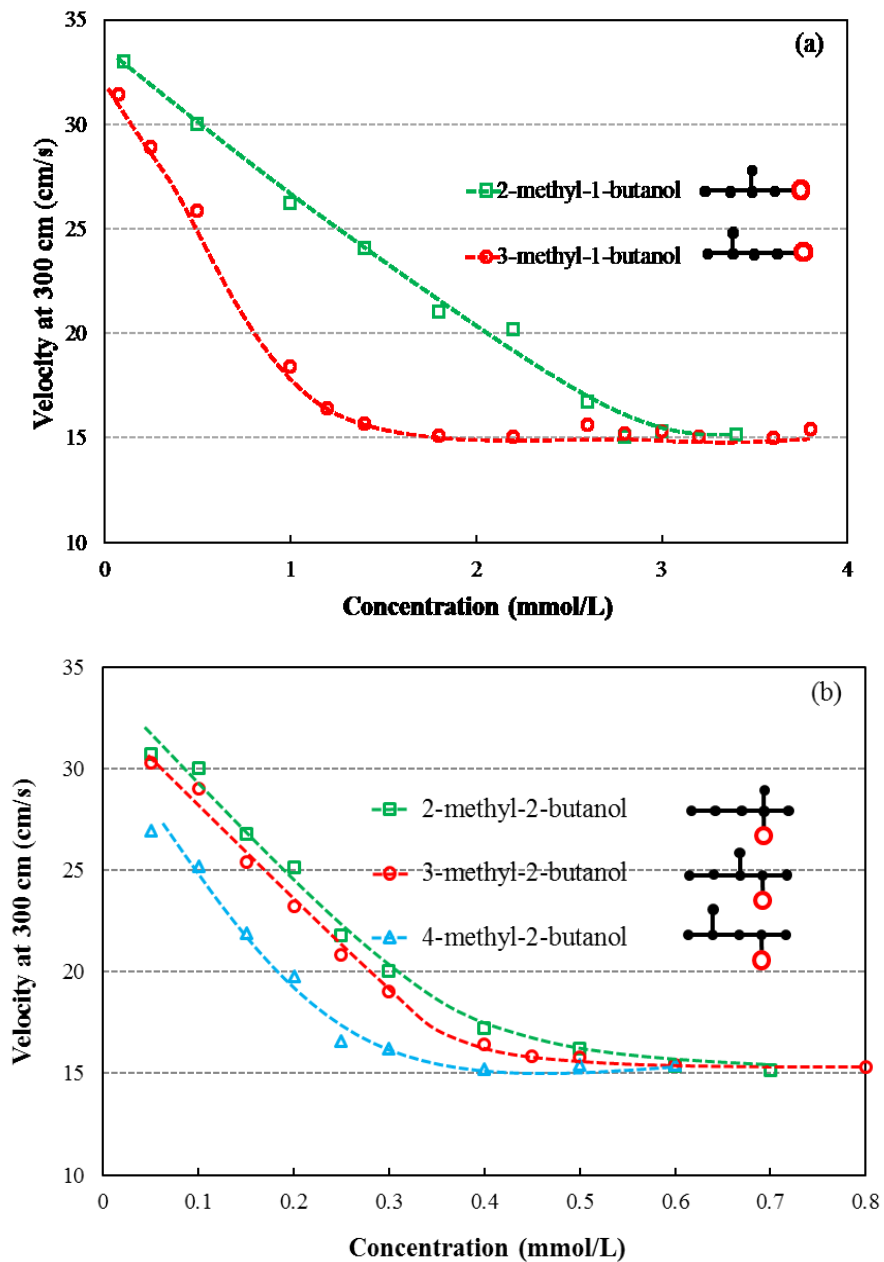


Figure 5.4 – Effect on velocity at 300 cm of the methyl branch position in alcohols: (a) five-carbon; (b) six-carbon

5.3.3 Concentration to reach minimum velocity at 300 cm, CMV

Following the established data reduction scheme, the CMVs were estimated and are summarized in Table 5.4 (alcohols) and Table 5.5 (diols). The further the methyl branch moves away from the hydroxyl head group, the lower the CMV.

Table 5.4 - CMVs for five- and six-carbon alcohols

| Name (Six carbon) | Position | | CMV (mmol/L) | Name (Five carbon) | Position | | CMV (mmol/L) |
|----------------------|------------------|----|-----------------|-----------------------|------------------|----|-----------------|
| | -CH ₃ | OH | | | -CH ₃ | OH | |
| 2-methyl-1-pentanol | 2 | 1 | 0.23 | 2-methyl-1-butanol | 2 | 1 | 1.95 |
| 2-methyl-2-pentanol | 2 | 2 | 0.4 | 2-methyl-2-butanol | 2 | 2 | 3.5 |
| 2-methyl-3-pentanol | 2 | 3 | 0.65 | 3-methyl-1-butanol | 3 | 1 | 1.25 |
| 3-methyl-1-pentanol | 3 | 1 | 0.14 | 3-methyl-2-butanol | 3 | 2 | 3.2 |
| 3-methyl-2-pentanol | 3 | 2 | 0.37 | 1-pentanol | - | 1 | 2.3 |
| 3-methyl-3-pentanol | 3 | 3 | 0.6 | 2-pentanol | - | 2 | 2.65 |
| 4-methyl-1-pentanol | 4 | 1 | 0.11 | 3-pentanol | - | 3 | 3.05 |
| 4-methyl-2-pentanol | 4 | 2 | 0.33 | | | | |
| 1-hexanol | - | 1 | 0.27 | | | | |
| 2-hexanol | - | 2 | 0.3 | | | | |
| 3-hexanol | - | 3 | 0.36 | | | | |

Table 5.5 - CMVs for five- and six-carbon diols

| Name (Six carbon) | Position | | CMV (mmol/L) | Name (Five carbon) | Position | | CMV (mmol/L) |
|----------------------|----------|----|-----------------|-----------------------|----------|----|-----------------|
| | OH | OH | | | OH | OH | |
| 1,2 - hexanediol | 2 | 1 | 0.18 | 1,2 - pentanediol | 2 | 1 | 1.8 |
| 1,5 - hexanediol | 5 | 1 | 0.4 | 1,4 - pentanediol | 4 | 1 | --- |
| 1,6 - hexanediol | 6 | 1 | 2.5 | 1,5 - pentanediol | 5 | 1 | 200 |

* ---: CMV not reached

5.4 Discussion

The effect of hydroxyl position in alcohols and diols and the effect of methyl branch in alcohols on bubble rise velocity and CMV were determined in this chapter. The data complement Chapter 4 where the chain length effect was determined.

A similar trend of hydroxyl position on bubble rise velocity was shown in both alcohols and diols: as the OH was closer to the terminal position the more the rise velocity decreased (for the same surfactant concentration), i.e., the more efficient the surfactant became in slowing the bubble down. The effect of the position of

the second hydroxyl group in diols is more pronounced than OH position effect in alcohols.

The methyl branch position effect was relative to the position of the OH group: with the methyl branch moving away from the OH the surfactant's ability to slow bubble rise increased.

The impact of the different structures is most likely related to the arrangement (packing) of molecules at the air/water interface (bubble surface). Two factors are at play: molecule orientation and the packing density, and hydrocarbon chain interaction effects. Surfactant orientation and packing density are closely related. Interfacial properties are strongly influenced by the surfactant molecular orientation at the interface (van Duynhoven et al. 2005). The orientation at the interface will depend on the structure, in particular the location of the hydrophobic and hydrophilic (OH in the case here) entities.

The effect of OH position on orientation with diols is illustrated for the six-carbon case in Fig. 5.5a. The two OHs in the terminal positions (1, 6-hexanediol) cause the molecule to orient close to horizontally at the air/water interface. When the second OH moves gradually to the 2C position the orientation of the molecule tilts with respect to the interface to approach vertical. It does not fully attain the vertical as both OH groups need to be accommodated on the water side of the interface. A similar series of orientations can be envisaged for the alcohols: the OH in the terminal position likely induces vertical orientation while the molecule

with OH in the middle of the molecule gives close to horizontal arrangement (Fig 5.5b).

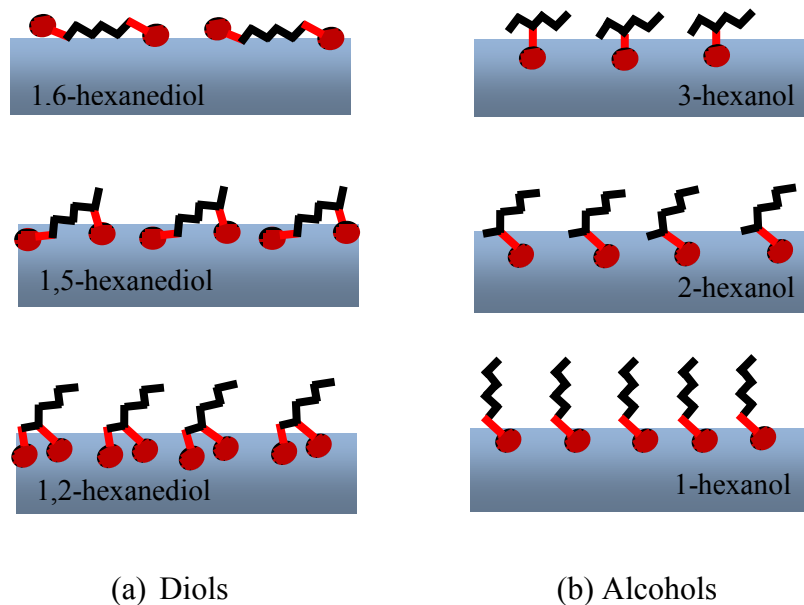


Figure 5.5 – Illustration of effect of hydroxyl position on packing density

The more vertical the arrangement the lower the area occupied per molecule which allows more surfactant molecules to be accommodated, and results in higher packing density. The higher the packing density the greater the surface tension gradients that are produced and thus the more effective the surfactant in slowing the bubble rise. This effect of orientation is seen in the velocity data and in the CMV data, where the greater effectiveness shows up as a lower CMV as OH migrates to the terminus (1 position in alcohols and the second OH at the 2 position in diols).

Another feature may further increase packing density. In both alcohols and diols as the OH migrates to the terminus the free length of hydrocarbon chain increases

which could result in chain-chain interaction. Székely et al. (2007) using small-angle neutron scattering in their study on five-carbon and six-carbon diols found that 1,2-diols exhibited strong chain-chain interaction compared to 1,5-pentanediol and 1,6-hexanediol. These chain interactions associated with the more vertical molecule orientations could result in a further increase in packing with its consequent effect on enhancing surface tension gradients and slowing bubble rise.

The location of methyl branch has a significant effect on slowing the bubble and thus on the CMV value. As the methyl group moves farther from the OH the surfactant is more effective in slowing down the bubble: e.g., 4-methyl-2-pentanol > 3-methyl-2-pentanol > 2-methyl-2-pentanol. The effect of methyl branch position on orientation and packing at the bubble surface is illustrated for two alcohols in Fig 5.6. The impact of methyl position on molecule orientation and packing density can be used to explain the ability to slow the bubble rise velocity.

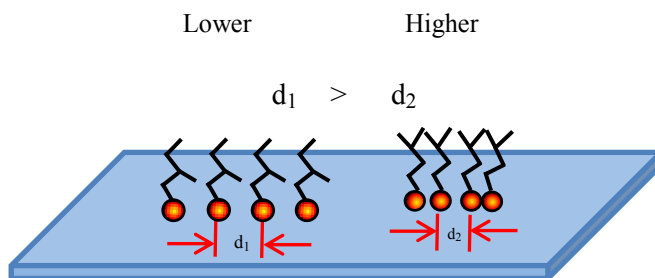


Figure 5.6 – Illustration of effect of methyl position on packing density

Two factors could control packing density with regard to methyl branch position. One is steric hindrance (Wheland 1960; Howarth 1998). The methyl branch on

the hydrocarbon chain restricts the molecule's rotational freedom which reduces the accommodation of the chains in optimal positions (Gradzielski 1998). This steric effect is probably greater the closer the methyl group to the OH which would increase the distance between adsorbed molecules (Fig 5.6).

A second factor is that the methyl group has an inductive effect on the hydroxyl group tending to repel electrons towards the O atom (Singh and Yadav 2010). This electron repulsion effect of alkyl groups is inversely proportional to the distance the alkyl group is from the O atom (Taft 1953; Kim et al. 2007). Moving the methyl group closer to the OH would intensify this electron repulsion and would tend to enlarge the electron cloud around the OH (Streitwieser et al. 1992; Catalán 1996). A consequence is that the distance between two hydroxyl groups of neighboring molecules increases (d_1 , Fig. 5.6) causing a reduction in the packing density. Other studies have shown that a methyl group near the hydroxyl group gave lower surfactant efficiency (Backlund et al. 1995; Ezrahi et al. 2005). Thus both the increased steric hindrance and electron repulsion effects associated with the methyl group approaching the OH group result in less effective slowing of the bubble, i.e., increased CMV as observed.

5.5 Summary

The effect of hydroxyl position in alcohols and diols and methyl branch position in alcohols was investigated in this chapter. The tests were conducted on 18 aliphatic alcohols (7 five-carbon alcohol isomers and 11 six-carbon alcohol isomers) and 6 alkyl diols (three five-carbon and three six-carbon alkyl diol

isomers). The results show that OH at one terminal is the most effective in reducing bubble rise velocity and reducing the concentration to reach minimum velocity (at 300 cm) or CMV. The location of the second OH in diols and OH in branched alcohols has a more pronounced effect than the position of the single OH in the alcohols. When the methyl branch is further away from the OH, the efficiency in slowing bubble velocity increases, i.e., a lower CMV is obtained. The effect of position of the OH and methyl groups is qualitatively explained by the impact on packing of the molecules on the bubble surface.

References

- Adkins, S. S., Chen, X., Nguyen, Q. P., Sanders, A. W. and Johnston, K. P. (2010). Effect of branching on the interfacial properties of nonionic hydrocarbon surfactants at the air–water and carbon dioxide–water interfaces. *Journal of Colloid and Interface Science* 346(2): 455-463.
- Backlund, S., Eriksson, F., Karlsson, S. and Lundsten, G. (1995). Enzymatic esterification and phase behavior in ionic microemulsions with different alcohols. *Colloid & Polymer Science* 273(6): 533-538.
- Catalán, J. (1996). Influence of inductive effects and polarizability on the acid–base properties of alkyl compounds. Inversion of the alcohol acidity scale. *Journal of Physical Organic Chemistry* 9(9): 652-660.
- Clayden, J. (2001). *Organic chemistry*. Oxford; New York, Oxford University Press.
- Cosgrove, T. (2005). *Colloid Science Principles, Methods and Applications*. Department of Chemistry University of Bristol, Bristol, UK, Blackwell Publishing Ltd.
- Ezrahi, S., Tuval, E., Aserin, A. and Garti, N. (2005). The effect of structural variation of alcohols on water solubilization in nonionic microemulsions: 2. Branched alcohols as solubilization modifiers: Results and interpretation. *Journal of Colloid and Interface Science* 291(1): 273-281.
- Frank, C., Frielinghaus, H., Allgaier, J. and Prast, H. (2007). Nonionic surfactants with linear and branched hydrocarbon tails: Compositional Analysis,

- Phase Behavior, and Film Properties in Bicontinuous Microemulsions. *Langmuir* 23(12): 6526-6535.
- Gibbs, A. and Pomonis, J. G. (1995). Physical properties of insect cuticular hydrocarons: The effects of chain length, methyl-branching and unsaturation. *Comparative Biochemistry and Physiology Part B: Biochemistry and Molecular Biology* 112(2): 243-249.
- Gradzielski, M. (1998). Effect of the cosurfactant structure on the bending elasticity in nonionic oil-in-water microemulsions. *Langmuir* 14(21): 6037-6044.
- Howarth, J. (1998). *Core Organic Chemistry*. New York, John Wiley & Sons Ltd.
- Kim, Y., Kay, B. D., White, J. M. and Dohnálek, Z. (2007). Inductive effect of alkyl chains on alcohol dehydration at bridge-bonded oxygen vacancies of TiO₂(110). *Catalysis Letters* 119(1-2): 1-4.
- Lin, I. J., Friend, J. P. and Zimmels, Y. (1973). The effect of structural modifications on the hydrophile--lipophile balance of ionic surfactants. *Journal of Colloid and Interface Science* 45(2): 378-385.
- Lin, I. J. and Metzger, A. (1971). Effect of dissolved paraffinic gases on the surface tension and critical micelle concentration (CMV) of aqueous solutions of dodecylamine hydrochloride (DACl). *The Journal of Physical Chemistry* 75(19): 3000-3004.
- Lin, I. J., Moudgil, B. M. and Somasundaran, P. (1974). Estimation of the effective number of -CH₂- groups in long-chain surface active agents. *Colloid & Polymer Science* 252(5): 407-414.

- Rosen, M. J. (2004). Surfactants and interfacial phenomena. Hoboken, New Jersey, John Wiley & Sons, Inc.
- Singh, J. and Yadav., L. D. S. (2010). Organic chemistry. Vol. 2. <http://site.ebrary.com/id/10417229>.
- Somasundaran, P. and Wang D. (2006). Chapter 5: Application of flotation agents and their structure–property relationships, Solution Chemistry Minerals and Reagents . W. Dianzuo, Elsevier. Volume 17: 143-201.
- Streitwieser, A., Heathcock, C. H. and Kosower, E. M. (1992). Introduction to Organic Chemistry, Times Roman and coudy Old Style by York Graphic Services, Inc.
- Székely, N. K., Almásy, L, Rădulescu, A. and Rosta, L. (2007). Small-angle neutron scattering study of aqueous solutions of pentanediol and hexanediol. Journal of Applied Crystallography 40: s307-s311.
- Taft, R. W. (1953). The general nature of the proportionality of polar effects of substituent groups in organic chemistry. Journal of the American Chemical Society 75(17): 4231-4238.
- van Duynhoven, J., Leika, A. and van der Hoeven, P. (2005). Quantitative assessment of alkyl chain branching in alcohol-based surfactants by nuclear magnetic resonance. Journal of Surfactants and Detergents 8(1): 73-82.
- Varadaraj, R., Bock, J., Zushma, S. and Brons, N. (1992). Influence of hydrocarbon chain branching on interfacial properties of sodium dodecyl sulfate. Langmuir 8(1): 14-17.

Wheland, G. W. (1960). *Advanced Organic Chemistry*. New York, John Wiley & Sons, Inc. London.

Chapter 6 – Effect of number of PO and EO units in polyglycols

6.1 Introduction

The physical/chemical properties of polyglycols are largely dependent on the specific and relative length of their hydrophobic and hydrophilic components (Wu et al. 2010; Rulison 2012). Varying the relative length of the hydrophobic to hydrophilic in the groups allows tailoring a molecule with a designed HLB, molecule weight (Laskowski and Woodburn 1998) and solubility (Pugh 2000). This chapter complements Chapter 4 where the effect of alkyl chain length (i.e., number of carbons, n) in polyglycols was determined. The chapter focuses on polypropylene glycols (PPG) and their alkyl ethers (PPGAE), and polyethylene glycols (PEG) and their alkyl ethers (PEGAE). The aim is to determine the effect of the number of propylene oxide (PO) units (m) and the number of ethylene oxide (EO) units (l) in their corresponding polyglycol.

The number of PO and EO units is closely related to the resulting properties of aqueous solutions of polyglycols. Güvelí et al. (1983) observed that the critical micelle concentration (CMC) of a series of PEGAE ($n = 16, l = 10, 18, 30, 60$) surfactants decreased as the EO chain length increased. With increasing number of EO units in PEGAE the adsorption free energy decreases (Güvelí et al. 1983). Kronberg et al. (1984) also found that with the increasing EO number, the adsorption free energy decreased and the cross-sectional molecular area increased.

A linear decrease of log CMC vs. the number of PO units (m) in PPGAE was reported by Kucharski and Chlebicki (1974).

Studies have shown that the chemical structure of polyglycol frothers affects flotation performance. Pugh (2000) studied commercial polypropylene glycol methyl ethers (i.e., n = 1) and showed that the longer the PO chain the higher the flotation yield at a fixed dosage (60 g/tonne). Tan et al. (2005) studied commercial PPGs (n = 0; m = 3, 6.5, 12.8, 16.5, 34) and found that foamability increased as the PO number increased. Laskowski et al. (2003) studied a range of polypropylene glycol methyl ethers (n = 1; m = 1, 2, 3, 4, 6.3) and found that with an increase in number of PO units the critical coalescence concentration (CCC) decreased. Zhang et al. (2012a) investigated a series of polyglycols from m = 1 to 17 and found that the CCC had an exponential relationship with the number of carbons in the alkyl chain (n) and with the number of PO units. They modeled CCC as an exponential function against HLB. Zhang et al. took the position that to understand commercial frothers a wide range of structures from the same family needed to be tested. This same argument is applied here. The objective of this chapter, therefore, is to determine the effect of the number of PO and EO units in their respective polyglycols on bubble rise velocity and the concentration to reach minimum velocity, CMV.

6.2 Reagents

The reagents in the study are listed in Table 6.1 and 6.2. In the polypropylene glycol family ($C_nH_{2n+1}-(OC_3H_6)_m-OH$) m = 1, 2, 3 and n = 0, 1, 3, 4 (n = 2 is not

available) were tested (Table 6.1), and in the polyethylene glycol family ($C_nH_{2n+1}-(OC_2H_4)_l-OH$) $l = 1, 2, 3$ and $n = 0, 1, 2, 3, 4$ were tested (Table 6.2). All the surfactants were purchased from Aldrich-Sigma with the highest purity (98% to 99.5%) available and were used as supplied.

Table 6.1 - Polypropylene glycol surfactants tested in this study

| Frother family | Name | Chemical structure | | | Mole weight |
|----------------|----------------------------------|-----------------------|---|---|-------------|
| | | Formula | n | m | |
| PPG | Propylene glycol | $H(OC_3H_6)OH$ | 0 | 1 | 76.09 |
| | Dipropylene glycol | $H(OC_3H_6)_2OH$ | | 2 | 134.18 |
| | Tripropylene glycol | $H(OC_3H_6)_3OH$ | | 3 | 192.26 |
| PPGAE | Propylene glycol methyl ether | $CH_3(OC_3H_6)OH$ | 1 | 1 | 90.12 |
| | Dipropylene glycol methyl ether | $CH_3(OC_3H_6)_2OH$ | | 2 | 148.20 |
| | Tripropylene glycol methyl ether | $CH_3(OC_3H_6)_3OH$ | | 3 | 206.28 |
| | Propylene glycol propyl ether | $C_3H_7(OC_3H_6)OH$ | 3 | 1 | 118.18 |
| | Dipropylene glycol propyl ether | $C_3H_7(OC_3H_6)_2OH$ | | 2 | 176.25 |
| | Tripropylene glycol propyl ether | $C_3H_7(OC_3H_6)_3OH$ | | 3 | 234.33 |
| | Propylene glycol butyl ether | $C_4H_9(OC_3H_6)OH$ | 4 | 1 | 132.20 |
| | Dipropylene glycol butyl ether | $C_4H_9(OC_3H_6)_2OH$ | | 2 | 190.28 |
| | Tripropylene glycol butyl ether | $C_4H_9(OC_3H_6)_3OH$ | | 3 | 248.36 |

Table 6.2 - Polyethylene glycol surfactants tested in this study

| Frother family | Name | Chemical structure | | | Mole weight |
|----------------|---------------------------------|-----------------------|---|---|-------------|
| | | Formula | n | l | |
| PEG | Triethylene glycol | $H(OC_2H_4)_3OH$ | 0 | 3 | 150.17 |
| PEGAE | Diethylene glycol methyl ether | $CH_3(OC_2H_4)_2OH$ | 1 | 2 | 120.15 |
| | Triethylene glycol methyl ether | $CH_3(OC_2H_4)_3OH$ | | 3 | 164.20 |
| | Ethylene glycol ethyl ether | $C_2H_5(OC_2H_4)OH$ | 2 | 1 | 90.12 |
| | Diethylene glycol ethyl ether | $C_2H_5(OC_2H_4)_2OH$ | | 2 | 134.17 |
| | Triethylene glycol ethyl ether | $C_2H_5(OC_2H_4)_3OH$ | | 3 | 178.23 |
| | Ethylene glycol propyl ether | $C_3H_7(OC_2H_4)OH$ | 3 | 1 | 104.15 |
| | Diethylene glycol propyl ether | $C_3H_7(OC_2H_4)_2OH$ | | 2 | 148.20 |
| | Ethylene glycol butyl ether | $C_4H_9(OC_2H_4)OH$ | 4 | 1 | 118.17 |
| | Diethylene glycol butyl ether | $C_4H_9(OC_2H_4)_2OH$ | | 2 | 163.23 |
| | Triethylene glycol butyl ether | $C_4H_9(OC_2H_4)_3OH$ | | 3 | 206.28 |

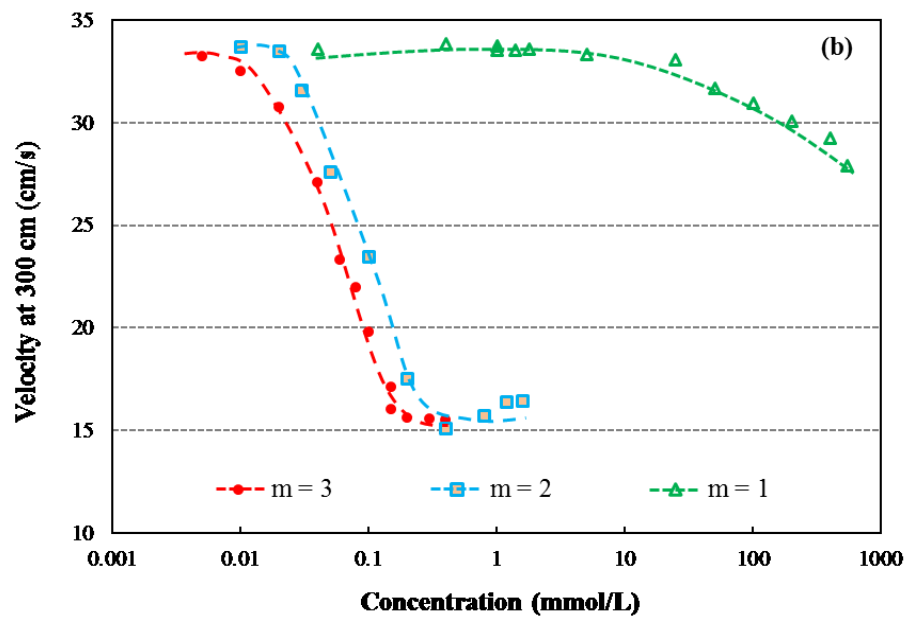
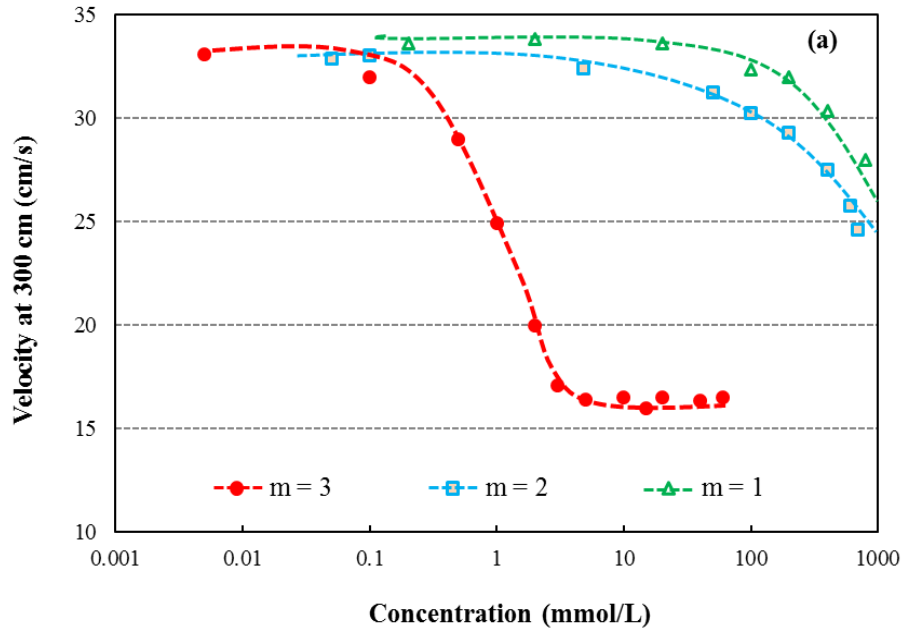
6.3 Results

6.3.1 Velocity at 300 cm and CMV

6.3.1.1 Polypropylene glycols (PPG) and their alkyl ethers (PPGAE)

Fig. 6.1 shows the velocity at 300 cm as a function of concentration for the polypropylene glycol family with $m = 1, 2, 3$ at four values of n , $n = 0$ (a), 1 (b), 3 (c), 4 (d). Fig. 6.1a shows the ability of PPG (i.e., $n = 0$) to slow the bubble depends strongly on m : for $m = 1$ and $m = 2$ the minimum velocity was not reached within the concentration range tested (up to 1.4 mol/L and 0.7 mol/L, respectively).

For PPGAE the ability to slow the bubble is governed by both alkyl chain length (n) and number of PO units (m). With increased n , the ability to reduce bubble rise velocity increases (i.e., the concentration required decreases, as concluded in Chapter 4). For the combination of lowest n ($= 1$) and lowest m ($= 1$) the minimum velocity was not reached up to the concentration 0.55 mol/L tested (Fig. 6.1b). With $m = 2$ the minimum velocity (15 cm/s) was reached at 3.5 mmol/l. For $n = 3$ and 4 the minimum velocity was reached for all three m values. The CMVs for PPG and PPGAE are summarized in Table 6.3.



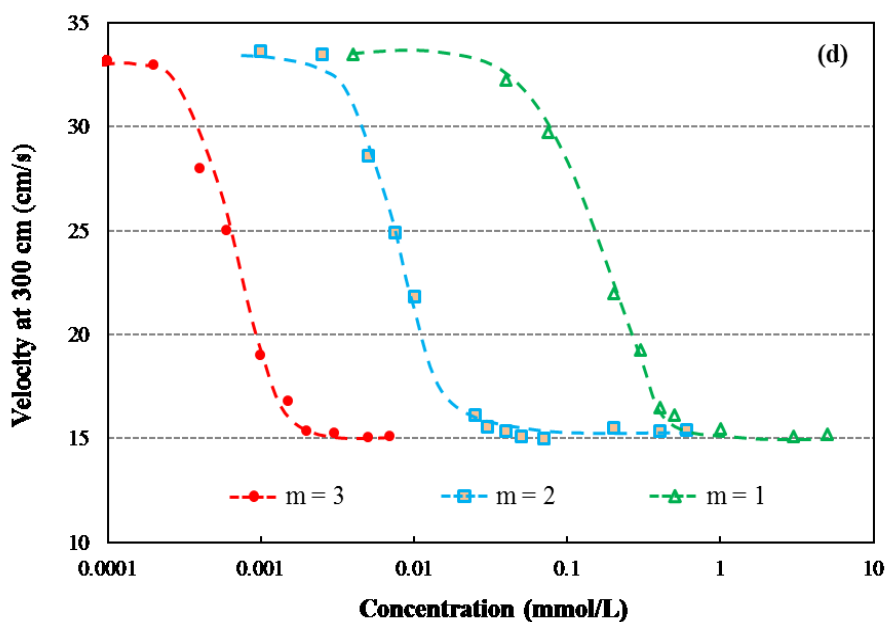
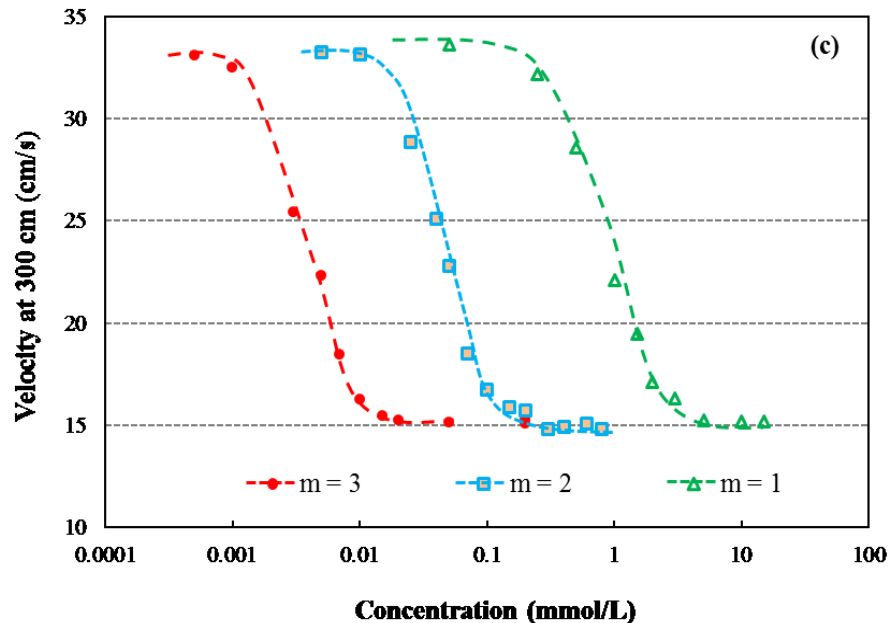
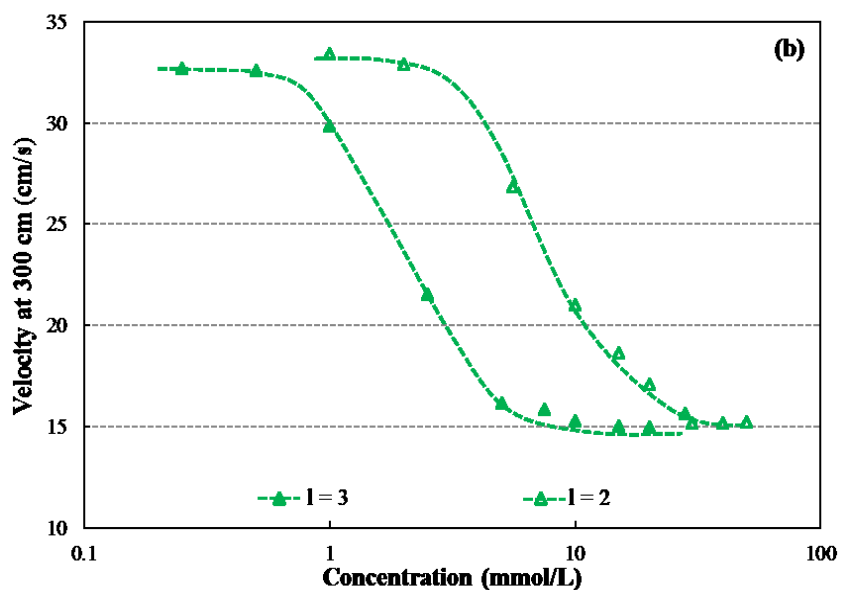
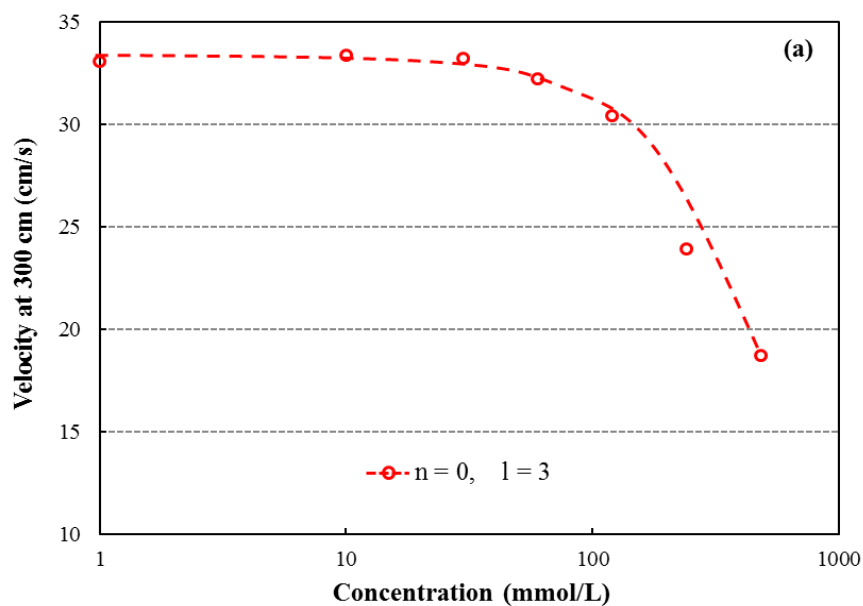


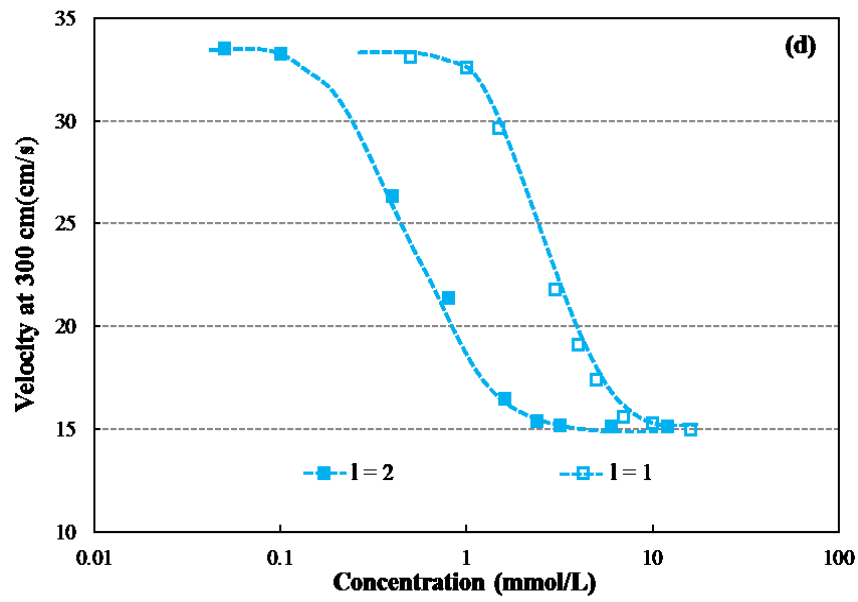
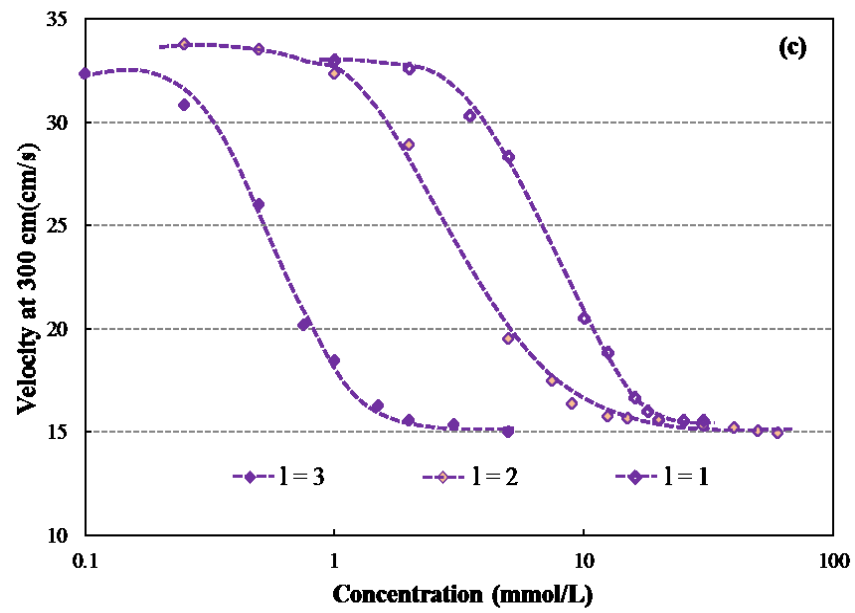
Figure 6.1 – Velocity at 300 cm as a function of concentration for polypropylene glycols and their alkyl ethers: (a) $n = 0$ (i.e., PPG); (b) $n = 1$; (c) $n = 3$; (d) $n = 4$

6.3.1.2 Polyethylene glycols (PEG) and their alkyl ethers (PEGAE)

Fig. 6.2 shows the velocity at 300 cm as a function of concentration for the polyethylene glycol family with $l = 1, 2, 3$ at four values of n , $n = 0$ (a) (i.e., PEG),

1 (b), 2 (c), 3 (d) and 4 (e). For triethylene glycol ($n = 0$; $l = 3$) minimum velocity was not achieved up to 0.48 mol/L (Fig 6.2a) so shorter EO chains ($n = 0$; $l = 1, 2$) were not tested. The CMV values for the polyethylene glycols are summarized in Table 6.3.





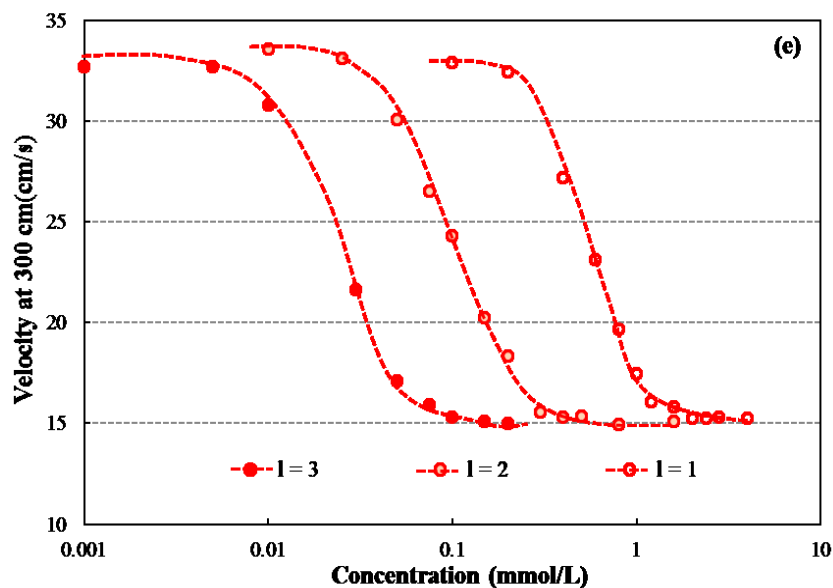


Figure 6.2 – Velocity at 300 cm as a function of concentration for polyethylene glycols and their alkyl ethers: (a) $n = 0$ (i.e., PEG); (b) $n = 1$; (c) $n = 2$; (d) $n = 3$; (e) $n = 4$

Table 6.3 - CMV for polyglycol ethers as function of PO/EO number

| Frother family | Name | n | m (PO) or l (EO) | CMV (mmol/L) | |
|----------------|--------------------------------------|--------------------------------------|------------------|--------------|--------|
| PPG | Propylene glycol | 0 | 1 | --- | |
| | Dipropylene glycol | | 2 | --- | |
| | Tripropylene glycol | | 3 | 4 | |
| PPGAE | Propylene glycol methyl ether | 1 | 1 | --- | |
| | Dipolypropylene glycol methyl ether | | 2 | 3.5 | |
| | Tripolypropylene glycol methyl ether | | 3 | 0.2 | |
| | PPGAE | Propylene glycol propyl ether | 3 | 1 | 3 |
| | | Dipolypropylene glycol propyl ether | | 2 | 0.14 |
| | | Tripolypropylene glycol propyl ether | | 3 | 0.01 |
| | PPGAE | Propylene glycol butyl ether | 4 | 1 | 0.5 |
| | | Dipolypropylene glycol butyl ether | | 2 | 0.024 |
| | | Tripolypropylene glycol butyl ether | | 3 | 0.0014 |
| PEG | Triethylene glycol | 0 | 3 | --- | |
| PEGAE | Diethylene glycol mono-methyl ether | 1 | 2 | 25 | |
| | Triethylene glycol mono-methyl ether | | 3 | 7 | |
| | PEGAE | Ethylene glycol mono-ethyl ether | 2 | 1 | 20 |
| | | Diethylene glycol mono-ethyl ether | | 2 | 10 |
| | | Triethylene glycol mono-ethyl ether | | 3 | 1.4 |
| | PEGAE | Ethylene glycol mono-propyl ether | 3 | 1 | 6.5 |
| | | Diethylene glycol mono-propyl ether | | 2 | 1.8 |
| | PEGAE | Ethylene glycol mono-butyl ether | 4 | 1 | 1.1 |
| | | Diethylene glycol mono-butyl ether | | 2 | 0.4 |
| | | Triethylene glycol mono-butyl ether | | 3 | 0.08 |

6.3.2 Effect of PO (m) number and EO (l) number on CMV

The log CMV as a function of PO (m) number and EO (l) number at a given alkyl carbon (n) number is shown in Fig. 6.3. The pattern for both PPGAE and PEGAE is that log CMV decreased as m/l increased in a series of self-similar linear plots shifting to lower CMV as n increased. These patterns are new findings.

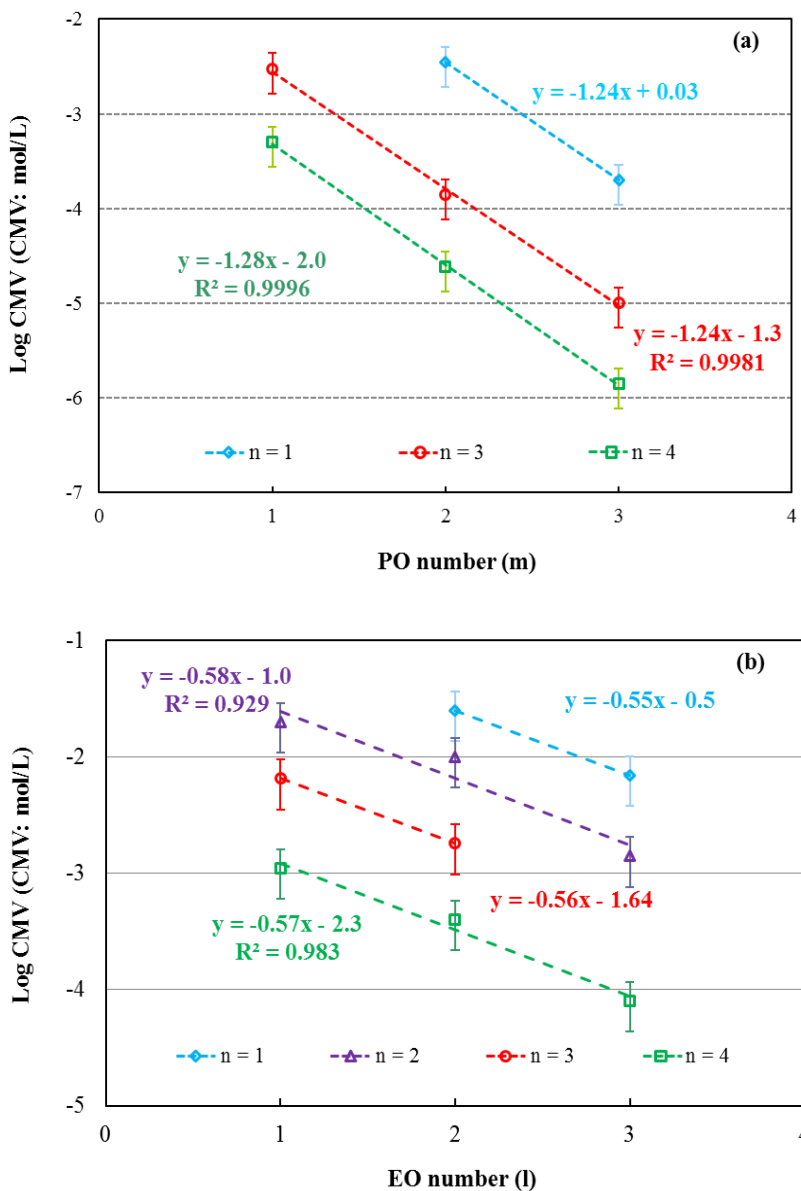


Figure 6.3 – Log CMV as a function of: (a) PO (m) number; (b) EO (l) number

6.4 Discussion

Bubble rise velocity in surfactant solution is dictated by the nature, amount and packing of surfactant accumulating on the bubble surface. The velocity profile, in particular the deceleration stage, is an indicator of this adsorption process (Sam et al. 1996). The surfactant adsorption density on the bubble surface depends on packing density which is related to the chemical structure, i.e., the nonpolar hydrophobic hydrocarbon chain and the polar hydrophilic head(s), in this case OH and $-O-$ linkages in the PO/EO units. Chapter 4 covered the effect of hydrocarbon chain length (n , number of carbons). In this chapter, the number of PO groups (m) and the number of EO groups (l), i.e., the PO and EO unit (or chain) length, were studied.

From the velocity profile the velocity at 300 cm was determined. The velocity at 300 cm was plotted as a function of concentration and m (PO number) in the polypropylene glycol alkyl ether family and as a function of l (EO number) in the polyethylene glycol alkyl ether family (as only one PPG, tripropylene glycol, reached CMV, PPG is not included in the plot). From the velocity at 300 cm vs. concentration plots the CMV were determined. With increasing m/l , the CMV decreases.

The number of propylene oxide (PO) and ethylene oxide (EO) units evidently plays an important role in slowing bubble rise and decreasing CMV. The mechanism is related to the structure and its impact on adsorption. At the air/water interface the polar $-O-$ linkages along the PO/EO unit chain length

cause the molecule to orientate horizontally (Schick 1962). This orientation gives multiple sites along the bubble surface for hydrogen bonding with neighboring water molecules. The rising motion of the bubble means constant breaking and forming of these H-bonds which can be considered to increase surface viscosity. Increasing the PO/EO unit number would increase the number of H-bonds increasing surface viscosity, and thus increasing drag and slowing bubble rise (Nguyen and Schulze 2004).

A linear relationship of log CMV as a function of m/l was found for both PPGAE and PEGAE families. The polyglycol surfactants share a common trait regardless of n (Fig. 6.3), namely a slope of ca. -1.25 against m in PPGAE family, and a slope of ca. -0.57 against l in the PEGAE family. Chapter 4 showed a linear relationship of log CMV against n in the PPGAE family with a slope of ca. -0.74 independent of m, and for the PEGAE family a slope of ca. -0.63 independent of l. Considering both the hydrocarbon chain effect (Chapter 4) and the PO/EO unit effect (this chapter) empirical equations can be proposed:

$$\text{For PPGAE: } \log [\text{CMV}] = -a \times n - b \times m + \text{constant 1} \quad 6.1$$

$$\text{For PEGAE: } \log [\text{CMV}] = -a \times n - b \times l + \text{constant 2} \quad 6.2$$

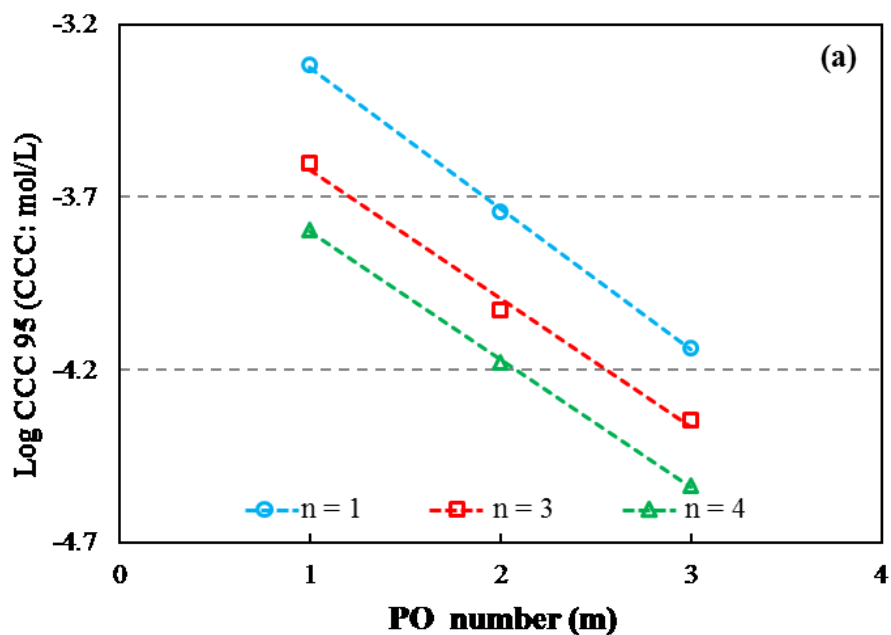
where a and b and are constants and are listed in Table 6.4

Table 6.4 - Constants in Eq. 6.1 and 6.2

| No. | Family | a | b | constant |
|-----|--------|------|------|----------|
| 1 | PPGAE | 0.74 | 1.25 | 0.862 |
| 2 | PEGAE | 0.63 | 0.57 | 0.212 |

These findings bear a similarity to those of a previous study relating critical coalescence concentration to carbon n number and m in PPGs (Zhang et al. 2012a) (see Chapter 4, Fig. 4.10). Zhang et al. (2012a; 2012b) determined the critical coalescence concentration (CCC) for some of the same surfactants used in the present study. They showed an exponential relationship between CCC and m and n, which can be re-arranged as in Fig. 6.4 to show the same log CCC vs. m or l trend as observed here for CMV.

Zhang et al. (2012a) went on to assess the CCC data against the hydrophilic-lipophilic balance (HLB) (Davis 1957). Following that lead, in Chapter 7 a similar analysis connecting CMV and HLB is attempted.



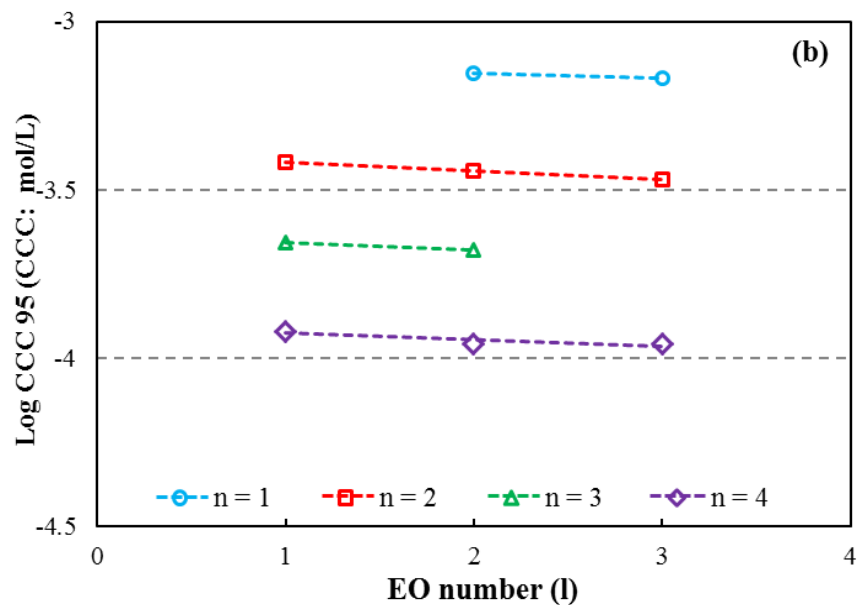


Figure 6.4 – Log CCC as a function of (a): PO (m) number; (b) EO (l) number

6.5 Summary

The aim of this chapter on polyglycols was to establish the impact of the number of propylene oxide (PO) m units and the number of ethylene oxide (EO) l units on bubble rise velocity and CMV. Twelve polypropylene glycol and their alkyl ethers with $m = 1, 2, 3$ and twelve polyethylene glycol and their alkyl ethers with $l = 1, 2, 3$ were investigated. The most significant findings were:

1. At a given alkyl group chain length and concentration bubble rise velocity decreases with the increase of m/l.
2. The decrease in velocity is argued to be due to role of the –O– linkages causing the molecule to orient horizontally at the bubble surface and increase surface viscosity because of H-bonding with neighboring water molecules.

3. At a given alkyl group chain length the log CMV decreases with the increase of m/l .
4. At given alkyl group chain length a series of self-similar linear plots of log CMV as a function of m/l was found.
5. Empirical relationships were established relating CMV to n (number of carbons in the alkyl chain) and m/l .
6. Using literature critical coalescence concentration (CCC) data a linear log CCC vs. m was shown, i.e., the same form as the log CMV vs. m relationship.

References

- Davies, J. T. (1957). A quantitative kinetic theory of emulsion type, I. Physical chemistry of the emulsifying agent. Gas/Liquid and Liquid/Liquid Interface Proceedings of the International Congress of Surface Activity: 426-438
- Güvelí, D. E., Davis, S. S. and Kayes, J. B. (1983). Critical micelle concentration, surface, volumetric, and hydrodynamic properties of polyoxyethylenemonohexadecyl ethers. *Journal of Colloid and Interface Science* 91(1): 1-11.
- Kronberg, B., Stenius, P. and Thorssell, Y. (1984). Adsorption of nonylphenol-poly(propylene oxide)-poly(ethylene oxide) nonionic surfactants on polystyrene latex. *Colloids and Surfaces* 12(0): 113-123.
- Kucharski, S. and Chlebicki, J. (1974). The effect of polyoxypropylene chain length on the critical micelle concentration of propylene oxide—ethylene oxide block copolymers. *Journal of Colloid and Interface Science* 46(3): 518-521.
- Laskowski, J. S., Tlhone, T., Williams, P. and Ding, K. (2003). Fundamental properties of the polyoxypropylene alkyl ether flotation frothers. *International Journal of Mineral Processing* 72(1-4): 289-299.
- Laskowski, J. S. and Woodburn, E. T. (1998). *Frothing in flotation II* Amsterdam, Netherlands Gordon and Breach Science Publishers.

- Nguyen, A. V. and Schulze, H. J. (2004). Colloidal Science of flotation, Surfactant science series New York, New York Basel. Vol. 118 pp: 70-73
- Pugh, R. J. (2000). Non-ionic polyethylene oxide frothers in graphite flotation. Minerals Engineering 13(2): 151-162.
- Rulison, C. (2012). Critical Micelle Concentration as a function of head group size for alkyl alcohol ethoxylates. Application notes # 201(Instrumentation and laboratory services for surface science): 1-5.
- Sam, A., Gomez, C. O. and Finch, J. A. (1996). Axial velocity profiles of single bubbles in water/frother solutions. International Journal of Mineral Processing 47(3-4): 177-196.
- Schick, M. J. (1962). Surface films of nonionic detergents—I. Surface tension study. Journal of Colloid Science 17(9): 801-813.
- Tan, S. N., Fornasiero, D., Sedev, R. and Ralston, J. (2005). The role of surfactant structure on foam behavior. Colloids and Surfaces A: Physicochemical and Engineering Aspects 263(1-3): 233-238.
- Wu, Y., Iglauer, S., Shuler, P. and Tang, Y. (2010). Branched alkyl alcohol propoxylated sulfate surfactants for improved oil recovery. Tenside Surf. Det. 47(3): 152-161.
- Zhang, W., Nasset, J. E., Rao, S. R. and Finch, J. A. (2012)a. Characterizing frothers through Critical Coalescence Concentration (CCC)95-

Hydrophile-Lipophile Balance (HLB) Relationship. Minerals 2(3): 208-227.

Zhang, W., Nasset, J. E., Rao, S. R. and Finch, J. A. (2012)b. Frother function-structure relationship: Dependence of CCC95 on HLB (in preparation.)

Chapter 7 – Relationship between CMV and HLB

7.1 Introduction

In this chapter, the relationship between concentration to reach minimum velocity (CMV) and the hydrophilic-lipophilic balance (HLB) is determined and the relationship between critical coalescence concentration (CCC) and HLB of Zhang et al. (2012) revisited. As background, HLB and CCC are briefly reviewed.

7.1.1 Hydrophilic-Lipophilic Balance (HLB)

A common method of characterizing surfactants is based on their hydrophilic-lipophilic balance (HLB) (Graciaa et al. 1982). The HLB concept was first proposed by Clayton in a series of patents in 1933 (Kunieda and Shinoda 1985). He pointed out that: “In a given homologous series of surfactants, there is a point of range in which the hydrophilic and lipophilic properties is balanced and an optimum efficiency is reached for the particular applications.” The concept is that since the surfactant molecule contains both hydrophilic and lipophilic (hydrophobic) groups the ratio of these two groups should determine its physiochemical behavior.

Subsequently, many methods have been proposed to calculate the HLB number (Griffin 1954; Davies 1957; Davies and Rideal 1961; Schick and Beyer 1963; Heusch 1970; Lo et al. 1972; Marszall and Lin 1978; Graciaa et al. 1989). Two commonly used methods are the Griffin method and the Davies method. Griffin (1954) proposed a semi-empirical HLB scale based on determination of the stability of emulsions for non-ionic surfactants. Davies (1957) introduced a

structural definition of HLB which tries to account for the effects of all the hydrophilic and lipophilic functional groups of a molecule. Davies assumed that HLB was an additive and constitutive indicator with hydrophilic and lipophilic (hydrophobic) group numbers assigned to various structural components. In the Davies method, both the structural layout of the molecule and the chemical formula are taken into consideration. The Davies equation (Eq. 7.1) allows us to calculate the HLB number of a surfactant as a sum of structural factors:

$$\text{HLB} = 7 + \Sigma (\text{hydrophilic group numbers}) + \Sigma (\text{hydrophobic group numbers}) \quad 7.1$$

The HLB value represents the relative tendency of a surfactant molecule to transfer from an aqueous to a hydrocarbon environment and vice versa (Marszall and Lin 1978). The commonly used HLB group numbers in Davies method relevant to the frother family studied here are listed in Table 7.1.

Table 7.1 - Selected group number HLB value used in Davies method

| Functional group | | Group HLB value |
|--------------------------|--|-----------------|
| Hydrophilic | -OH | 1.9 |
| | -O- | 1.3 |
| Lipophilic (Hydrophobic) | >CH-; -CH ₂ -; -CH ₃ ; | -0.475 |

All the HLB numbers calculated in this study are based on the Davies equation. Examples of calculation are given for MIBC (4-methyl-2-pentanol) (Eq. 7.2), where we have one OH group and 6 C in the alkyl group (i.e. C₆H₁₃), and tripropylene glycol butyl ether (Eq. 7.3) (C₄H₉(OC₃H₆)₃OH), where we have 13 C in the alkyl chain, three O atoms and one OH groups.

$$\text{HLB (MIBC)} = 7 + 1.9 - (6 \times 0.475) = 6.05 \quad 7.2$$

$$\begin{aligned} \text{HLB (Tripropylene glycol butyl ether)} &= 7 + 1.9 + (1.3 \times 3) - (13 \times 0.475) \\ &= 6.625 \end{aligned} \qquad 7.3$$

The range of HLB numbers for nonionic surfactants is from 1-20, while for ionic surfactants (e.g., sodium dodecyl sulphate) it may be as high as 40 (Kruglyakov 2000). The HLB number for flotation frothers varies from 4 to 10 (Waldhoff and Spilker 2005). Surfactants with HLB numbers >10 have an affinity for water (hydrophilic, or lipid insoluble) and those with HLB numbers < 10 have an affinity for organic environments (lipophilic, or water insoluble). As an aide-memoire, as the HLB number decreases this means that the surfactant molecule is becoming more hydrophobic (lipophilic) and less water-soluble.

The relationship between HLB and various properties of surfactants has been the subject of many studies (Ross et al. 1959; Schott 1969; Boyd et al. 1972; Lin 1972; Lin and Marszall 1976; Morgen et al. 1977; Little 1978; Salager et al. 1980; Kunieda and Shinoda 1985; Rabaron et al. 1993; Verdinelli et al. 2008). Harris and Jia (2000) showed that the HLB number of a frother can be related to flotation recovery. They noted two important structural features of a frother: a hydrophobic group to lower the HLB number and to increase surface activity, and the arrangement of oxygen atoms and alkyl groups in the molecular chain. Laskowski [2003] and Pugh [2000] discussed a link between frother functions and HLB. Successful frothers appear to have HLB values close to 6 (Laskowski 1993; Laskowski 2004). Zhang et al. (2012a) related the critical coalescence concentration (CCC) to HLB for a series of surfactants from two frother families,

alcohols and polypropylene glycols. They modeled the relationship in a series of exponential equations dependent on the family and showed that the CCC for commercial frothers could be predicted from the model.

7.1.2 Critical Coalescence Concentration (CCC)

The commonly used tool to characterize frothers is to plot the Sauter mean bubble size (D_{32}) as a function of concentration (Cho and Laksowski 2002). The Sauter mean diameter (size), developed by Sauter in the late 1920s (Sauter 1928), is defined as the diameter of a sphere that has the same volume/surface area ratio as the bubble size distribution. The Sauter mean bubble size decreases exponentially as a function of frother concentration to reach a minimum size at a certain concentration (Aveyard 1991). The ability of frother to reduce bubble size is usually ascribed to reduced bubble coalescence (Harris 1976).

Cho and Laskowski (2002) introduced the term ‘critical coalescence concentration (CCC)’ to refer to the minimum concentration required to produce the minimum size bubble, arguing it corresponded to the concentration that completely prevented bubble coalescence. They used a graphical method to estimate CCC. The CCC has been shown to decrease with increasing frother molecular weight and is claimed to be a material constant independent of machine type and geometry (Grau et al. 2005). Laskowski (2003) showed that frothers with low CCC values had low HLB numbers, but no general correlation emerged based on the few commercial frothers tested.

Recognizing the difficulty of identifying the end point of an exponential function, Nasset et al. (2007) adopted a three-parameter model to fit the Sauter mean bubble size-concentration relationship and extracted a CCC95, the concentration giving 95% bubble size reduction compared to water only. Zhang et al. (2012a) developed relationships between CCC95 and HLB by using virtually all the available surfactants from two frother families, alcohols and polyglycols (polypropylene glycols and their ethers). Empirical models were developed for the polyglycols and 1-alcohols showing that each family exhibits a unique CCC95-HLB relationship dependent on frother structure variables, e.g., alkyl chain length (n , number of carbons) and number of propylene oxide groups (m). They did question the unique numbers assigned to all OH and CH groups regardless of location in the molecule, a factor that made it impossible to include isomers in the CCC95-HLB relationships.

7. 2 HLB, CMV and CCC values

Tables 7.2 and 7.3 give the HLB number (from the Davies equation), the CMV values (Chapters 4 and 6), and the CCC95 values (Zhang et al. 2012a; Zhang et al. 2012b) for the alcohol and polyglycol families, respectively. The CCC and CCC95 data were shown to be similar, and often the term CCC will be substituted for CCC95 for discussion purposes. The structure variables are the hydrocarbon n number and the PO/EO (m/l) number.

Table 7.2 - Aliphatic alcohols: HLB, CMV and CCC

| Alcohols | Name | n | HLB | CMV | CCC95 ^{1,*} |
|----------|-----------------|---|---------------|----------|----------------------|
| | | | Davies method | (mmol/L) | (mmol/L) |
| Alcohols | 1-butanol | 4 | 7.00 | 20 | 0.85 |
| | 1-pentanol | 5 | 6.53 | 2.3 | 0.29 |
| | 1-hexanol | 6 | 6.05 | 0.27 | 0.11 |
| | 1-heptanol | 7 | 5.58 | 0.06 | 0.072 |
| Diols | 1,2-propanediol | 3 | 9.38 | ---- | ---- |
| | 1,2-butanediol | 4 | 8.90 | 20 | ---- |
| | 1,2-pentanediol | 5 | 8.43 | 1.8 | ---- |
| | 1,2-hexanediol | 6 | 7.95 | 0.18 | ---- |

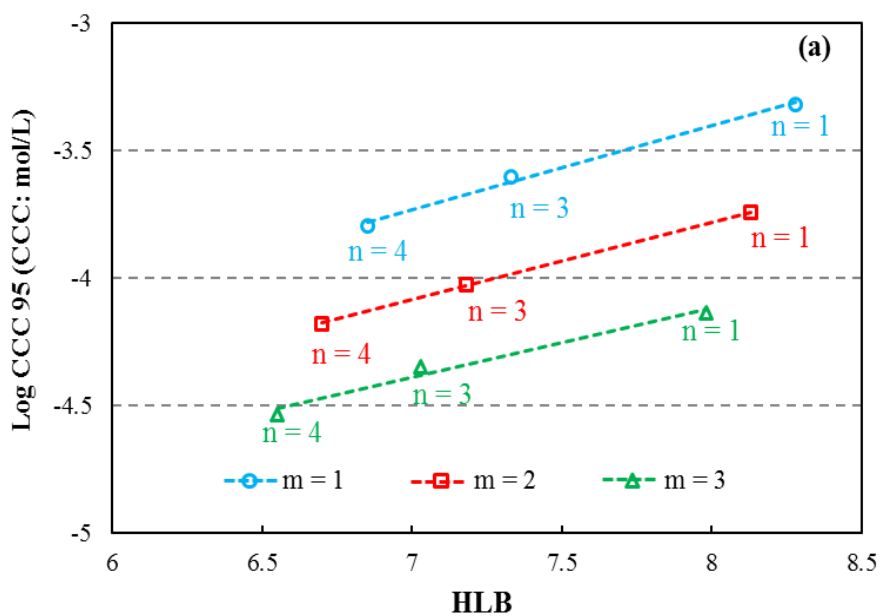
Table 7.3 - Polypropylene and polyethylene alkyl glycol ethers: HLB, CMV and CCC

| Frother family | Name | n | m /l | HLB | CMV | CCC95 ^{2,3} |
|----------------|---------------------------|---|------|---------------|----------|----------------------|
| | | | | Davies method | (mmol/L) | (mmol/L) |
| PPGAE | Propylene glycol ether | 1 | 1 | 8.30 | - | 0.48 |
| | | 3 | | 7.35 | 3 | 0.25 |
| | | 4 | | 6.88 | 0.5 | 0.16 |
| | Dipropylene glycol ether | 1 | 2 | 8.18 | 3.5 | 0.18 |
| | | 3 | | 7.23 | 0.14 | 0.094 |
| | | 4 | | 6.75 | 0.024 | 0.066 |
| | Tripropylene glycol ether | 1 | 3 | 8.05 | 0.2 | 0.073 |
| | | 3 | | 7.10 | 0.01 | 0.045 |
| | | 4 | | 6.63 | 0.0014 | 0.029 |
| PEGAE | Ethylene glycol ether | 2 | 1 | 8.3 | 20 | 0.38 |
| | | 3 | | 7.83 | 6.5 | 0.22 |
| | | 4 | | 7.35 | 1.1 | 0.12 |
| | Diethylene glycol ether | 1 | 2 | 9.13 | 25 | 0.7 |
| | | 2 | | 8.65 | 10 | 0.36 |
| | | 3 | | 8.75 | 1.8 | 0.21 |
| | | 4 | | 7.70 | 0.4 | 0.11 |
| | | 6 | | 6.75 | 0.025 | 0.068 |
| | Triethylene glycol ether | 1 | 3 | 9.48 | 7 | 0.68 |
| | | 2 | | 9.00 | 1.4 | 0.34 |
| | | 4 | | 8.05 | 0.08 | 0.11 |

*: CCC95 from literature (1: Zhang 2012; 2: Zhang, et al., 2012a and 3: Zhang, et al. 2012b)

7.3 CCC vs. HLB

Zhang et al. (2012a) showed that the CCC–HLB relationship depended on the n (number of carbons in alkyl chain) and m (number of propylene oxide groups). They used an exponential equation to fit the data but that also suggests a log-based relationship could be substituted. Based on their results, Figs 7.1 and 7.2 show the log CCC versus the HLB for PPGAE as a function of n and m and PEGAE as a function of n and l , respectively. Each member of the family shares a similar trend (slope), i.e., the trends are self-similar.



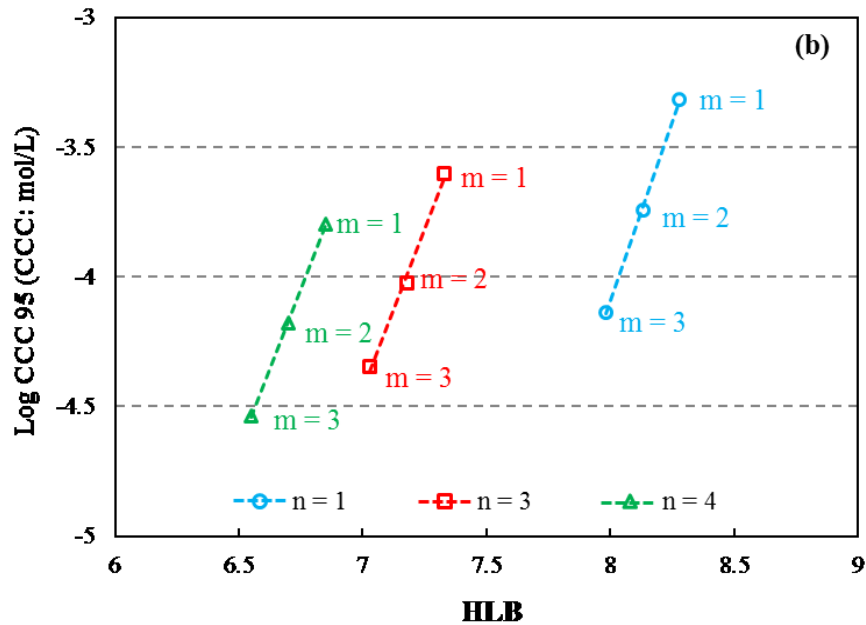
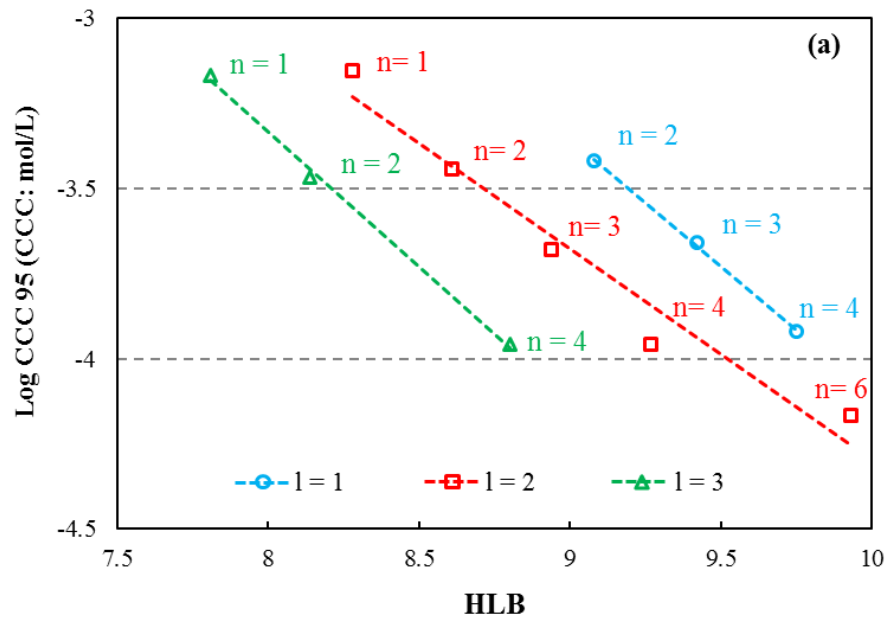


Figure 7.1 – Log CCC vs. HLB for PPGAE family as a function of: (a) carbon (n); (b) PO (m) number (dashed lines are least squares best fit)



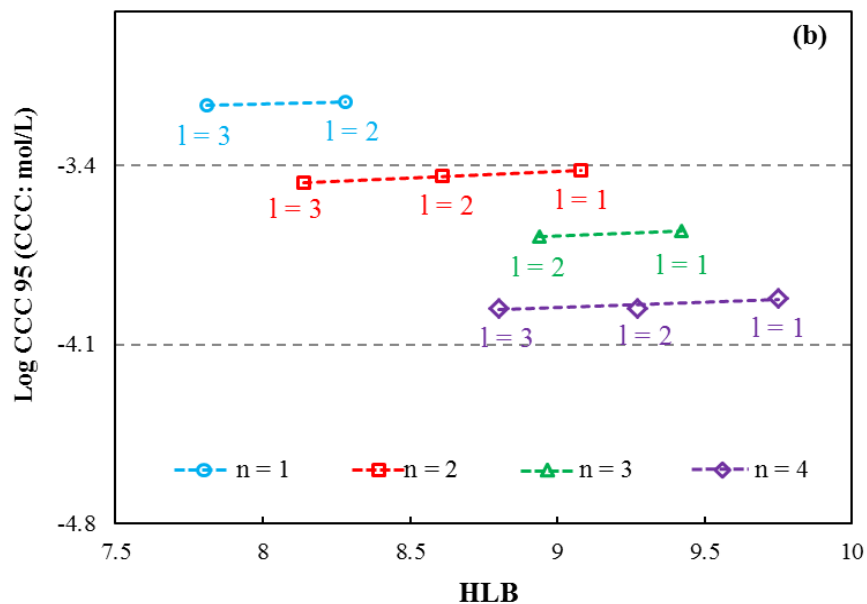
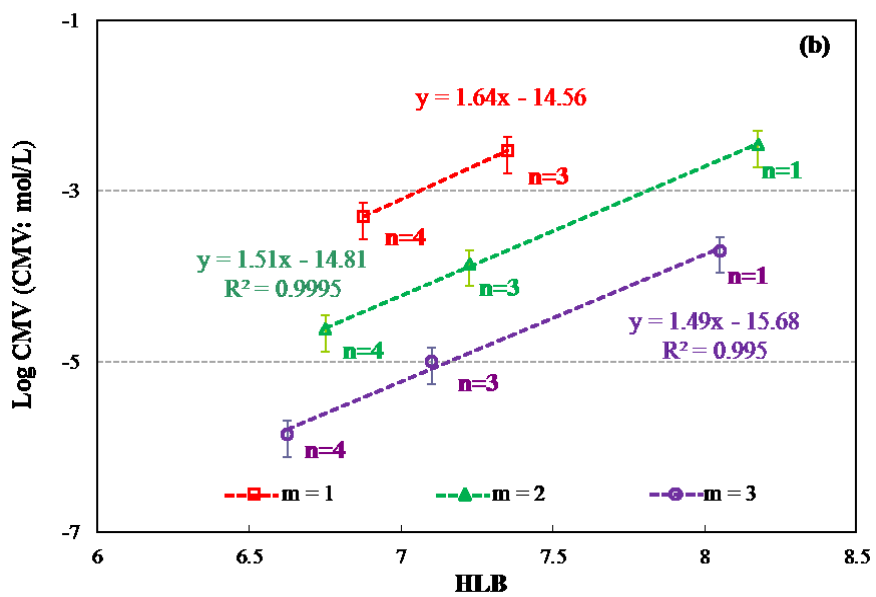
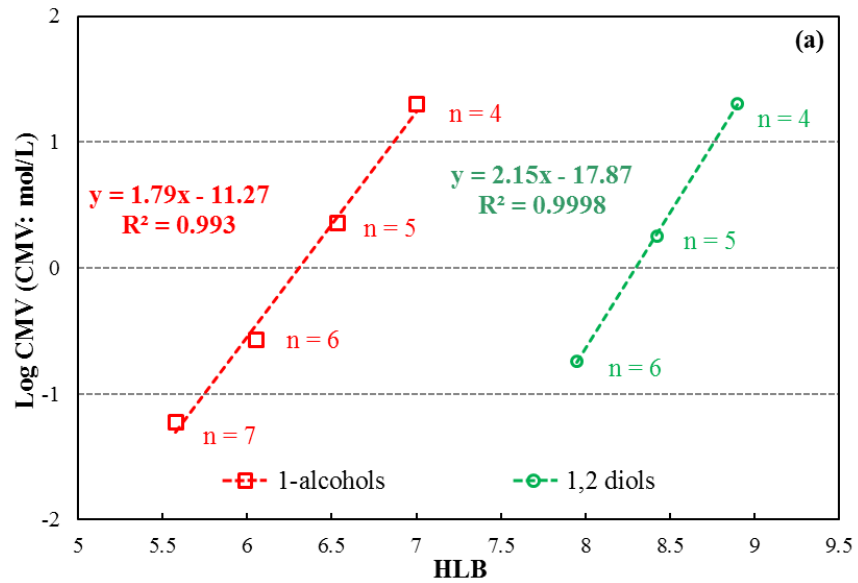


Figure 7.2 – Log CCC vs. HLB for PEGAE family as a function of: (a) carbon (n); (b) EO (l) number (dashed lines are least squares best fit)

7.4 CMV vs. HLB

7.4.1 Effect of alkyl chain length (n)

Fig. 7.3 shows log CMV versus HLB as a function of n, the number of carbons in the alkyl group for the four surfactant types tested: aliphatic and diols (Fig. 7.3a), PPGAE (Fig. 7.3b) and PEGAE (Fig. 7.3c). A linear relationship is observed, log CMV increasing as n decreases, i.e. the as the molecule becomes more hydrophilic. Each member of the family share a similar trend (slope), i.e., the trends are self-similar.



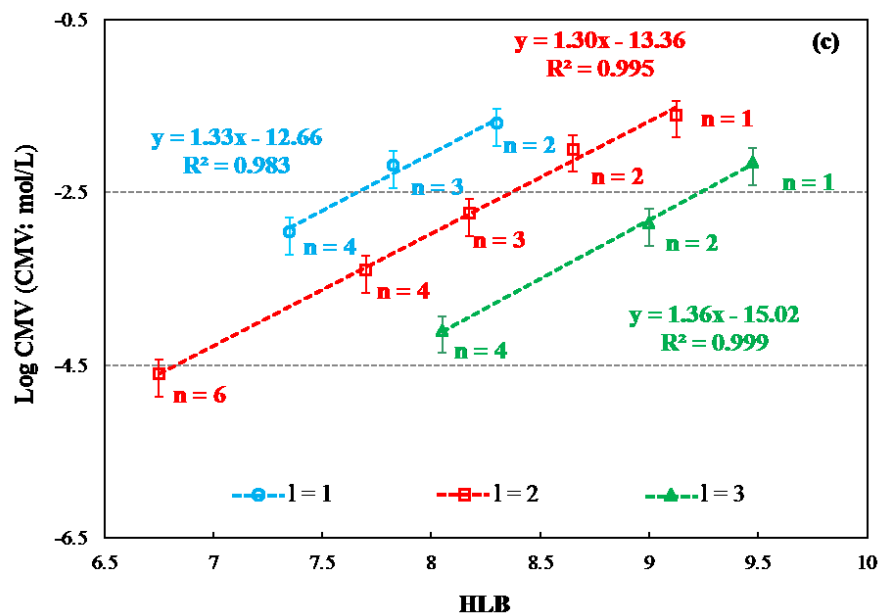


Figure 7.3 – Log CMV versus HLB as a function of n: (a) 1-alcohols and 1, 2 diols; (b) PPGAE; (c) PEGAE (dashed lines are least squares best fit)

7.4.2 Effect of PO/EO group (m/l) number

Fig. 7.4 shows log CMV versus HLB as a function of the number of PO/EO units for PPGAE (Fig. 7.4a) and PEGAE (Fig. 7.4b). The results are a series of self-similar linear log CMV–HLB trends dependent on m (number of PO groups) in the polypropylene glycol ethers or the l (number of EO groups) in polyethylene glycol ethers. The direction of the trend switches from PPGAE to PEGAE as increasing m in the former decreases HLB (surfactant becomes more hydrophobic) while increasing l in the latter increases HLB (the EO group is hydrophilic).

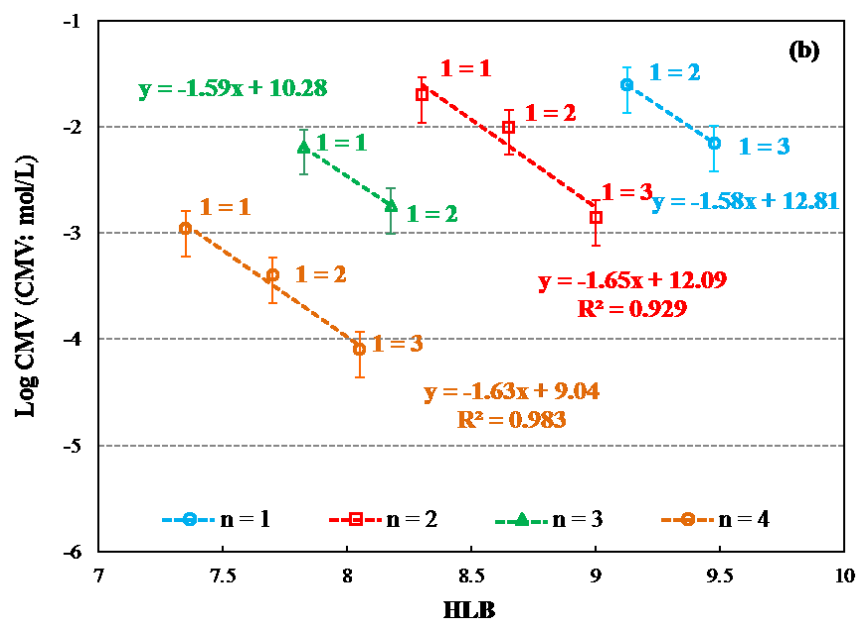
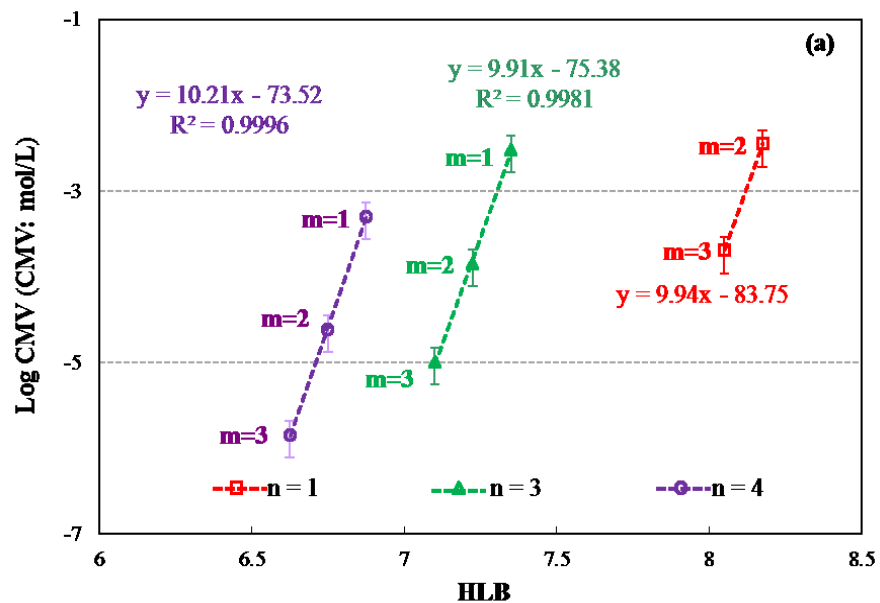
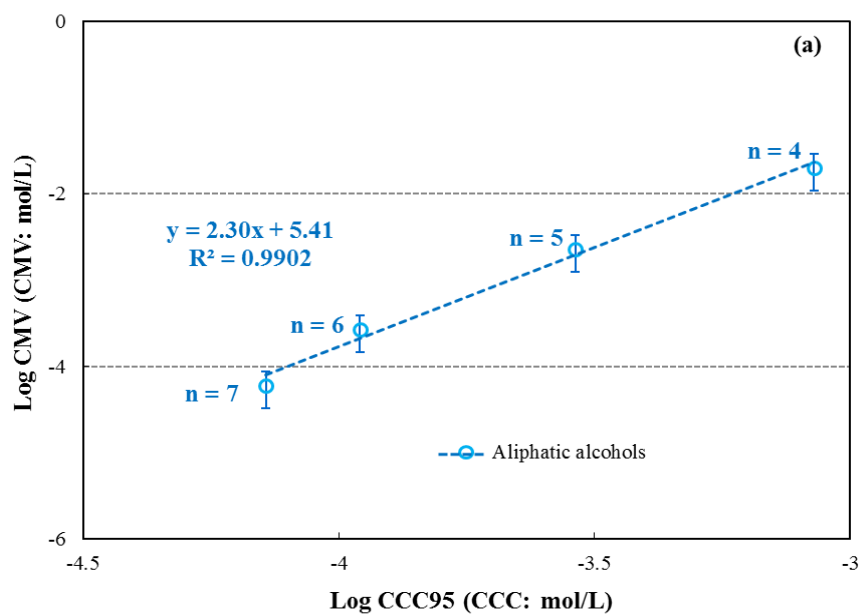


Figure 7.4 – Log CMV versus HLB value as a function of m or 1: (a) PPGAE; (b) PEGAE (dashed lines are least squares best fit)

7.4 Relationship between CMV and CCC

Since both log CCC and log CMV show linearly dependence on HLB this implies there is a relationship between CMV and log CCC. Fig. 7.5 shows log CMV versus log CCC95 as a function of n for the aliphatic alcohols (Fig. 7.5 a), polypropylene glycol alkyl ethers (Fig. 7.5b) and polyethylene glycol alkyl ethers (Fig.7.5c). Fig. 7.6 shows log CMV versus log CCC95 as a function of m/l for PPGAE (Fig. 7.6a) and PEGAE (Fig. 7.6b). As expected, a linear relationship was observed in each case.



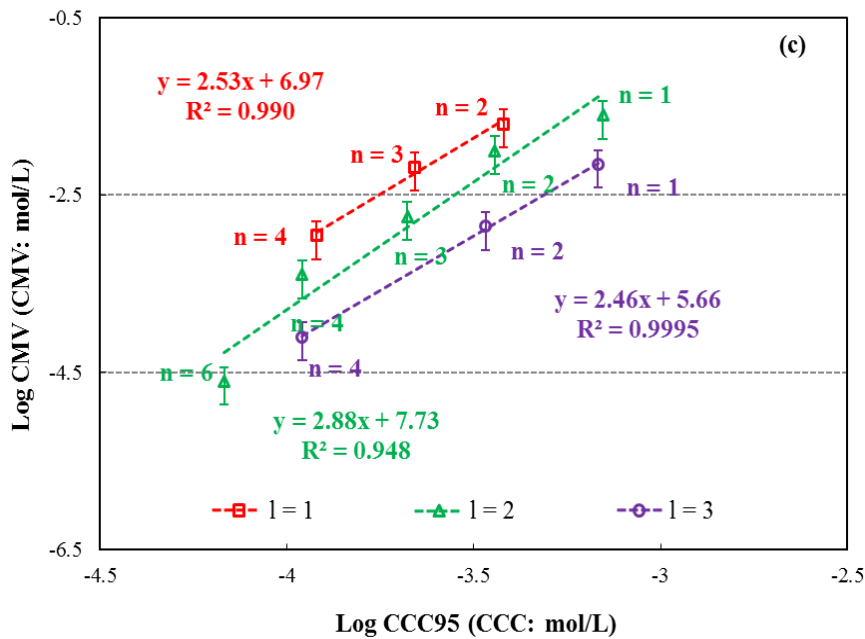
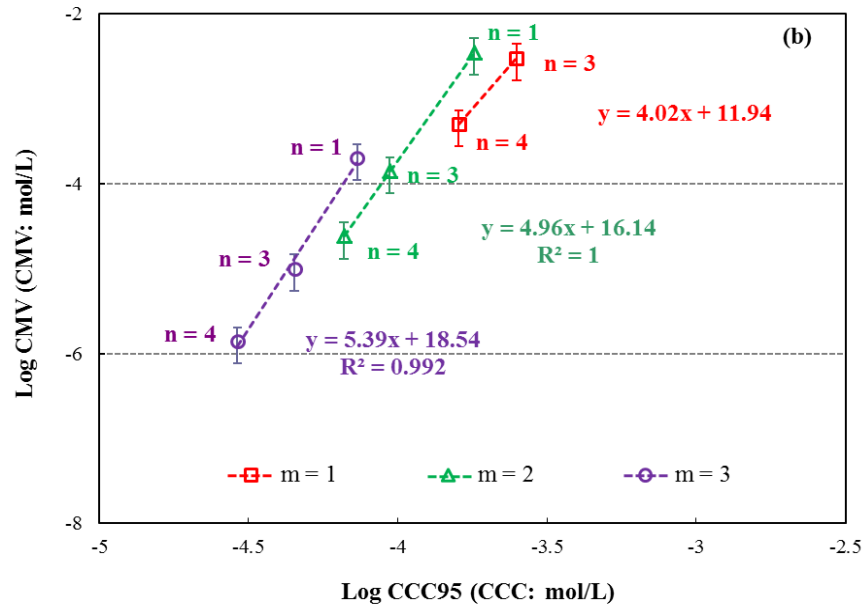


Figure 7.5 – Log CMV versus log CCC95 as a function of n: (a) 1-alcohols; (b) PPGAE; (c) PEGAE (dashed lines are least squares best fit)

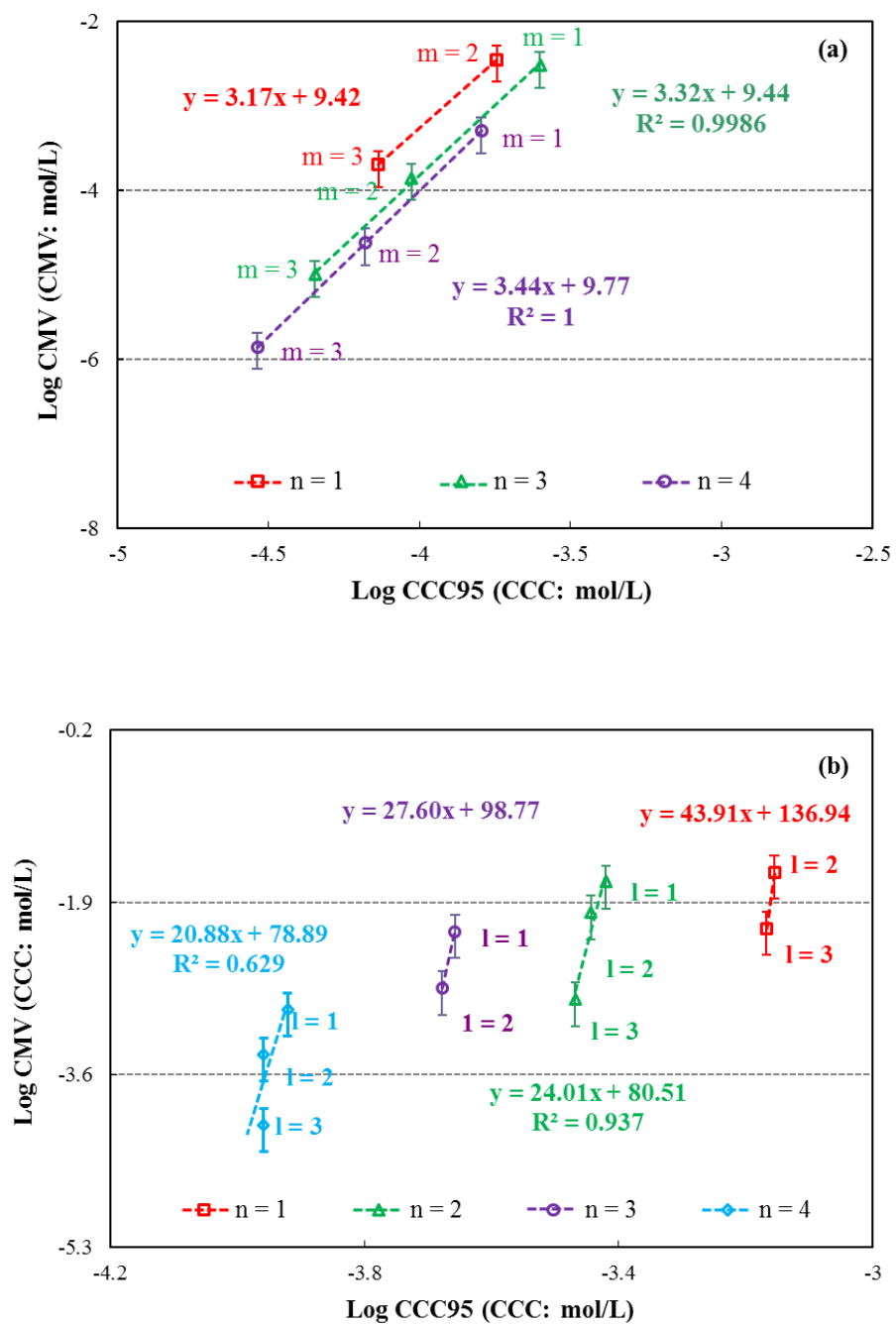


Figure 7.6 – Log CMV versus log CCC95 as a function of m or l: (a) PPGAE; (b) PEGAE

7.5 Discussion

In flotation systems, two frother functions are to decrease bubble size and reduce bubble rise velocity. The former function can be characterized by the CCC value, and the latter, as introduced in this thesis, can be characterized by the CMV. The ambition of this chapter is to link these two frother functions to a measure of frother structure, the HLB number.

As a structural indicator, HLB expresses a balance between the hydrophilic and hydrophobic parts of a molecule. Using the Davies equation, HLB decreases as the number of carbons in the alkyl group increases and as the number of PO (m) groups in PPGAE but increases as the number of EO groups (l) in PEGAE increase. Nevertheless, as l increases in PEGAE both CMV and CCC decrease as is the case when m increases in PPGAE, although less sharply. This means the direction of the trend switches between PPGAE and PEGAE such that there is no general outcome, for example that increasing frother hydrophobicity decreases CCC or CMV.

The CMV–HLB trends follow those discussed in previous chapters: \log CMV was linearly related with carbon n number (Chapter 4), and m/l number (Chapter 6). As adding unit n , m or l alters HLB in constant proportion the linear trends with HLB are expected.

Zhang et al. (2012a) modeled the CCC95–HLB relationship for polyglycols and 1-alcohols, showing that each family exhibited a unique exponential function dependent on frother structure variables, e.g., alkyl chain length (n) and number

of propylene oxide groups (m). The form of their relationships implied the log CCC vs. HLB demonstrated here for their data. Linear models arguably more readily reveal the common family traits discussed by Zhang et al. Once log CCC vs. HLB was established it follows that log CMV is linearly related to log CCC. This relationship between CMV and CCC held for all three examples, the alcohol, PPGAE, and PEGAE cases.

The relationship between CMV and CCC suggests a common mechanism, i.e., the mechanism causing bubble size reduction when produced in a swarm is related to the mechanism causing the individual bubbles to slow down. Identifying the connection is aided by expressing both functions in terms of surfactant concentration. The common mechanism may be the surface tension gradients produced at the air-water interface in the presence of surfactants. The role of these gradients on slowing bubble rise is well established (Dukhkin et al. 1998), if still the subject of debate (Tomiyama 2002). Finch et al. (2008) pointed out that these same gradients can be at play in promoting bubble size reduction by causing bubble breakup. Regardless of establishing the common mechanism, this is the first time evidence has been presented that bubble size reduction and bubble rise velocity share something in common. The mechanism(s) deserves to be identified as it appears to be the basis for the frother functions in the pulp zone of flotation machines.

7.6 Summary

A structure-function approach to characterizing frothers is explored using the hydrophile-lipophile balance (HLB) to represent the structure and the concentration to reach minimum velocity (CMV) to represent the bubble rise velocity function. All the surfactants showed log CMV was linearly related to HLB. This relationship was also shown for a second frother function, bubble size reduction represented by the critical coalescence concentration (CCC). The CMV and CCC are shown to be correlated which argues for a common mechanism controlling bubble rise velocity and bubble size reduction.

References

- Aveyard, R. (1991). Column flotation: A selected review. Part I. *International Journal of Mineral Processing* 33(1-4): 343-354.
- Boyd, J., Parkinson, C. and Sherman, P. (1972). Factors affecting emulsion stability, and the HLB concept. *Journal of Colloid and Interface Science* 41(2): 359-370.
- Cho, Y. S. and Laskowski, J. S. (2002). Effect of flotation frothers on bubble size and foam stability. *International Journal of Mineral Processing* 64(2-3): 69-80.
- Davies, J. T. (1957). A quantitative kinetic theory of emulsion type, I. Physical chemistry of the emulsifying agent. *Gas/Liquid and Liquid/Liquid Interface Proceedings of the International Congress of Surface Activity*: 426-438
- Davies, J. T. and Rideal E. K. (1961). *Interfacial phenomena* New York, Academic Press.
- Dukhin, S. S., Miller, R. and Loglio, G. (1998). Physico-chemical hydrodynamics of rising bubble. *Studies in Interface Science*. D. Möbius and R. Miller, Elsevier. Volume 6: 367-432.
- Finch, J. A., Nasset, J. E. and Acuña, C. (2008). Role of frother on bubble production and behaviour in flotation. *Minerals Engineering* 21(12-14):

949-957.

Graciaa, A., Barakat, Y., El-Emary, M., Fortney, L., Schechter, R. S., Yiv, S. and Wade, W. H. (1982). HLB, CMC, and phase behavior as related to hydrophobe branching. *Journal of Colloid and Interface Science* 89(1): 209-216.

Graciaa, A., Lachaise, J., Marion, G. and Schechter, R. S. (1989). A study of the required hydrophile-lipophile balance for emulsification. *Langmuir* 5(6): 1315-1318.

Grau, R. A., Laskowski, J. S. and Heiskanen, K. (2005). Effect of frothers on bubble size. *International Journal of Mineral Processing* 76(4): 225-233.

Griffin, W. C. (1954). Calculation of HLB Values of Non-Ionic Surfactants. *Journal of the Society of Cosmetic Chemists* 4: 259.

Harris, C. C. (1976). Flotation Machines. In *flotation*, A. M. Gaudin Memorial Volume, Fuerstenau, M. C., Ed.; AIME; New York, NY, USA. Vol 2: 753-815

Harris, G. H. and Jia, R. (2000). An improved class of flotation frothers. *International Journal of Mineral Processing* 58(1-4): 35-43.

Heusch, R. (1970). Eine experimentelle Methode zur Bestimmung des HLB-Wertes von Tensiden. *Colloid & Polymer Science* 236(1): 31-38.

- Kruglyakov, P. M. (2000). Hydrophile-lipophile balance of surfactants and solid particles: physicochemical aspects and applications; Chapter 3 Hydrophile-lipophile balance of surfactants. *Studies in Interface Science*. New York, Elsevier. Volume 9: 146-266.
- Kunieda, H. and Shinoda, K. (1985). Evaluation of the hydrophile-lipophile balance (HLB) of nonionic surfactants. I. Multisurfactant systems. *Journal of Colloid and Interface Science* 107(1): 107-121.
- Laskowski, J. S. (1993). Frothers and Flotation Froth. *Mineral Processing and Extractive Metallurgy Review* 12(1): 61-89.
- Laskowski, J. S. (2003). Fundamental properties of flotation frothers. *Proceedings of 22nd international mineral processing congress, Cape town, South African Institute of mining and metallurgy*.
- Laskowski, J. S. (2004). Testing Flotation Frothers. *Physicochemical Problems of Mineral Processing*, (2004) (38): 13-22.
- Lin, I. J. (1972). Hydrophile-lipophile balance (hlb) of fluorocarbon surfactants and its relation to the critical micelle concentration (cmc). *The Journal of Physical Chemistry* 76(14): 2019-2023.
- Lin, I. J. and Marszall, L. (1976). CMC, HLB, and effective chain length of surface-active anionic and cationic substances containing oxyethylene groups. *Journal of Colloid and Interface Science* 57(1): 85-93.

- Little, R. C. (1978). Correlation of surfactant hydrophile-lipophile balance (HLB) with solubility parameter. *Journal of Colloid and Interface Science* 65(3): 587-588.
- Lo, I., Legras, T., Seiller, M., Choix, M. and Puisieux, F. (1972). Emulsions. IV. Determination of the critical HLB of various oil phases. *Les émulsions. IV. Détermination du HLB critique de différentes phases huileuses.* 30(3): 211-222.
- Marszall, L. and Lin, I. (1978). Partition coefficient, HLB and effective chain length of surface-active agents *Emulsions. A. Weiss, Springer Berlin / Heidelberg.* 63: 99-104.
- Morgen, J. C., Schechter, R. S., Wade, W. H., Shah, D.O. (1977). *Improved oil recovery by surfactant and polymer flooding*, New York, Academic Press.
- Nesset, J. E., Finch, J. A. and Gomez, C. O.(2007). Operating variables affecting the bubble size in forced-air mechanical flotation machines. *Proceedings of the AusIMM Mill Operators Conference.* Fremantle, Australia: 55-65.
- Pugh, R. J. (2000). Non-ionic polyethylene oxide frothers in graphite flotation. *Minerals Engineering* 13(2): 151-162.
- Rabaron, A., Cavé, G., Puisieux, F. and Seiller, M. (1993). Physical methods for measurement of the HLB of ether and ester non-ionic surface-active agents: ¹H-NMR and dielectric constant. *International Journal of Pharmaceutics* 99(1): 29-36.

- Ross, S., Chen, E. S., Becher, P. and Ranauto, H. J. (1959). Spreading Coefficients and Hydrophile-Lipophile Balance of Aqueous Solutions of Emulsifying Agents. *The Journal of Physical Chemistry* 63(10): 1681-1683.
- Salager, J. L., Quintero, L., Ramos, E. and Anderez, J. M. (1980). Properties of surfactant/oil/water emulsified systems in the neighborhood of the three-phase transition. *Journal of Colloid and Interface Science* 77(1): 288-289.
- Sauter, J. (1928). Die Grössenbestimmung der in Gemischnebeln von Verbrennungskraftmaschinen vorhandenen Brennstoffteilchen. *VDI-Forschungsheft Nr. 279* (312).
- Schick, M. J. and Beyer, E. A. (1963). Foaming properties of nonionic detergents. *Journal of the American Oil Chemists' Society* 40(2): 66-68.
- Schott, H. (1969). Hydrophile-lipophile balance and micelle formation of nonionic surfactants. *Journal of Pharmaceutical Sciences* 58(9): 1131-1133.
- Tomiyaama, A., Celata, G. P., Hosokawa, S. and Yoshida, S. (2002). Terminal velocity of single bubbles in surface tension force dominant regime. *International Journal of Multiphase Flow* 28(9): 1497-1519.
- Verdinelli, V., Messina, P. V., Schulz, P. C. and Vuano, B. (2008). Hydrophile-lipophile balance (HLB) of n-alkane phosphonic acids and their salts.

Colloids and Surfaces A: Physicochemical and Engineering Aspects
316(1-3): 131-135.

Waldhoff, H. and Spilker, R. (2005). Handbook of Detergents, Part C: Analysis. Surfactant Science Series, Volume 123, New York. Journal of the American Chemical Society 127(13): 4984-4984.

Zhang, W. (2012). Frothers and Frother Blends: A Structure – Function Study (Ph. D dissertation). Department of Mining and Materials. Montreal, McGill University.

Zhang, W., Nasset, J. E., Rao, S. R. and Finch, J. A. (2012) a. Characterizing Frothers through Critical Coalescence Concentration (CCC)95-Hydrophile-Lipophile Balance (HLB) Relationship. Minerals 2(3): 208-227.

Zhang, W., Nasset, J. E., Rao, S. R. and Finch, J. A. (2012) b. Frother Function-Structure Relationship: Dependence of CCC95 on HLB (in preparation).

Chapter 8 – CMV vs. HLB modified to include isomers

8.1 Introduction

One disadvantage of the Davies method is that the hydrophile-lipophile balance (HLB) is calculated to be the same for isomers whereas it is evident that the concentration to reach minimum velocity (CMV) does vary with isomers in the alcohol data, as does the critical coalescence concentration (CCC) for alcohols (Zhang 2012) and the critical micelle concentration (CMC) for ionic surfactants (Lin et al. 1973; Lin et al. 1974). In effect the HLB can be considered to apply to straight-chain hydrocarbon surfactants (e.g., 1-alcohols) with no branching (e.g., of OH or $-\text{CH}_3$ groups). Wu et al. (2005) have shown that position isomerism may strongly affect the HLB number of a surfactant. What is needed is a way to modify the HLB number to include isomers.

A few attempts have been made to modify the HLB group numbers to allow for position isomerism. Lin et al. (1973; 1974) tried to relate HLB to CMC by introducing an effective number (n_{eff}) for $-\text{CH}_2-$ groups for branched surfactants in a modification of the Davies equation:

$$HLB = 7 + \Sigma (\text{hydrophilic group numbers}) + \Sigma (-0.475 \times n_{\text{eff}}) \quad 8.1$$

where -0.475 is the HLB group number for the hydrocarbon ($-\text{CH}_2-$) group. The effect of branching is analogous to reduction in n_{eff} of 1–1.5 $-\text{CH}_2-$ units associated with a decrease in hydrophobic character (Lin et al. 1973).

In Chapter 5, the effect on CMV of the position of hydroxyl group and methyl branch in eighteen five- and six-carbon alcohol isomers was determined. The purpose of this chapter is to modify the Davies HLB by adding a position coefficient for the OH group and the $-CH_3$ branch to extend the relationship between CMV and HLB to include isomers.

8.2 Relationship between CMV and HLB in alcohol isomers

8.2.1 Effect of hydroxyl group position

Fig. 8.1 shows log CMV as a function hydroxyl position in five- and six-carbon alcohols. A similar linear relationship is shown for both with a slope ca. 0.06.

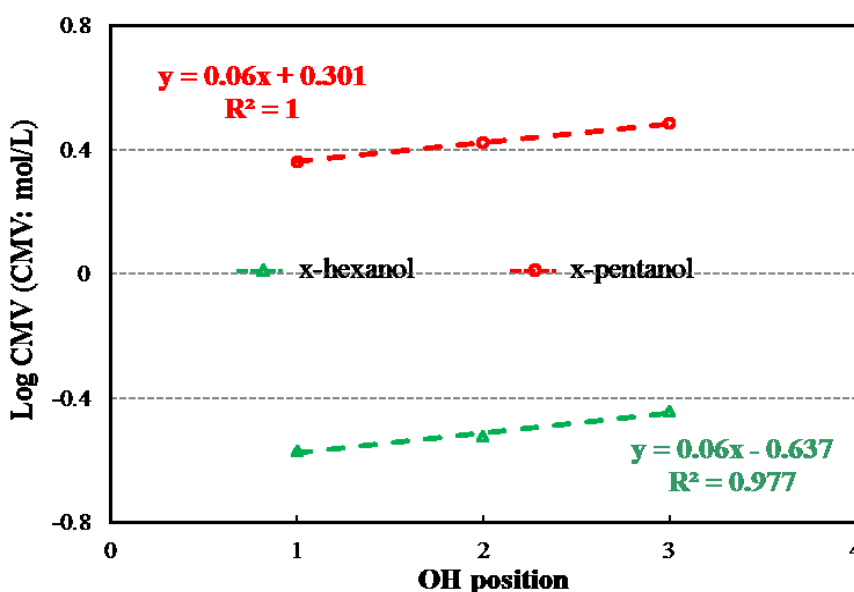
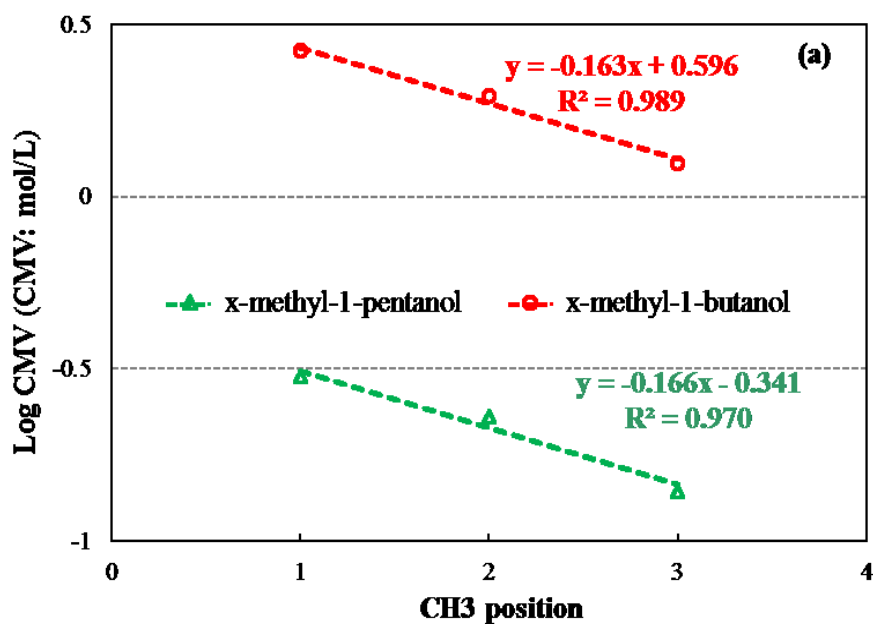


Figure 8.1 – Log CMV as a function of hydroxyl position in five/six alcohols (x indicates the position of hydroxyl group)

8.2.2 Effect of methyl branch position

The effect of methyl branch position is related to the position of the hydroxyl group. Fig. 8.2 shows log CMV as a function of methyl branch position in five-

/six-carbon alcohols with OH located at 1C (Fig. 8.2a), 2C (Fig. 8.2b) and 3C (Fig. 8.2c). In Fig. 8.2a with OH in the 1C position, the three isomers of the 5-carbon alcohol and the three isomers of the 6-carbon alcohols are seen to comprise parallel (self-similar) linear relationships with slope ca. 0.164. (Note, to maintain a consistent numbering system for the methyl position, the convention adopted is to start with, for example 1-methyl-1-pentanol for the six-carbon case, rather than the alternative nomenclature 2-hexanol (Ezrahi et al. 2005). Although there are fewer isomers based with OH in the 2 and 3 positions the linear relationship between log CMV and position of the -CH₃ group is consistent.



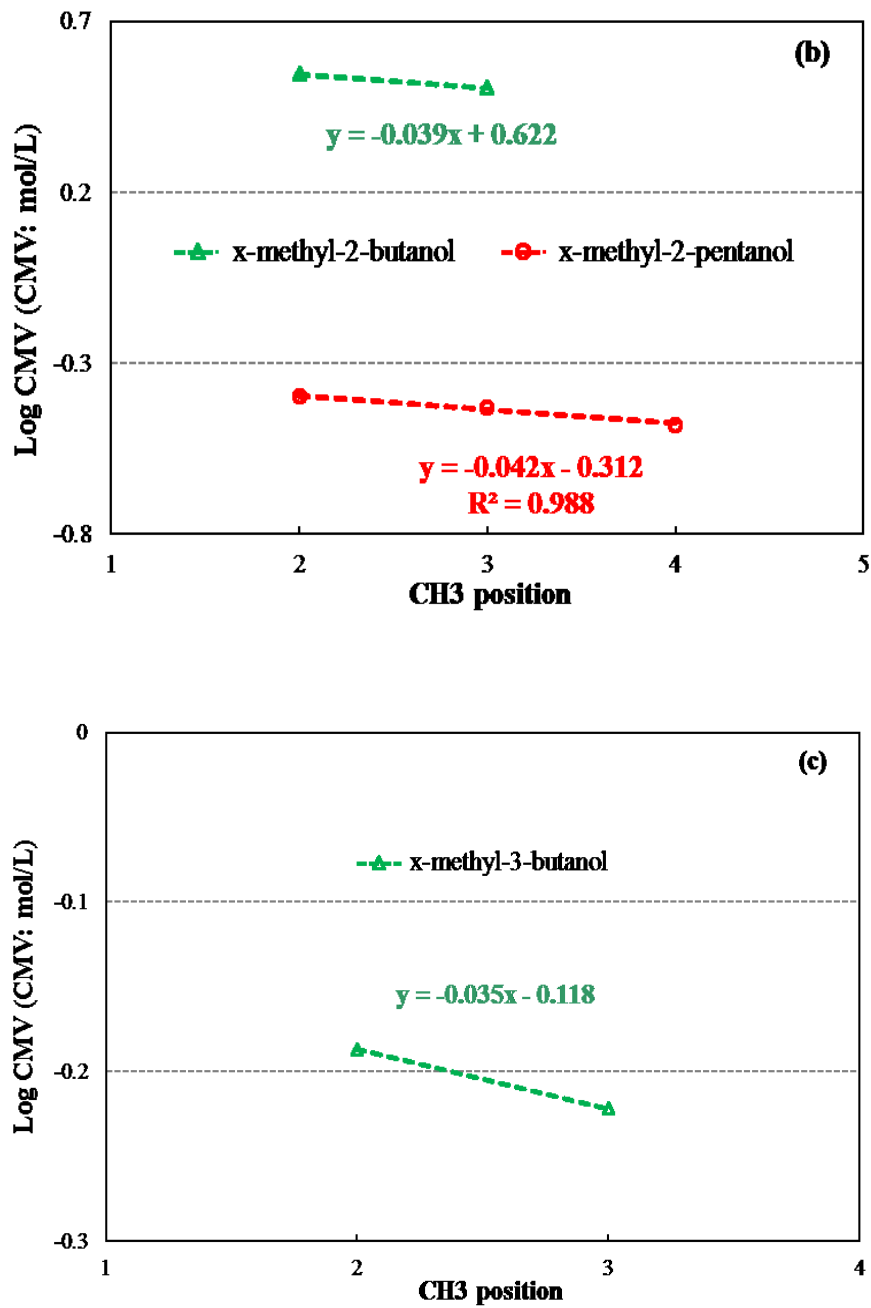


Figure 8.2 – Log CMV as a function of methyl branch position in five-/six-carbon alcohols with hydroxyl group located at: (a) 1C; (b) 2C; (c) 3C position (x indicates the methyl branch position)

8.3 HLB modification in isomers

To modify HLB the effect of the position of the hydroxyl group and the methyl branch in the alcohol isomers needs to be accounted for. The method of Lin et al. (1973, 1974) was to consider the isomer as a straight chain of an equivalent (or effective) number of carbons, n_{eff} , based on Davies equation. In the method developed here the HLB modification focuses on the type of group (OH or $-\text{CH}_3$) and the position, for the rest of the molecule the calculation of HLB is not altered.

8.3.1 Hydroxyl position

Based on the argument that the Davies HLB applies to the straight chain isomer $\text{HLB}_{\text{OH}} = 1.9$ can be taken to apply to the hydroxyl group being at one end of the hydrocarbon chain. Fig. 8.1 showed $\log \text{CMV}$ was a linear function of OH position with a slope of ca. 0.06 for both the five- and six-carbon alcohol isomers. Taking this position effect into consideration, a modification coefficient for position of the OH group is introduced as:

$$C_{x-\text{OH}} = 1 + (a - 1) \times (1 + k_{\text{OH}}) \quad 8.2$$

where a is the position of the hydroxyl group and k_{OH} is the slope from the experimental $\log \text{CMV}$ vs. hydroxyl position, i.e., 0.06. For example, the modified hydroxyl HLB group number for OH located at the 2C position is:

$$\text{HLB}_{2-\text{OH}} = 1.9 \times C_{2-\text{OH}} = 1.9 \times [1 + (2 - 1) \times (1 + 0.06)] = 2.01 \quad 8.3$$

and for the 3C position:

$$\text{HLB}_{3-\text{OH}} = 1.9 \times C_{3-\text{OH}} = 1.9 \times [1 + (3 - 1) \times (1 + 0.06)]$$

$$= 2.13 \quad 8.4$$

8.3.2 Methyl branch position

The results in Chapter 5 showed that the methyl branch position effect in alcohols is related to hydroxyl position. Fig. 8.2 shows the change of methyl position with OH at 1C (Fig.8.2a) had a slope ca. 0.164, with OH at 2C (Fig.8.2b) a slope ca. 0.04, and at 3C (Fig.8.2c) a slope ca. 0.035. Taking the methyl position effect into consideration, the modification coefficient for the methyl branch position is:

$$C_{x-CH_3} = 1 + (b - 1) \times (1 + k_{-CH_3/OH}) \quad 8.5$$

where b is the position of methyl branch and $k_{-CH_3/OH}$ is the slope of the experimental log CMV vs. methyl position where $k_{-CH_3/OH} = 0.164, 0.04, 0.035$ for hydroxyl group at 1C, 2C, 3C positions, respectively. For example, for OH at 2C position for 3-methyl-2-pentanol, the modification coefficient for the HLB group number for the methyl branch is:

$$C_{3-CH_3} = 1 + (3 - 1) \times 0.04 \quad 8.6$$

Taking both the hydroxyl position and methyl branch position modification coefficients into account two example calculations of the modified HLB number for a molecule are given:

3-methyl-1-pentanol (OH at 1C position and a methyl branch at 3C position):

$$\begin{aligned} \text{HLB} &= 7 - 5 \times 0.475 - [1 + (3 - 1) \times 0.164] \times 0.475 + 1.9 \\ &= 5.89 \end{aligned} \quad 8.7$$

3-methyl-2-pentanol (OH at 2C position and a methyl branch at 3C position):

$$\begin{aligned} \text{HLB} &= 7 - 5 \times 0.475 - [1 + (3 - 1) \times 0.04] \times 0.475 + 1.9 \times [1 + (2 - 1) \times 0.06] \\ &= 6.13 \end{aligned} \qquad 8.8$$

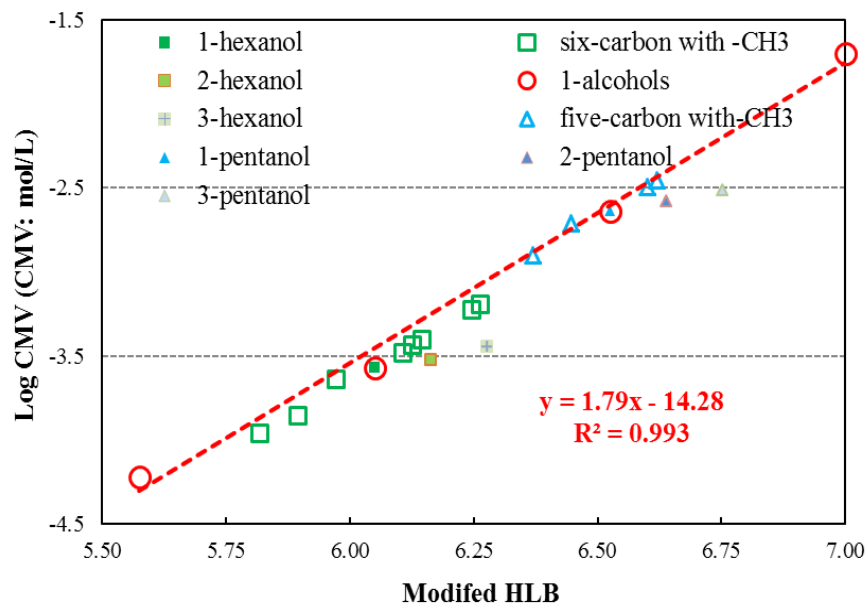


Figure 8.3 – Log CMV as a function of modified HLB (dashed line is best fit for 1-alcohols)

Using the proposed modification coefficients, log CMV vs. modified HLB is plotted in Fig 8.3. The dash line shows the best fit-in trend for 1-alcohols. From the figure, it is observed that after the modification, x-pentanol and x-hexanol (x here stands for 2 and 3) are still not in the same trend line as the 1-alcohols. The location of the OH in the 2 and 3 positions can be considered to divide the molecule into a straight chain section and a branch (Backlund et al. 1995; Ezrahi et al. 2005). For example, for 2-hexanol the six-carbon chain can be separated into one five-carbon chain and a methyl branch. The now “branched” hydrocarbon chain the HLB can be modified by adding the branch modification

coefficient into the calculation. The modified HLB number for 2-hexanol is then calculated as:

$$\text{HLB} = 7 - 5 \times 0.475 - 0.475 \times [1 + 0.164] + 1.9 (1 + 0.06) = 6.09 \quad 8.9$$

and the modified HLB number for 3-hexanol is calculated as:

$$\begin{aligned} \text{HLB} &= 7 - 5 \times 0.475 - 0.475 \times [1 + 2 \times 0.164] + 1.9 \times (1 + 2 \times 0.06) \\ &= 6.12 \end{aligned} \quad 8.10$$

The relationship of log CMV as a function of re-modified HLB number for five- and six-carbon alcohol isomers is re-plotted in Fig 8.4, where a single trend is observed for all the alcohols.

The final modification coefficients are listed in Table 8.1 with the modified HLB numbers for the alcohol isomers listed in Table 8.2.

Table 8.1 - Hydroxyl group and methyl branch position modification coefficient

| Structure variable | | Position | Modification coefficient | |
|--------------------|-----------|----------|--------------------------|-------------------|
| | | | OH | -CH ₃ |
| OH | | 1 | 1 | - |
| | | 2 | 1 + (2-1) * 0.06 | 1 + 0.164 |
| | | 3 | 1 + (3-1) * 0.06 | (1+2*0.164) |
| -CH ₃ | OH at C-1 | 4 | 1 | 1 + (4-1) * 0.164 |
| | | 3 | | 1 + (3-1) * 0.164 |
| | | 2 | | 1 + (2-1) * 0.164 |
| | OH at C-2 | 4 | 1 + (2-1) * 0.06 | 1 + (4-1) * 0.04 |
| | | 3 | | 1 + (3-1) * 0.04 |
| | | 2 | | 1 + (2-1) * 0.04 |
| | OH at C-3 | 3 | 1 + (3-1) * 0.06 | 1 + (3-1) * 0.035 |
| | | 2 | | 1 + (2-1) * 0.035 |

Table 8.2 - Modified HLB in five-/six-carbon alcohol isomers

| Family | Name | CMV (mmol/L) | Position | | HLB | |
|-------------|----------------|-----------------|------------------|----|--------|----------|
| | | | -CH ₃ | OH | Davies | Modified |
| Five carbon | 3-M-1-butanol | 1.25 | 3 | 1 | 6.53 | 6.37 |
| | 3-M-2-butanol | 3.2 | 3 | 2 | | 6.60 |
| | 2-M-1-butanol | 1.95 | 2 | 1 | | 6.45 |
| | 2-M-2-butanol | 3.5 | 2 | 2 | | 6.62 |
| | 1-pentanol | 2.3 | - | 1 | | 6.53 |
| | 2-pentanol | 2.65 | - | 2 | | 6.56 |
| | 3-pentanol | 3.05 | - | 3 | | 6.59 |
| Six carbon | 4-M-1-pentanol | 0.11 | 4 | 1 | 6.05 | 5.82 |
| | 4-M-2-pentanol | 0.33 | 4 | 2 | | 6.11 |
| | 3-M-1-pentanol | 0.14 | 3 | 1 | | 5.89 |
| | 3-M-2-pentanol | 0.37 | 3 | 2 | | 6.13 |
| | 3-M-3-pentanol | 0.6 | 3 | 3 | | 6.24 |
| | 2-M-1-pentanol | 0.23 | 2 | 1 | | 5.97 |
| | 2-M-2-pentanol | 0.4 | 2 | 2 | | 6.15 |
| | 2-M-3-pentanol | 0.65 | 2 | 3 | | 6.26 |
| | 1-hexanol | 0.27 | - | 1 | | 6.05 |
| | 2-hexanol | 0.3 | - | 2 | | 6.09 |
| | 3-hexanol | 0.36 | - | 3 | | 6.12 |

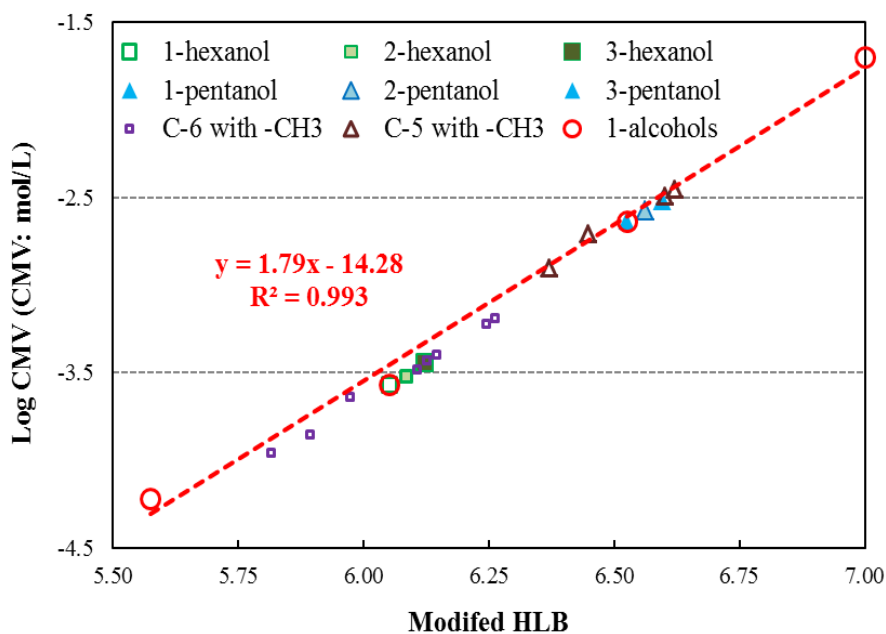


Figure 8.4 – Log CMV as a function of modified HLB including x-hexanol/x-pentanol as branch chained (x stands for 2 or 3)

8.4 Discussion

The structural alcohol isomer system was studied to try to generate a universal CMV vs. HLB trend, i.e., one that held for all the isomers. The idea was to modify the OH and methyl branch HLB group number to account for position in such a manner that the resulting modified HLB number would lie on the same linear log CMV vs. HLB trend observed for the straight chain alcohols (1-alcohols). The starting point was the observation that log CMV vs. position of OH and methyl branch was linear and exhibited a common slope. This permitted a modification coefficient to be designed to modify the HLB group number to account for position of the hydroxyl and methyl branch.

For 2-alcohols and 3-alcohols, initially the modified HLB did not fully fit the trend. Some studies have shown that 2-alcohols and 3-alcohols could be considered as branched alcohols (Backlund et al. 1995; Ezrahi et al 2005). The HLB group modification for the methyl branch was then added. Fig 8.4 showed the re-modified HLB number now did fall on the common alcohol log CMV vs. HLB linear trend line. Since no such further modification was needed for alcohols with OH in the 2 or 3 position with a methyl branch implies there is no additional “branching” due to the OH position effect.

The argument for separation into two parts for the 2- and 3-alcohol cases is that the electron cloud of the hydroxyl could cause a bending in the chain. However, for 2 or 3-alcohols with a methyl branch, e. g., 3-methyl-2-pentanol, the steric hindrance from methyl branch could induce an opposing effect and the main hydrocarbon chain remains straight.

Lin and co-workers (Lin et al. 1973; Lin and Marszall 1976) modified HLB by introducing n_{eff} to allow for the effect of the position of the head group in ionic surfactants. To illustrate, when the polar head in 14-carbon alkyl sulfates was located at 1C, the effective carbon number was taken as 14 in the Davies equation; however, when the polar group was at 7C the effective carbon number was 11.9 (Lin and Marszall 1976). This shows the alkyl sulphonate with the polar group at 7C was effectively less hydrophobic than when the polar group was at 1C. A similar approach to estimate an n_{eff} could be adopted here. Instead of altering the group numbers they could be fixed and then the number of carbons adjusted to derive the n_{eff} that makes HLB for isomers fit the log CMV vs. HLB trend found for the 1-alcohols. Alternatively given the approach here, the n_{eff} that gives the same modified HLB number in Table 8.2 could be calculated. The result would be that for modified HLB values greater than the n-carbon 1-alcohol base case HLB then $n_{\text{eff}} < n$, and the molecule is less hydrophobic the base case, and for HLB values less than the base case then $n_{\text{eff}} > n$ and the molecule is more hydrophobic. While n_{eff} could be estimated it does not seem to have physical meaning (other than showing whether a molecule is more or less hydrophobic compared to the straight chain case). A modification that changes the HLB group number to account for position of the group in isomers seems the more direct route.

As discussed in Chapter 7, log CCC is linearly related to HLB (and consequently log CMV is linearly related to log CCC). As Zhang et al. (2012) noted a relationship to HLB could not be extended to include 2- and 3-alcohols because

HLB did not alter to reflect the effect of OH position. That is, they had the same problem as here. The natural question is whether the OH group HLB number modified for position derived here also fits the CCC data. Fig. 8.5 explores this showing the approximately linear trend for log CCC vs. 1-alcohols with 4 to 7 carbons and including the data for 2- and 3-alcohol isomers with 5 and 6 carbons taking the modified HLB from Table 8.2. The isomers show the increased HLB from the base 1-alcohol case trends with increasing CCC, just as the CMV also trended. The five-carbon case, however, showed the isomers had a more marked effect on increasing the CCC compared to the six-carbon case. This suggests that the modified HLB group number for the OH position effect derived here is not entirely universal. The CCC database for alcohol isomers is limited and more need to be tested. It may be that correlating any parameter to HLB to include isomers may have to derive the modification appropriate to the parameter. The approach here for the CMV parameter may be applicable but a general solution to determine HLB for isomers is still to be designed.

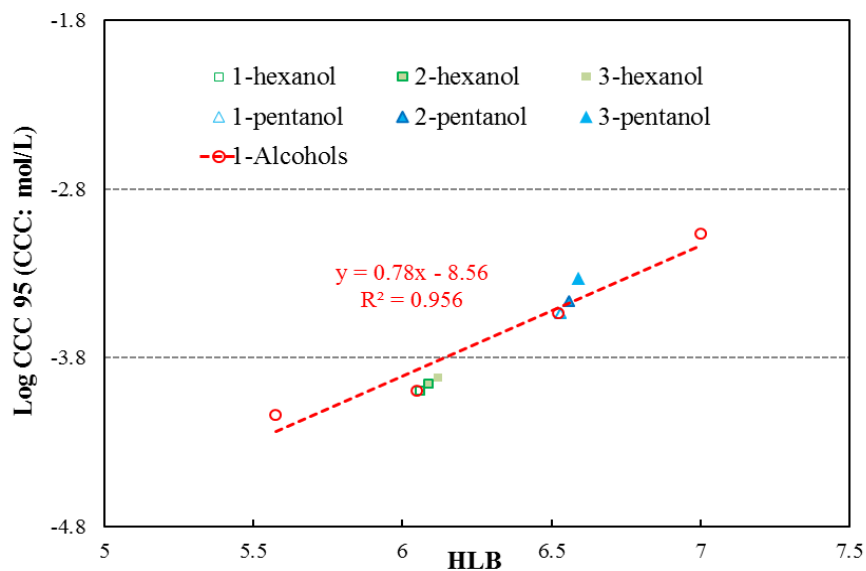


Figure 8.5 – Log CCC as a function of modified HLB number (CCC 95 from literature: Zhang 2012)

8.5 Summary

An approach to modify the hydroxyl group and methyl branch HLB number was explored in seven five-carbon and eleven six-carbon alcohols. Empirical modification coefficients were developed for both OH and $-\text{CH}_3$ branch positions based on the observed linear log CMV vs. group position. All the alcohol isomer data fell on the same log CMV vs. modified HLB number. Extension to CCC data for alcohol isomers to fit to log CCC vs. modified HLB was partially successful.

References

- Backlund, S., Eriksson, F., Karlsson, S. and Lundsten, G. (1995). Enzymatic esterification and phase behavior in ionic microemulsions with different alcohols. *Colloid & Polymer Science* 273(6): 533-538.
- Ezrahi, S., Tuval, E., Aserin, A. and Garti, N. (2005). The effect of structural variation of alcohols on water solubilization in nonionic microemulsions: 2. Branched alcohols as solubilization modifiers: Results and interpretation. *Journal of Colloid and Interface Science* 291(1): 273-281.
- Lin, I. J., Friend, J. P., and Zimmels, Y. (1973). The effect of structural modifications on the hydrophile—lipophile balance of ionic surfactants. *Journal of Colloid and Interface Science* 45(2): 378-385.
- Lin, I. J. and Marszall, L. (1976). CMC, HLB, and effective chain length of surface-active anionic and cationic substances containing oxyethylene groups. *Journal of Colloid and Interface Science* 57(1): 85-93.
- Lin, I. J., Moudgil, B. M. and Somasundaran, P. (1974). Estimation of the effective number of -CH₂- groups in long-chain surface active agents. *Colloid & Polymer Science* 252(5): 407-414.
- Wu, J., Y., Xu, Y. M., Dabros, T. and Hamza, H. (2005). Effect of EO and PO positions in nonionic surfactants on surfactant properties and demulsification performance. *Colloids and Surfaces A: Physicochemical and Engineering Aspects* 252(1): 79-85.

Zhang, W. (2012). Frothers and Frother Blends: A Structure – Function Study (Ph. D dissertation), McGill University.

Chapter 9 – Conclusions, claims to original research and suggestions for future work

9.1 Conclusions

Frothers are used in mineral flotation to control bubble size, slow bubble rise velocity and stabilize the froth phase. The aim of this thesis is to determine the structure effect on bubble rise velocity. The tests were conducted in a 350 cm column with over 50 surfactants of the alcohol, diol, polypropylene glycol and alkyl ether, polyethylene glycol and alkyl ether families. A 1.45 mm size bubble was employed in all the measurements. The velocity at 300 cm was determined and concentration to reach minimum velocity at 300 cm (CMV) was estimated graphically. The following conclusions can be drawn from this study:

9.1.1 Experimental setup

The experimental procedures to obtain the necessary replication were established.

- Minimum gas injection rate was used to minimize launch effects on bubble rise velocity.
- The cleanliness of the system was verified by verifying the bubble rise velocity profile in tap water prior to every test.

9.1.2 Structural effect

9.1.2.1 Position effect of hydroxyl group and methyl branch in alcohols

- The hydroxyl group at the 1C position gives the most efficient structure to reduce bubble rise velocity and thus the lowest CMV.

- The closer the hydroxyl locates to the center the less effective the structure in slowing bubble rise and the higher the CMV.
- The position of the second OH in diols has a pronounced impact: the closer the two OHs to the terminal position the lower the CMV.
- The effect of OH position is associated with orientation and packing of molecule on the bubble surface: the OH in the terminal position allows more vertical orientation and denser packing resulting in larger surface tension gradients that increase drag and slow the bubble rise.
- The effect of the methyl branch position depends on the location of the OH: as the methyl moves further from the OH, the more effective the structure in slowing bubble and the lower the CMV. Again, orientation and packing are considered the mechanism.
- Log CMV shows a linear relationship with the hydroxyl and methyl branch position.

9.1.2.2 Chain length effect in alcohols and polyglycols

- In alcohols and polyglycols, increase in hydrocarbon (alkyl) chain length (n, number of carbons) decreases CMV.
- The effect of increasing alkyl chain length was attributed to increase in surface activity that increase surface tension gradients coupled with increased chain-chain interaction that increases packing that further increase surface tension gradients.
- At a given alkyl chain length, the CMV decreases as propoxy (PO) or ethoxy (EO) chain length increases in the corresponding polyglycol.

- The effect of increasing PO and EO is attributed to increased H-bonding with water molecules via the –O– linkage that increases surface viscosity.
- Linear relationships between log CMV and the number of carbons in the alkyl group (n) and number of PO groups (m) and EO groups (l) in the corresponding polyglycol was found.
- Each family was characterized by a series of self-similar trends in log CMV vs. n or m/l number.

9.1.2.3 Relationship of CMV with HLB, CCC95 with HLB, and CMV with CCC95

- Excluding isomers, log CMV has a linear relationship with HLB.
- Excluding isomers, log CCC95 has a linear relationship with HLB.
- Thus log CMV has a linear relationship with log CCC95.

9.1.2.4 Modified HLB

- Using modification coefficients modified HLB group numbers to accounts for position of OH and methyl groups in isomers of alcohols were derived.
- Log CMV has a linear relationship with modified HLB that includes isomers.

9.2 Claims for original research

- Refined measurement techniques in the study of single bubble velocity have provided the necessary reproducibility.

- Provided an extensive (over 50 surfactants), reliable experimental database for frother structure-function relationship studies.
- The first to use the concentration to reach minimum velocity (CMV) as a frother characteristic and derive relationships between CMV and aspects of frother structure, e.g. number of carbons in alkyl group in alcohols and polyglycols, and number of propoxy (PO) and ethoxy (EO) groups in polyglycols.
- The first to demonstrate the position effect of methyl branch and hydroxyl group in alcohols on bubble rise velocity.
- The first to show that CMV is related to hydrophile-lipophile balance (HLB) and that CMV is related to critical coalescence concentration (CCC).
- Empirical models developed system to modify HLB for alcohol isomers.

9.3 Recommendations for future work

- Determining bubble rise velocity profile requires a lot of time. A technique is needed to determine the bubble velocity profile automatically.
- Investigate polyglycols with various methyl branches in polypropylene glycol alkyl ethers and polyethylene glycol alkyl ethers to accomplish the position effect of methyl group in polyglycols.
- Model velocity profiles to determine the physical parameters of dynamic surfactant adsorption and desorption on a rising bubble surface.

- Investigate surfactant types containing different functional groups (e.g. ethyl groups) to extend the modification of HLB group values.

Appendix

Table A – 1. Velocity profiles at 0.4 mmol/L

| 1-pentanol | | | | 1-hexanol | | | |
|----------------------|------------------------|----------------------|------------------------|----------------------|------------------------|----------------------|------------------------|
| June-2011 | | May-2011 | | Dec-2011 | | Oct-2011 | |
| Distance (cm) | Velocity (cm/s) | Distance (cm) | Velocity (cm/s) | Distance (cm) | Velocity (cm/s) | Distance (cm) | Velocity (cm/s) |
| 0.72 | 21.56 | 0.22 | 6.71 | 0.85 | 25.43 | 0.94 | 28.34 |
| 3.00 | 39.88 | 1.48 | 30.88 | 2.29 | 17.86 | 2.55 | 19.92 |
| 5.14 | 37.44 | 3.62 | 33.35 | 3.49 | 18.00 | 3.86 | 19.34 |
| 6.82 | 32.81 | 5.84 | 33.18 | 4.70 | 18.29 | 5.13 | 18.64 |
| 9.00 | 32.63 | 8.05 | 33.35 | 5.91 | 18.29 | 6.31 | 16.98 |
| 11.18 | 32.63 | 10.28 | 33.53 | 7.12 | 18.00 | 7.47 | 17.74 |
| 12.80 | 32.43 | 17.00 | 34.24 | 8.31 | 17.71 | 8.64 | 17.30 |
| 14.48 | 32.31 | 20.29 | 33.18 | 9.49 | 17.57 | 9.78 | 16.98 |
| 16.70 | 32.25 | 26.89 | 33.00 | 10.67 | 17.86 | 10.93 | 17.49 |
| 18.81 | 32.13 | 29.11 | 33.53 | 11.83 | 16.86 | 12.09 | 17.23 |
| 20.94 | 32.63 | 46.55 | 32.66 | 12.93 | 16.14 | 13.22 | 16.79 |
| 23.14 | 32.38 | 78.96 | 32.15 | 13.98 | 15.43 | 14.37 | 17.62 |
| 25.28 | 31.94 | 110.89 | 31.72 | 15.06 | 16.86 | 15.52 | 16.98 |
| 27.38 | 31.88 | 140.41 | 31.51 | 16.17 | 16.43 | 16.66 | 17.04 |
| 29.50 | 31.88 | 161.38 | 31.36 | 17.24 | 15.71 | 17.78 | 16.60 |
| 46.29 | 31.46 | 179.15 | 31.38 | 25.81 | 16.10 | 26.75 | 16.84 |
| 77.59 | 31.13 | 205.11 | 31.00 | 41.95 | 16.18 | 43.37 | 16.39 |
| 108.54 | 30.79 | 235.95 | 30.68 | 58.10 | 16.12 | 59.67 | 16.20 |
| 138.26 | 30.70 | 266.23 | 29.87 | 74.07 | 15.82 | 75.99 | 16.45 |
| 168.99 | 30.75 | 295.82 | 29.31 | 89.91 | 15.87 | 92.30 | 16.17 |
| 200.53 | 30.28 | 324.77 | 28.60 | 105.85 | 16.01 | 108.50 | 16.22 |
| 230.45 | 29.58 | 340.96 | 28.32 | 121.65 | 15.58 | 124.40 | 15.59 |
| 259.76 | 29.04 | | | 137.15 | 15.42 | 140.10 | 15.80 |
| 288.61 | 28.68 | | | 156.53 | 15.92 | 157.94 | 15.70 |
| 318.01 | 28.24 | | | 172.34 | 15.48 | 173.70 | 15.88 |
| 338.67 | 27.97 | | | 184.41 | 15.89 | 187.41 | 15.77 |
| | | | | 200.19 | 15.67 | 203.20 | 15.81 |
| | | | | 215.92 | 15.81 | 219.05 | 15.89 |
| | | | | 231.72 | 15.78 | 234.85 | 15.71 |
| | | | | 247.41 | 15.60 | 250.64 | 15.86 |
| | | | | 263.04 | 15.66 | 266.54 | 15.95 |
| | | | | 278.75 | 15.77 | 282.48 | 15.92 |
| | | | | 294.56 | 15.84 | 298.34 | 15.80 |
| | | | | 310.38 | 15.81 | 318.92 | 15.85 |
| | | | | 325.97 | 15.37 | 334.82 | 15.82 |
| | | | | 337.25 | 15.39 | 341.02 | 15.87 |

Table A-2. Bubble velocity profiles in water at different times

| Aug-10 | | Dec-10 | | Mar-11 | | Jun-11 | |
|---------------|-----------------|---------------|-----------------|---------------|-----------------|---------------|-----------------|
| Distance (cm) | Velocity (cm/s) | Distance (cm) | Velocity (cm/s) | Distance (cm) | Velocity (cm/s) | Distance (cm) | Velocity (cm/s) |
| 0.65 | 19.41 | 0.53 | 15.75 | 0.78 | 23.49 | 0.39 | 11.82 |
| 2.40 | 33.18 | 2.16 | 33.30 | 2.71 | 34.29 | 1.88 | 32.82 |
| 4.64 | 33.88 | 4.39 | 33.45 | 5.02 | 35.06 | 4.12 | 34.24 |
| 6.88 | 33.53 | 6.63 | 33.90 | 7.37 | 35.49 | 6.41 | 34.41 |
| 9.14 | 34.24 | 8.89 | 33.75 | 9.73 | 35.31 | 8.71 | 34.77 |
| 11.42 | 34.06 | 11.14 | 33.75 | 12.09 | 35.49 | 11.02 | 34.41 |
| 12.77 | 34.22 | 13.40 | 34.20 | 13.86 | 35.40 | 13.31 | 34.41 |
| 15.04 | 34.05 | 15.68 | 34.20 | 16.20 | 35.50 | 15.60 | 34.24 |
| 18.22 | 34.06 | 17.95 | 33.75 | 19.15 | 35.66 | 17.90 | 34.77 |
| 19.92 | 33.89 | 20.21 | 34.05 | 20.92 | 35.20 | 20.22 | 34.94 |
| 21.61 | 33.88 | 22.48 | 34.05 | 22.66 | 34.89 | 22.52 | 34.06 |
| 24.54 | 33.64 | 24.74 | 33.90 | 25.58 | 34.80 | 24.81 | 34.59 |
| 26.80 | 33.21 | 27.01 | 34.05 | 27.93 | 34.70 | 27.11 | 34.24 |
| 28.41 | 34.06 | 29.28 | 34.05 | 29.69 | 35.49 | 29.41 | 34.77 |
| 30.66 | 33.53 | 31.54 | 33.90 | 32.04 | 34.89 | 31.71 | 34.41 |
| 48.52 | 33.48 | 49.53 | 33.72 | 50.75 | 35.11 | 49.94 | 34.15 |
| 81.84 | 33.15 | 83.08 | 33.38 | 85.63 | 34.65 | 83.99 | 33.95 |
| 114.94 | 33.05 | 116.27 | 33.00 | 120.18 | 34.46 | 117.92 | 33.92 |
| 150.16 | 33.01 | 150.35 | 32.96 | 154.49 | 34.17 | 151.69 | 33.62 |
| 183.22 | 33.12 | 183.29 | 32.90 | 188.57 | 33.98 | 185.39 | 33.78 |
| 214.16 | 33.18 | 214.92 | 32.55 | 222.26 | 33.41 | 219.07 | 33.58 |
| 247.52 | 33.54 | 247.47 | 32.56 | 255.47 | 33.00 | 252.66 | 33.60 |
| 280.65 | 33.71 | 279.85 | 32.20 | 288.23 | 32.53 | 286.15 | 33.39 |
| 315.09 | 33.92 | 315.06 | 31.85 | 320.34 | 31.68 | 319.38 | 33.07 |
| 337.76 | 33.41 | 338.39 | 31.65 | 339.28 | 31.06 | 340.19 | 33.03 |

Table A-3. Bubble velocity profiles in presence of 1, 2-butanol

| water | | 1 mM | | 8 mM | | 30mM | | 60 mM | |
|------------|-------------|------------|-------------|------------|-------------|------------|-------------|------------|-------------|
| Dist. (cm) | Vel. (cm/s) | Dist. (cm) | Vel. (cm/s) | Dist. (cm) | Vel. (cm/s) | Dist. (cm) | Vel. (cm/s) | Dist. (cm) | Vel. (cm/s) |
| 0.39 | 11.64 | 0.73 | 21.91 | 0.14 | 4.31 | 0.38 | 11.31 | 0.66 | 19.76 |
| 1.86 | 32.64 | 2.59 | 33.82 | 1.28 | 29.81 | 1.73 | 29.31 | 2.14 | 24.53 |
| 4.09 | 34.27 | 4.85 | 34.09 | 3.38 | 33.19 | 3.68 | 29.06 | 3.72 | 22.94 |
| 6.38 | 34.36 | 7.15 | 34.91 | 5.58 | 32.63 | 5.58 | 28.11 | 5.21 | 21.88 |
| 8.68 | 34.45 | 9.46 | 34.27 | 7.76 | 32.81 | 7.45 | 27.86 | 6.66 | 21.53 |
| 10.98 | 34.73 | 11.77 | 35.09 | 9.95 | 33.00 | 9.29 | 27.51 | 8.08 | 21.18 |
| 12.72 | 34.85 | 13.52 | 34.97 | 11.59 | 32.31 | 10.67 | 27.63 | 9.11 | 21.53 |
| 15.03 | 34.91 | 15.82 | 34.51 | 13.78 | 32.13 | 12.44 | 27.69 | 10.33 | 21.18 |
| 17.93 | 34.91 | 18.70 | 34.45 | 16.50 | 32.63 | 14.60 | 25.03 | 11.85 | 20.35 |
| 19.66 | 34.50 | 20.42 | 34.27 | 18.13 | 32.13 | 15.84 | 24.17 | 12.75 | 19.65 |
| 21.37 | 34.56 | 22.15 | 34.36 | 19.68 | 31.96 | 17.02 | 23.14 | 13.62 | 19.65 |
| 24.24 | 34.43 | 25.00 | 34.18 | 22.34 | 31.71 | 18.89 | 22.47 | 15.09 | 18.29 |
| 26.55 | 34.45 | 27.27 | 34.30 | 24.51 | 31.75 | 20.37 | 21.97 | 16.25 | 17.65 |
| 28.28 | 34.64 | 28.99 | 34.25 | 26.09 | 31.69 | 21.44 | 21.17 | 17.13 | 17.65 |
| 30.59 | 34.55 | 31.26 | 33.73 | 28.20 | 31.50 | 22.82 | 20.31 | 18.28 | 16.76 |
| 48.92 | 34.35 | 49.22 | 33.66 | 44.55 | 30.60 | 33.33 | 19.66 | 26.96 | 16.25 |
| 83.21 | 34.34 | 82.71 | 33.33 | 74.52 | 29.34 | 52.28 | 18.26 | 43.12 | 16.08 |
| 116.96 | 33.27 | 116.01 | 33.26 | 102.98 | 27.59 | 70.12 | 17.41 | 59.14 | 15.95 |
| 151.34 | 33.26 | 151.32 | 32.97 | 129.87 | 26.19 | 87.23 | 16.82 | 74.99 | 15.74 |
| 184.59 | 33.24 | 184.14 | 32.62 | 156.09 | 24.61 | 104.11 | 16.92 | 90.62 | 15.52 |
| 216.72 | 33.22 | 214.72 | 32.89 | 180.19 | 23.53 | 120.89 | 16.66 | 106.21 | 15.67 |
| 249.83 | 33.01 | 247.43 | 32.53 | 202.55 | 22.75 | 137.31 | 16.17 | 122.06 | 16.02 |
| 282.95 | 33.22 | 279.85 | 32.32 | 224.99 | 22.14 | 156.92 | 16.47 | 137.76 | 15.38 |
| 317.09 | 32.87 | 315.11 | 31.83 | 246.83 | 21.54 | 173.39 | 16.48 | 157.24 | 15.38 |
| 338.86 | 32.75 | 338.41 | 31.45 | 268.08 | 20.96 | 186.54 | 16.42 | 172.64 | 15.48 |
| | | | | 288.90 | 20.68 | 202.88 | 16.25 | 184.01 | 15.52 |
| | | | | 306.71 | 20.37 | 218.98 | 15.97 | 199.54 | 15.55 |
| | | | | 326.89 | 20.08 | 234.97 | 16.01 | 215.02 | 15.41 |
| | | | | 342.27 | 19.92 | 250.98 | 16.01 | 230.49 | 15.52 |
| | | | | | | 267.05 | 16.13 | 246.00 | 15.51 |
| | | | | | | 283.05 | 15.87 | 261.37 | 15.24 |
| | | | | | | 298.92 | 15.86 | 276.88 | 15.79 |
| | | | | | | 320.12 | 15.93 | 292.51 | 15.47 |
| | | | | | | 336.10 | 16.20 | 307.44 | 15.40 |
| | | | | | | 342.00 | 16.00 | 324.12 | 15.82 |
| | | | | | | | | 339.79 | 15.44 |

Table A-4. Bubble velocity profiles in presence of 0.5 mmol/L dipropylene glycol ether

| Methyl ether | | Propyl ether | | Butyl ether | |
|---------------------|------------|---------------------|------------|--------------------|------------|
| Con.(mmol/L) | Vel.(cm/s) | Con.(mmol/L) | Vel.(cm/s) | Con.(mmol/L) | Vel.(cm/s) |
| 0 | 0 | 0 | 0 | 0 | 0 |
| 0.64 | 19.20 | 0.38 | 11.55 | 0.01 | 0.45 |
| 2.39 | 33.20 | 1.73 | 28.80 | 0.63 | 17.85 |
| 4.65 | 34.80 | 3.65 | 28.65 | 1.75 | 15.75 |
| 6.96 | 34.40 | 5.52 | 27.45 | 2.78 | 15.30 |
| 9.27 | 34.80 | 7.36 | 27.75 | 3.81 | 15.45 |
| 11.59 | 35.00 | 9.19 | 27.30 | 4.83 | 15.30 |
| 13.35 | 34.60 | 10.56 | 26.65 | 5.60 | 15.80 |
| 15.69 | 34.60 | 12.36 | 26.35 | 6.62 | 15.80 |
| 18.59 | 34.40 | 14.57 | 26.10 | 7.89 | 15.30 |
| 20.31 | 34.20 | 15.87 | 25.75 | 8.66 | 15.65 |
| 22.03 | 34.60 | 17.14 | 25.50 | 9.42 | 15.30 |
| 24.91 | 34.80 | 19.27 | 25.25 | 10.70 | 15.10 |
| 27.21 | 34.20 | 20.86 | 25.45 | 11.72 | 15.35 |
| 28.93 | 34.40 | 22.12 | 25.50 | 12.49 | 15.75 |
| 31.21 | 34.00 | 23.91 | 25.20 | 13.52 | 15.15 |
| 49.32 | 33.95 | 37.41 | 25.32 | 21.67 | 15.30 |
| 83.12 | 33.65 | 62.43 | 24.72 | 37.06 | 15.47 |
| 116.48 | 33.07 | 87.23 | 24.88 | 52.47 | 15.36 |
| 151.47 | 32.58 | 112.17 | 25.00 | 67.85 | 15.39 |
| 183.83 | 32.06 | 137.11 | 24.87 | 83.24 | 15.39 |
| 213.23 | 31.01 | 161.94 | 24.80 | 98.55 | 15.24 |
| 243.65 | 29.84 | 186.54 | 24.40 | 113.73 | 15.11 |
| 272.86 | 28.57 | 210.72 | 23.96 | 128.93 | 15.29 |
| 299.89 | 27.31 | 234.60 | 23.79 | 144.19 | 15.23 |
| 326.43 | 25.86 | 258.28 | 23.57 | 160.44 | 15.25 |
| 342.73 | 25.00 | 281.72 | 23.31 | 175.73 | 15.35 |
| | | 313.24 | 22.93 | 190.06 | 15.35 |
| | | 336.14 | 22.73 | 205.41 | 15.36 |
| | | 342.19 | 22.65 | 220.84 | 15.50 |
| | | | | 236.28 | 15.37 |
| | | | | 251.60 | 15.28 |
| | | | | 266.87 | 15.25 |
| | | | | 282.13 | 15.28 |
| | | | | 297.54 | 15.54 |
| | | | | 319.31 | 15.56 |
| | | | | 334.86 | 15.50 |
| | | | | 341.16 | 15.82 |

Table A-5. Effect of velocity at 300 cm of OH position in alcohols

| Five-carbon | | | | | |
|--------------------|------------|-------------------|------------|-------------------|------------|
| 1-pentanol | | 2-pentanol | | 3-pentanol | |
| Con.(mmol/L) | Vel.(cm/s) | Con.(mmol/L) | Vel.(cm/s) | Con.(mmol/L) | Vel.(cm/s) |
| 0.08 | 31.76 | 0.5 | 31.00 | 0.3 | 32.56 |
| 0.40 | 29.33 | 1.0 | 26.51 | 0.5 | 32.04 |
| 0.57 | 28.22 | 1.4 | 23.16 | 1.0 | 29.26 |
| 1.20 | 22.20 | 1.8 | 21.32 | 1.4 | 26.74 |
| 1.25 | 21.75 | 2.2 | 17.81 | 1.8 | 22.26 |
| 1.40 | 20.59 | 2.6 | 16.19 | 2.2 | 20.71 |
| 1.70 | 19.39 | 2.8 | 15.43 | 2.6 | 18.69 |
| 1.80 | 18.37 | 3.0 | 15.71 | 2.8 | 17.38 |
| 2.20 | 16.83 | 3.2 | 15.06 | 3.0 | 16.89 |
| 2.27 | 15.62 | 3.6 | 15.59 | 3.2 | 17.39 |
| 2.60 | 15.02 | 4.0 | 15.49 | 3.6 | 16.61 |
| 2.84 | 15.69 | 5.0 | 15.39 | 3.8 | 16.55 |
| 3.69 | 15.23 | 6.0 | 15.19 | 4.0 | 16.23 |
| 3.97 | 15.23 | 7.0 | 15.29 | 4.8 | 15.66 |
| 4.00 | 15.13 | | | 5.0 | 15.68 |
| 4.25 | 15.29 | | | 6.0 | 15.52 |
| 4.54 | 15.33 | | | 8.0 | 15.22 |
| 6.81 | 14.90 | | | 10.0 | 15.21 |
| 13.61 | 15.03 | | | | |

| Six-carbon | | | | | |
|-------------------|------------|------------------|------------|------------------|------------|
| 1-hexanol | | 2-hexanol | | 3-hexanol | |
| Con.(mmol/L) | Vel.(cm/s) | Con.(mmol/L) | Vel.(cm/s) | Con.(mmol/L) | Vel.(cm/s) |
| 0.05 | 32.86 | 0.05 | 32.65 | 0.05 | 33.35 |
| 0.075 | 29.58 | 0.075 | 30.43 | 0.075 | 31.35 |
| 0.10 | 26.40 | 0.10 | 28.50 | 0.10 | 29.44 |
| 0.15 | 23.46 | 0.15 | 24.68 | 0.15 | 26.30 |
| 0.20 | 20.13 | 0.20 | 21.86 | 0.20 | 24.64 |
| 0.25 | 17.65 | 0.25 | 19.06 | 0.25 | 19.69 |
| 0.3 | 16.58 | 0.3 | 17.35 | 0.3 | 18.35 |
| 0.4 | 15.35 | 0.4 | 16.35 | 0.4 | 17.34 |
| 0.5 | 15.35 | 0.6 | 15.79 | 0.6 | 16.35 |
| 0.6 | 15.52 | 0.8 | 15.25 | 0.8 | 15.55 |
| 0.8 | 15.16 | | | | |

Table A-6. Velocity at 300 cm vs. concentration for five-carbon isomers

| 3-methyl-1-butanol | | 3-methyl-2-butanol | | 2-methyl-1-butanol | | 2-methyl-2-butanol | |
|---------------------------|----------------|---------------------------|----------------|---------------------------|----------------|---------------------------|----------------|
| Con. (mmol/L) | Vel. (cm/s) | Con. (mmol/L) | Vel. (cm/s) | Con. (mmol/L) | Vel. (cm/s) | Con. (mmol/L) | Vel. (cm/s) |
| 0.1 | 31.41 | 0.1 | 33.00 | 0.1 | 33.00 | 0.1 | 33.90 |
| 0.3 | 28.93 | 0.5 | 30.00 | 0.5 | 30.00 | 0.5 | 32.29 |
| 0.5 | 25.86 | 1.0 | 26.25 | 1.0 | 26.25 | 1.0 | 28.74 |
| 1.0 | 18.41 | 1.4 | 24.09 | 1.4 | 24.09 | 1.8 | 26.11 |
| 1.2 | 16.42 | 1.8 | 21.03 | 1.8 | 21.03 | 2.2 | 23.72 |
| 1.4 | 15.66 | 2.2 | 20.19 | 2.2 | 20.19 | 2.6 | 20.20 |
| 1.8 | 15.10 | 2.6 | 16.74 | 2.6 | 16.74 | 3.0 | 18.71 |
| 2.2 | 15.02 | 2.8 | 15.05 | 2.8 | 15.05 | 3.6 | 15.96 |
| 2.6 | 15.63 | 3.0 | 15.34 | 3.0 | 15.34 | 4.0 | 16.07 |
| 2.8 | 15.20 | 3.4 | 15.14 | 3.4 | 15.14 | 4.8 | 15.36 |
| 3.0 | 15.33 | | | | | 5.2 | 15.45 |
| 3.2 | 15.06 | | | | | 5.6 | 15.25 |
| 3.6 | 15.00 | | | | | 6.0 | 15.14 |
| 3.8 | 15.40 | | | | | 8.0 | 15.04 |

Table A-7. Velocity at 300 cm vs. concentration for six-carbon isomers

| 3-methyl-1-pentanol | | 3-methyl-2-pentanol | | 3-methyl-3-pentanol | |
|----------------------------|------------|----------------------------|------------|----------------------------|------------|
| Con.(mmol/L) | Vel.(cm/s) | Con.(mmol/L) | Vel.(cm/s) | Con.(mmol/L) | Vel.(cm/s) |
| 0.01 | 19.64 | 0.05 | 30.29 | 0.05 | 30.52 |
| 0.05 | 17.64 | 0.10 | 29.03 | 0.10 | 29.60 |
| 0.10 | 15.84 | 0.15 | 25.43 | 0.15 | 28.12 |
| 0.15 | 15.47 | 0.20 | 23.23 | 0.20 | 27.21 |
| 0.2 | 15.32 | 0.25 | 20.81 | 0.25 | 25.02 |
| 0.3 | 15.32 | 0.3 | 19.04 | 0.3 | 23.80 |
| 0.4 | 15.43 | 0.4 | 16.41 | 0.4 | 21.33 |
| 0.5 | 15.73 | 0.45 | 15.83 | 0.5 | 17.97 |
| | | 0.5 | 15.81 | 0.6 | 16.40 |
| | | 0.6 | 15.41 | 0.7 | 15.64 |
| | | 0.8 | 15.31 | 0.8 | 15.04 |
| 2-methyl-1-pentanol | | 2-methyl-2-pentanol | | 2-methyl-3-pentanol | |
| Con.(mmol/L) | Vel.(cm/s) | Con.(mmol/L) | Vel.(cm/s) | Con.(mmol/L) | Vel.(cm/s) |
| 0.05 | 26.04 | 0.05 | 30.74 | 0.075 | 32.41 |
| 0.10 | 23.15 | 0.10 | 30.01 | 0.15 | 30.98 |
| 0.15 | 19.58 | 0.15 | 26.78 | 0.20 | 28.52 |
| 0.20 | 16.85 | 0.20 | 25.16 | 0.25 | 26.81 |
| 0.25 | 16.01 | 0.25 | 21.81 | 0.30 | 25.16 |
| 0.30 | 15.62 | 0.30 | 20.05 | 0.40 | 22.37 |
| 0.40 | 15.23 | 0.40 | 17.22 | 0.50 | 20.24 |
| 0.50 | 14.75 | 0.50 | 16.24 | 0.60 | 17.19 |
| 0.60 | 14.65 | 0.60 | 15.35 | 0.70 | 16.49 |
| | | 0.70 | 15.15 | 0.80 | 16.19 |

Table A-8. Effect of velocity at 300 cm of position of second OH in diols

| Five-carbon | | | | | |
|-------------------------|------------|-------------------------|------------|------------------------|------------|
| 1, 2-pentanediol | | 1, 4-pentanediol | | 1,5-pentanediol | |
| Con.(mmol/L) | Vel.(cm/s) | Con.(mmol/L) | Vel.(cm/s) | Con.(mmol/L) | Vel.(cm/s) |
| 0.05 | 31.72 | 0.05 | 32.66 | 0.1 | 32.88 |
| 0.1 | 30.41 | 0.5 | 31.56 | 2 | 32.95 |
| 0.2 | 26.66 | 1.0 | 29.82 | 6 | 32.22 |
| 0.3 | 24.71 | 1.4 | 28.07 | 10 | 29.69 |
| 0.4 | 21.98 | 1.9 | 23.74 | 15 | 24.58 |
| 0.5 | 19.76 | 5.0 | 21.26 | 50 | 20.85 |
| 0.6 | 19.36 | 10 | 16.56 | 100 | 19.00 |
| 0.7 | 18.01 | 20 | 15.56 | 150 | 15.51 |
| 0.8 | 17.39 | 40 | 15.26 | 200 | 16.31 |
| 0.9 | 17.04 | | | 250 | 16.22 |
| 1.0 | 16.73 | | | | |
| 1.2 | 16.58 | | | | |
| 1.4 | 16.03 | | | | |
| 1.6 | 15.78 | | | | |
| 1.8 | 15.04 | | | | |
| 2.0 | 14.89 | | | | |
| 2.5 | 15.04 | | | | |
| 5.0 | 15.39 | | | | |

| Six-carbon | | | | | |
|------------------------|------------|------------------------|------------|------------------------|------------|
| 1, 2-hexanediol | | 1, 5-hexanediol | | 1, 6-hexanediol | |
| Con.(mmol/L) | Vel.(cm/s) | Con.(mmol/L) | Vel.(cm/s) | Con.(mmol/L) | Vel.(cm/s) |
| 0.01 | 32.36 | 0.075 | 30.15 | 0.05 | 31.44 |
| 0.03 | 28.88 | 0.10 | 28.48 | 0.1 | 31.13 |
| 0.05 | 20.31 | 0.15 | 23.29 | 0.2 | 30.31 |
| 0.08 | 17.64 | 0.20 | 22.38 | 0.3 | 29.55 |
| 0.10 | 16.70 | 0.30 | 17.48 | 0.4 | 28.65 |
| 0.15 | 16.51 | 0.40 | 16.80 | 0.5 | 27.41 |
| 0.20 | 15.35 | 0.60 | 15.71 | 0.6 | 25.58 |
| 0.60 | 15.35 | 0.80 | 15.72 | 0.8 | 21.74 |
| | | 1.0 | 15.43 | 1.2 | 18.88 |
| | | 1.2 | 15.39 | 1.6 | 17.38 |
| | | | | 1.9 | 16.39 |
| | | | | 2.2 | 15.95 |
| | | | | 2.5 | 15.73 |
| | | | | 2.8 | 15.80 |
| | | | | 3.0 | 15.70 |